TUDelft

Delft University of Technology

Electrical Engineering, Mathematics and Computer Science

Delft Institute of Applied Mathematics

A Study of Pair Correlation Functions Using Classical DFT

A thesis submitted to the
Delft Institute of Applied Mathematics
in partial fulfillment of the requirements

for the degree

MASTER OF SCIENCE
in
APPLIED MATHEMATICS

by

J. de Gussem

Delft, The Netherlands
October, 2012

TUDelft

MSc thesis APPLIED MATHEMATICS

A Study of Pair Correlation Functions
Using Classical DFT

J. de Gussem

Delft University of Technology

Daily supervisor

Prof. dr. ir. C. Vuik

Reviewers

Dr. ir. F. Vermolen

October 2012

Responsible professor

Prof. dr. ir. C. Vuik

Dr. J. Thijssen

Delft, the Netherlands

DELFT UNIVERSITY of TECHNOLOGY

Abstract

Electrical Engineering, Mathematics and Computer Science
Numerical Analysis

Master of Science

A Study of Pair Correlation Functions Using Classical DFT

by Joost de GUSSEM

At the heart of physics of fluids are particle distribution functions. If all of these functions of a fluid are known, the state can be fully described. With a universal theory of particle distribution functions, physics of fluids is done. Of particular interest is the radial distribution function (rdf), which is related to the second particle distribution function, because the average excess internal energy, pressure and isothermal compressibility naturally follow from it. Here the function is obtained for 'soft' particles by calculating the density profile around a particle fixed in the origin, acting as an external potential. This is called the test-particle method. In order to theoretically describe 'soft' particles, the short ranged (repulsive) forces and the long ranged (usually attractive) forces of the interaction potential are separated. The repulsive forces are calculated from a weighted density theory (FMT) and the long ranged forces are added as a 'small' perturbation. The FMT has been proven to be accurate, but in order to describe the perturbation well we need to know how particles correlate for larger inter-particle separations in inhomogeneous systems. In particular for inhomogeneous systems it is difficult to say something about this but we can distinguish approximations for high and low densities. The result is a 1D non-linear integral equation with squares, cubes, fractions and logarithms in the *weighted* form of the unknown for the reference system and a perturbation which is linear in the unknown. The results are satisfactory for high and low densities, but for the intermediate range the results are less satisfactory. For a range of high densities we obtain a measure for the short-ranged correlations by fitting with MD results.

Acknowledgments

I would like to acknowledge and extend my gratitude to my supervisor Professor Kees Vuik, who always read my work very carefully and asked a lot of questions about the underlying physics of the problem. This resulted in an extensive introduction to the field of statistical physics. Also I would like to thank Erin McGarrity for providing me with a lot of simulation data. Without those data I would have been able to write this report.

Contents

Chapter 1

Introduction

There has been a long history in the search for distribution functions of uniform fluids. These functions describe the (short ranged) correlations between particles which are essential to describe liquids theoretically. If in particular the radial distribution function (rdf) g is known, thermodynamic properties of a system can be obtained via a number of different routes. In general, correlation functions depend of the size, shape and orientation of the particles, as well as the way the particles interact (that is, the interaction potential). General expressions for correlation functions leave these variables open. In
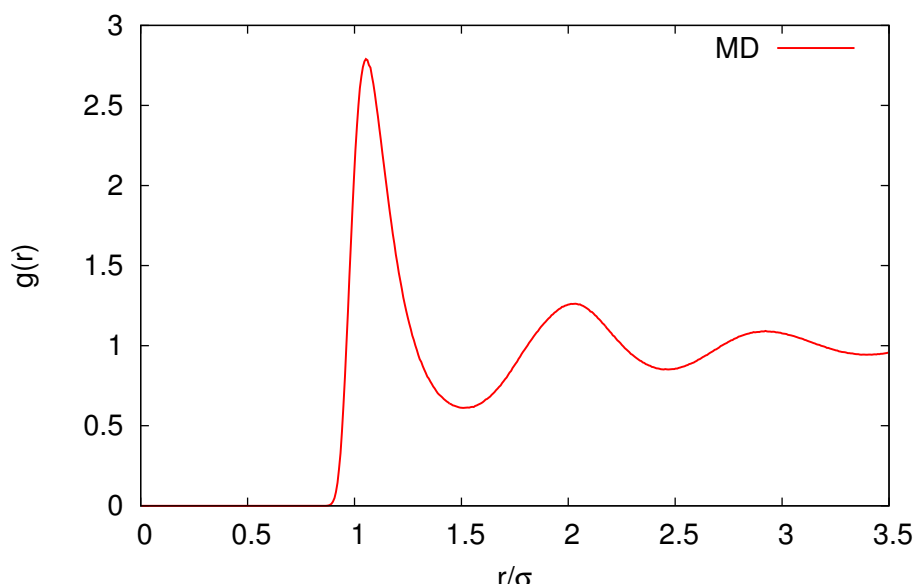

Figure 1.1: A sample radial distribution function g for spherical particles calculated using molecular dynamics (MD).[1] The horizontal axis is normalized by the particle diameter σ.

figure 1.1 a typical radial distribution function is shown for soft spherical particles in a homogeneous system with a 'high' density. When particles get close together they strongly repel; this is indicated by the region where g is 0 in the figure. Around $r=\sigma$, particles can align to the particle in the origin in a layer or a shell, sometimes referred to as a 'solvation shell'. Due to this first shell, there is a region around $r=3\sigma/2$ where it is less likely to find particles, indicated by the local minimum. Around $r=2$ there is another layer, since particles will align to the first solvation shell. The peak in this second solvation shell is smaller than the first peak because the particles are farther away from the origin and the interactions between the particles are weaker. For low densities the ordering is less apparent, because the average distance between the particles is larger. Typically only one local maximum occurs.

One of the earliest attempts to determine the structure and thermodynamics of a uniform classical fluid is done by Born and Green.[2] They assume that the forces between particles are pairwise additive and use a low density argument to arrive at the nonlinear integral equation for the rdf g,

$$-\nabla_1[\ln g(\mathbf{r}_1, \mathbf{r}_2) + \beta\phi(\mathbf{r}_1, \mathbf{r}_2)] = \beta\rho \int \nabla_1\phi(\mathbf{r}_1, \mathbf{r}_3)g(\mathbf{r}_1, \mathbf{r}_3)[g(\mathbf{r}_2, \mathbf{r}_3) - 1]\mathrm{d}\mathbf{r}_3.$$
(1.1)

Given a temperature $T = k_B/\beta$, where k_B is the Boltzmann constant, a density ρ and a pairwise interaction potential ϕ, the equation can be solved numerically. It turns out that the results due to this equation are satisfactory only at low densities.[3] Better results can be obtained from the OZ equation [4], named after Ornstein and Zernike. Already in the second decade of the last century they proposed to split the effects of particles in a direct and an indirect way. The direct contribution is defined to be given by the *direct* correlation function, denoted by c. The indirect part is due to the influence of molecule 1 on a third molecule, labeled 3, which in turn affects molecule 2, directly and indirectly. Mathematically this means that for homogeneous densities

$$h(r) = c(r) + \rho \int c(\mathbf{r}')h(|\mathbf{r} - \mathbf{r}'|)\mathrm{d}\mathbf{r}',$$
(1.2)

where h is the *total* correlation function. This is equal to the radial distribution function subtracted by the ideal (kinetic part): $h = g - 1$. Hence the name total correlation function because it takes into account all the correlations, but no kinetic energy. Since there are two unknowns in the above equation (c and h), a closure relation, or an initial guess for an iteration procedure, is needed. Percus argued that g can be obtained by calculating the density

profile around a particle fixed in the origin, while other particles move in the force field of the fixed particle.[6] When the fixed particle is treated as a perturbation this idea can (with the Yvon equation [5]) be shown to lead to the mean spherical approximation (MSA)

$$c(r) = -\beta\phi(r), \qquad (1.3)$$

where ϕ is the potential describing the pairwise interactions between the particles. When the potential is steeply repulsive at short range this leads to very poor results.[5] Better results can be obtained by an expansion of the density around an uniform state, leading to

$$g(r) = \mathrm{e}^{-\beta\phi(r)+\rho\int c(\mathbf{r}')h(\mathbf{r}-\mathbf{r}')\mathrm{d}\mathbf{r}'} = \mathrm{e}^{-\beta\phi(r)+h(r)-c(r)}, \qquad (1.4)$$

where the last step follows from the OZ equation (1.2). Expression (1.4) is called the *hypernetted chain* (HNC) approximation.[7] In combination with the OZ equation it can be written as an integral equation, [5]

$$\ln g(r)+\beta\phi(r) = \rho\int[g(|\mathbf{r}-\mathbf{r}'|)-1][g(\mathbf{r})-1-\ln g(\mathbf{r}')-\beta\phi(\mathbf{r}')]\mathrm{d}\mathbf{r}', \qquad (1.5)$$

which can be solved iteratively.[8] The Percus-Yevick equation [9],

$$g(r) = \mathrm{e}^{-\beta\phi(r)}\left(1+\rho\int c(\mathbf{r}')h(\mathbf{r}-\mathbf{r}')\mathrm{d}\mathbf{r}'\right) = \mathrm{e}^{-\beta\phi(r)}[1+h(r)-c(r)], \qquad (1.6)$$

gives better results although it can be shown to take less interactions than the HNC approximation into account. So it must be due to a cancellation of errors that it performs better.[5] In combination with the OZ equation, to eliminate c, one obtains

$$\mathrm{e}^{\beta\phi(r)}g(r) = 1 + \rho\int[g(|\mathbf{r}-\mathbf{r}'|)-1]g(\mathbf{r}')(1-\mathrm{e}^{\phi(\mathbf{r}')})\mathrm{d}\mathbf{r}'. \qquad (1.7)$$

The HNC and PY-equation are the most influential equations in recovering the radial distribution function. They have been studied a lot and various approximation schemes or solution methods have been investigated (e.g. [10, 11, 12]). Most models with non-trivial interaction potentials are only applicable in a certain density or temperature range.

Apart from the OZ equation, one can as aforementioned obtain correlation functions by calculating the density profile around a hard particle as an external force. It was shown by Percus that the single particle density distribution (that is, the density profile) in the presence of a single particle acting

3

as an external potential, is exactly equal to the pair distribution function of a homogeneous system. In the context of classical density functional theory (CDFT or classical DFT), this boils down to the minimum of a functional of an inhomogeneous (spatially varying) number density $\rho(\mathbf{r})$. Density functional theory (DFT) was developed in the 1970s, by Ebner, Saam and Stroud in 1976.[13]. In order to describe state properties of inhomogeneous systems accurately, we can use a smoothed density approximation (SDA) which takes density variations around a point into account. This is in contrast with local density approximations which treat non-uniform fluids as if it were locally uniform; it does not take into account the (non-homogeneous) environment. The smoothed densities can be defined in terms of the number densities ρ_i and weight functions, which can be scalars $\omega_i^{(\alpha)}$, or vectors $\boldsymbol{\omega}_i^{(\alpha)}$,

$$
\begin{aligned}
\overline{\rho}_\alpha(\mathbf{r}) &= \sum_{i=1}^{\nu} \int \rho_i(\mathbf{r}')\omega_i^{(\alpha)}(\mathbf{r}-\mathbf{r}')\mathrm{d}\mathbf{r}', \\
\overline{\boldsymbol{\rho}}_\alpha(\mathbf{r}) &= \sum_{i=1}^{\nu} \int \rho_i(\mathbf{r}')\boldsymbol{\omega}_i^{(\alpha)}(\mathbf{r}-\mathbf{r}')\mathrm{d}\mathbf{r}',
\end{aligned}
\tag{1.8}
$$

where the sum runs over all the ν species in the system.[14] The vector weights occur in general, because the density changes are directional dependent. The equation of state for *smoothed* density approximations should for uniform densities be equal to *local* density approximations. Thus Rosenfeld proposed in an influential paper a model with three linearly independent weights (two scalar weights and one vector weight) to describe the free energy of inhomogeneously distributed hard particles.[15] The weights are not based on homogeneous fluid properties but on the geometrical properties of spheres (radius, surface area, volume) and as a result, it is now referred to as fundamental measure theory (FMT). For homogeneous fluids, Rosenfeld's theory (RF) results in the PY compressibility equation for mixtures, which is an exact solution of equation (1.6) for hard spheres.[16, 17] Later an expression was derived which reduces to the Carnahan-Starling (CS) expression for mixtures in bulk fluids, called the White Bear (WB) version.[18] The CS expression is obtained from a recursive relation which closely follow the coefficients of the virial expansion for hard spheres and is therefore sometimes called semi-emphirical.[19] This is also generalized to mixtures [20] and is more accurate than the PY solution because it implicitly takes higher order terms into account.[5]

Non-local smoothed density theories have found a wide range of applications among which are non-spherical molecules [21, 22, 23, 24], mixtures

involving rods, platelets, spheres and polymers [25], freezing of fluids [26, 27], nucleation [28], polymers [29] and dynamical properties [30]. Of course research has been done to add other forces to hard spheres, for example associating bonds [31]. Surprisingly, no work has been done to obtain radial distribution functions for soft particles. Yu et al. obtained results in 2002 for hard spheres using the FMT in combination with Percus' test-particle method. These curves are much more informative than correlations around other external potentials, because they actually have a physical meaning as mentioned before. In this work we will calculate the density profile of soft particles around a soft particle fixed in the origin, acting as an external potential. We will do so using various judicious guesses for the correlations of the long ranged forces. We will also exploit the freedom of the arbitrariness in the way the interaction potential is split into a reference system and the perturbation. This is an important degree of freedom, since we want the perturbation to vary as smoothly as possible as a function of space giving rise to relatively small inter-particle forces. The reference system (i.e., the soft repulsive part) is subsequently linked to the hard-sphere system, described by the WB or RF functional via an effective diameter. There is no general theory for the effective diameter for inhomogeneous systems and it may differ from system to system.[32, 33] For homogeneous systems, equations for the effective diameter can be found from an optimization principle.[5]

In chapter 2 we extensively discuss all the theory concerning the physics of the problem. It is useful in order to understand the complexity of the problem and the significance of the results. Next, in chapter 3 the main research question is described with an overview of the equations we solve at the end. We describe several models that differ in the way the particles correlate with each other with respect to the long ranged interactions. Model 1 uses a mean field approximation which should be exact in the high density limit, since the short ranged repulsions dominate and the attractions act as a uniform background field. Here we can exploit the freedom to define the perturbation as convenient as possible. We distinguish two possibilities in model 1A and 1B. This is further explained at the end of the theory chapter. Model 2 uses a low density approximation (also called modified mean field) which should, as the name suggests, give better results for low densities. This model follows from the exact low density of the correlations in terms of the interaction potential as is also shown in the last section of the theory chapter. In chapter 4 something is said about integral equations which naturally arise in the study of correlation functions. In chapter 5 specifications of the discretization of the equations are given. The results and conclusions follow in chapter 6 and 7 respectively.

Chapter 2

Physics

2.1 Thermodynamics

We will start with the first law of thermodynamics. It provides the basic definition of internal energy and it reflects the conservation of energy,

$$\mathrm{d}U = \delta Q + \delta W, \qquad \text{(1th law)} \qquad (2.1)$$

where δQ is the infinitesimal heat intake into a well-defined system and δW is the work done *on* the system. The infinitesimal heat and work in the equations above are denoted by 'δ', rather than exact differentials denoted by 'd', because they do not describe the state of any system, they cannot be obtained by differentiation. The integral of an inexact differential depends on the particular path taken through the space of thermodynamic parameters, while the integral of an exact differential depends only on the initial and final states. Under certain circumstances the inexact differentials can be expressed in exact differentials.

For *quasi-static* transformations, the thermodynamic processes are performed slowly so that the system is always in equilibrium. This means that at any state of the process, the thermodynamic coordinates of the system exist and can in principle be calculated. For infinitesimal quasi-static transformations we can in general write the work into a set of *generalized displacement* {$\mathbf{x}$} and their conjugate *generalized forces* {$\mathbf{J}$} as mechanical work, and the chemical work μ_k associated with a fluctuating number of particles N_k for all species present in the system, showing here,

$$\delta W = \sum_i J_i \mathrm{d}x_i + \sum_k \mu_k \mathrm{d}N_k. \qquad (2.2)$$

The set of such conjugate coordinates need to be specified per system, see table 2.1 for some common examples. Note that the pressure is by conven-

Table 2.1: Generalized forces and their displacements.

System	Generalized force		Generalized displacement	
Wire	tension	τ	length	L
Film	surface tension	γ	area	A
Fluid	pressure	$-p$	volume	V
Magnetic	magnetic field	H	magnetization	M
Dielectric	electric field	E	polarization	P
Chemical	chemical potential	μ	particle number	N

tion calculated from the force exerted *on* the walls. The displacements are usually extensive quantities, that is, they are proportional to the system size, as opposed to the forces which are intensive, which means that they are independent of the system size.

Since the first law, eq. (2.1), is completely symmetric with respect to initial and final states of an evolving system, it does not account for a preferred direction of a process. The second law expresses that no process can have as a sole result that heat is transferred from a system of lower temperature to a system of higher temperature. A mathematical way to express the second law is called Clausius' theorem which states that for any cyclic transformation, we have for the heat increment supplied to the system,

$$\oint \frac{\delta Q}{T} \leq 0. \qquad \text{(2nd law)} \qquad (2.3)$$

Here equality holds for *reversible* cycles, since by traversing the integration path in the opposite direction, the heat transfer flips sign and the cyclic integral is both non-negative and non-positive by the above theorem. From this it follows that for a reversible process, the integral of δQ_{rev} is independent of the path taken. Moreover, since entropy ('disorder') is a state function, we can always connect the initial and final state of a process with an imaginary reversible process. Then we can write, using Clausius theorem,

$$\mathrm{d}S \geq \frac{\delta Q}{T} \quad \text{with} \quad \mathrm{d}S \equiv \frac{\delta Q_{\text{rev}}}{T}. \qquad \text{(classical)} \qquad (2.4)$$

which is the classical definition of entropy. Thus, the entropy of a system increases when irreversible processes occur, and it is maximal in the state of thermodynamic equilibrium. This definition of entropy only holds near equilibrium and it makes no reference to the microscopic nature of matter. A microstate is the most detailed description possible of the state of a system,

e.g. for a gas this means knowing the position and momentum of all particles in the system. A *general* way to define entropy, which can -for processes close to equilibrium- shown to be equivalent to the first, is,

$$S \equiv -k_B \sum_i P_i \ln P_i = k_B \ln \mathcal{Q}, \qquad \text{(statistical)} \qquad (2.5)$$

where P_i is the probability that the system is in the ith microstate, summing over all possible microstates (with $\sum P_i = 1$) and k_B is the Boltzmann constant. This expression is minimal for the delta function distribution $P_i = \delta_{i,j}$ and maximal for the uniform distribution as shown on the right-hand side. The right hand side follows from the *fundamental postulate of statistical thermodynamics* which states that,

$$\begin{array}{c} \text{for a given isolated system in equilibrium} \\ \text{each accessible microstate is equally probable,} \end{array} \qquad (2.6)$$

or $P_i = 1/\mathcal{Q}$ where $\mathcal{Q}$ is the number of microstates at a particular energy. So for the right hand side of (2.5) an assumption is made about the microstates, so it is not general anymore. But for a macroscopic system an expression of thermodynamic quantities in macroscopic properties (such as pressure, volume, temperature or internal energy) is more useful since it is not possible -or even necessary- to obtain all the microscopic information P_i of the system. Moreover, this is constantly changing since the particles exchange energy and there is a vast amount of microstates corresponding to a single macrostate, because the number of particles (molecules) in a system is usually very large. The fundamental postulate (2.6) is necessary, in order to conclude that for a system in equilibrium, the thermodynamic macrostate, which would result from the largest number of microstates, is also by far the most probable. For small systems the exact expression for entropy with P_i for every microstate can still be used.

A consequence of the first two thermodynamic laws is the *fundamental thermodynamic relation*. This relation expresses that a reversible (hence quasi-static) change in internal energy $\mathrm{d}U$ can be expressed in terms of infinitesimal changes in entropy S and other external displacements $\mathrm{d}x_i$ and particles of several species $\mathrm{d}N_i$, for example volume $\mathrm{d}V$ and a single species $\mathrm{d}N$,

$$\mathrm{d}U = T\mathrm{d}S + \sum_i J_i \mathrm{d}x_i + \sum_k \mu_k \mathrm{d}N_k \quad \text{e.g.} \quad \mathrm{d}U = T\mathrm{d}S - p\mathrm{d}V + \mu \mathrm{d}N. \quad (2.7)$$

Here T is the temperature in the system, p the pressure and μ is the chemical potential which is the amount of work required to add a particle to the system. Equation (2.7) simplifies if for example the volume of the system is

constant ($\mathrm{d}V{=}0$) or the number of particles in the system is fixed ($\mathrm{d}N{=}0$). Therefore it is sometimes convenient to evaluate systems in a specific ensemble with constant macroscopic conditions. We will proceed by discussing some ensembles and find definitions for some earlier mentioned intrinsic thermodynamic properties on the way.

2.2 Statistical Mechanics

Statistical mechanics is a probabilistic approach to equilibrium macroscopic properties of large numbers of degrees of freedom. Rather than following the evolution of an individual microstate, it examines the ensemble of microstates corresponding to a given macrostate. Moreover one seeks to find probabilities for the equilibrium ensemble and -in contrast to kinetic theory- does not care about *how* various systems evolve to a state of equilibrium.

In a specific ensemble some parameters are fixed. An isolated system (both mechanically and thermally) is called a *microcanonical* or (N, V, E) ensemble for which the number of particles, the volume and the total energy are held constant. Similarly, an isolated system which can exchange energy in the form of heat with a large thermal reservoir (so large that it is at constant temperature) is called a *canonical* or (N, V, T) ensemble. An isothermal-isobaric or (N, p, T) ensemble, also called the *Gibbs canonical* ensemble, is a generalized canonical ensemble in which the internal energy changes by addition of both heat and work. Thermal equilibrium is obtained by heat exchange with the reservoir and mechanical equilibrium by for example a piston in order to maintain constant pressure. It is in particular useful for studying chemical reactions, since they are usually carried out under constant pressure. A system which can, besides heat, also exchange particles with the reservoir is called the grand canonical or (μ, V, T) ensemble. These ensembles will be discussed next.

We start with an isolated system unable to exchange energy with the surrounding. If two such isolated systems with initial energy E_1 and E_2 respectively are brought into contact, by allowing heat exchange between them, the internal states will shift. So the total energy is $E{=}E_1{+}E_2$ and we work in the microcanonical ensemble (N, V, E). Since the overall energy is fixed, the total allowed phase space is computed from,

$$\mathcal{Q}(E) = \int \mathrm{d}E_1 \mathcal{Q}_1(E_1)\mathcal{Q}_2(E{-}E_1) = \int \mathrm{d}E_1 \mathrm{e}^{(S_1(E_1)+S_2(E-E_1))/k_B}, \qquad (2.8)$$

where $\mathcal{Q}_1$ and $\mathcal{Q}_2$ and S_1 and S_2 are the number of microstates and entropy of system 1 with energy E_1 and 2 with energy $E_2{=}E{-}E_1$ respectively. Besides
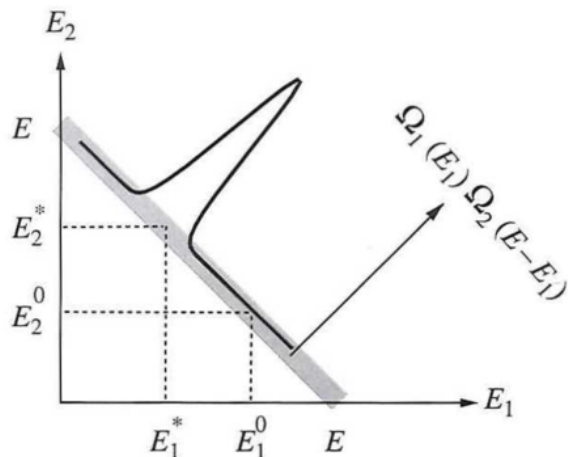
Figure 2.1: The joint number of states of two systems in contact with total energy $E=E_1+E_2$ (as indicated by the grey line) is overwhelmingly larger at the equilibrium energies (E_1^* and E_2^*) as indicated by the black curve.[36]

that we used equation (2.5) to express the number of microstates for a fixed energy into a corresponding amount of entropy. The extensive property of entropy indicates that S_1 and S_2 are proportional to the numbers of particles in each system, making the integrand in the above equation an exponentially large quantity, see figure 2.1. Since k_B is 'small', the integral in equation (2.8) can be approximated from the maximum of the integrand by the saddle point approximation (see equation (A.4)),

$$S(E)=k_B\ln\mathcal{Q}(E)\approx S_1(E_1^*)+S_2(E_2^*) \quad \text{and} \quad \left.\frac{\partial S_1}{\partial E_1}\right|_{\mathbf{x}_1} = \left.\frac{\partial S_2}{\partial E_2}\right|_{\mathbf{x}_2} \qquad (2.9)$$

gives the position of the maximum (i.e. E_1^* and $E_2^*=E-E_1^*$). Although all joint microstates are equally likely, the above results indicate that there is an exponentially larger number of states in the vicinity of (E_1^*, E_2^*), as can be seen in figure 2.1. After the exchange of energy takes place, the combined system explores a whole new set of microstates, that is the grey line in figure 2.1. The probabilistic arguments provide no information on the dynamics of the evolution among these microstates, or on the amount of time needed to establish equilibrium. However, once sufficient time has elapsed, the system is overwhelmingly likely to be at a state with internal energies (E_1^*, E_2^*). At this equilibrium point, the above maximum condition is satisfied, specifying a relation between two functions of state: internal energy and entropy, thus being equivalent to empirical temperatures. We can therefore define the

temperature T as,

$$\frac{1}{T} \equiv \left.\frac{\partial S}{\partial E}\right|_{\mathbf{x}=(V,N)}. \tag{2.10}$$

Note that this is consistent with the fundamental relation eq. (2.7). This holds in all ensembles where the other external variables (in this ensemble V and N) are temporarily held constant.

The above statistical definition of equilibrium rests upon the presence of many degrees of freedom $n_f \gg 1$ making it exponentially unlikely in n_f that the combined systems are found with component energies different from (E_1^*, E_2^*). By this construction, the equilibrium point has a larger number of accessible states than any other starting point (that is, $\mathcal{Q}_1(E_1^*)\mathcal{Q}_2(E_1^*) \geq \mathcal{Q}_1(E_1)\mathcal{Q}_2(E_2)$ for all possible E_1 and E_2). In the process of evolving to more likely states, there is an irreversible loss of information, accompanied by an increase in entropy,

$$\Delta S = S(E_1^*) + S(E_2^*) - (S(E_1) + S(E_2)) \geq 0, \tag{2.11}$$

which is another formulation of the second law of thermodynamics. The increase in entropy is,

$$\Delta S = \left(\left.\frac{\partial S}{\partial E}\right|_{\mathbf{x}} - \left.\frac{\partial S}{\partial E}\right|_{\mathbf{x}}\right)\Delta E_1 = \left(\frac{1}{T_1} - \frac{1}{T_2}\right)\Delta E_1 \geq 0, \tag{2.12}$$

that is, heat spontaneously flows from the hotter to the colder body, which is an equivalent formulation of the second law as we discussed before. Note that we used Δ to denote that we are (initially) not in equilibrium.

In order to make clear that the macrostate with the largest possible amount of microstates, is indeed by far the most likely one, consider an isolated system in the microcanonical ensemble with N oscillators and q units of energy. Such a system is often referred to as an *Einstein solid*. Since the system cannot exchange energy with the surroundings, the energy is conserved and the q energy units can be divided over N particles with equal probability (by assumption, see equation (2.6)). The number of microstates corresponding to given q and N is just the number of ways of choosing q out of $q+N-1$ degrees of freedom (where we subtract 1 since the total amount of energy is conserved) i.e.,

$$\mathcal{Q}(N,q) = \binom{q+N-1}{q}. \tag{2.13}$$

Now examine two such systems A and B which can exchange energy but not particles, as we did before, and take $n_A=300$, $n_B=200$, $q_{\text{total}}=100$. Figure 2.2

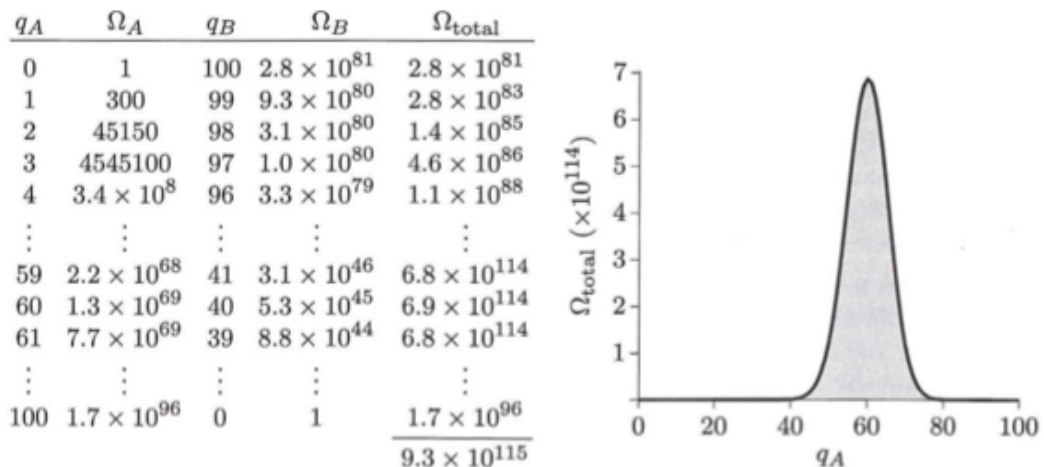| q_A	Ω_A	q_B	Ω_B	Ω_{total}
0	1	100	2.8×10^{81}	2.8×10^{81}
1	300	99	9.3×10^{80}	2.8×10^{83}
2	45150	98	3.1×10^{80}	1.4×10^{85}
3	4545100	97	1.0×10^{80}	4.6×10^{86}
4	3.4×10^{8}	96	3.3×10^{79}	1.1×10^{88}
$\vdots$	$\vdots$	$\vdots$	$\vdots$	$\vdots$
59	2.2×10^{68}	41	3.1×10^{46}	6.8×10^{114}
60	1.3×10^{69}	40	5.3×10^{45}	6.9×10^{114}
61	7.7×10^{69}	39	8.8×10^{44}	6.8×10^{114}
$\vdots$	$\vdots$	$\vdots$	$\vdots$	$\vdots$
100	1.7×10^{96}	0	1	1.7×10^{96}
				9.3×10^{115}

Figure 2.2: Macrostates and multiplicities of a system of tow Einstein solids, with 300 and 200 oscillators respectively, sharing a total of 100 units of energy.[37]

shows that the macrostate with sixty energy units in system A is 10^{33} times more likely than the least likely macrostate.

Although the probability of the most likely macrostate is only about 7%, the probability falls off very sharply as q_A differs from 60. The probability of finding q_A to be smaller than 30 or larger than 90 is less than one in a million, these are the 'tails' in figure 2.2. So apart from small fluctuations around q_A=60, the macrostate is known with high certainty; this is a *probabilistic* phenomenon, not absolutely certain, but extremely likely. Moreover, usually we examine systems with not just a few hundred of particles, but more like 10^{23}, which is the order of magnitude of Avogado's number defined as the number of elementary entities (molecules) per mole of substance. Generally, such a number is too large to work with and usually approximations are made, often based on the most likely macrostate.

Next consider a system in the canonical (N, V, T) ensemble where the energy in the system is not constant. It can be shown that the probability that the system is in a particular microstate i with energy level E_i is,

$$p_i = \mathcal{Z}^{-1}\mathrm{e}^{-\beta E_i} \quad \text{with} \quad \mathcal{Z} = \sum_i \mathrm{e}^{-\beta E_i}, \tag{2.14}$$

as normalization constant. This $\mathcal{Z}$ is also called the *partition function* and $\beta \equiv 1/k_B T$. The term 'exp$(-\beta E_i)$' is the relative probability of the energy states and it is known as the *Boltzmann factor*. Note that, unlike a microcanonical ensemble, energy is a random variable. We find an expression for the probability distribution $p(E)$ as a function of the energy by summing

over all microstates with a specific energy,

$$p(E) = \sum_i p_i \delta(E_i - E) = \mathcal{Z}^{-1} \mathrm{e}^{-\beta E} \sum_i \delta(E_i - E)$$
$$= \mathcal{Z}^{-1} \mathrm{e}^{-\beta E} \mathcal{Q}(E) = \mathcal{Z}^{-1} \mathrm{e}^{-\beta(E-TS)} = \mathcal{Z}^{-1} \mathrm{e}^{-\beta F(E)}, \qquad (2.15)$$

where we used respectively eq. (2.14), the definition of the number of microstates $\mathcal{Q}(E)$ with energy E and its relation to entropy eq. (2.5). Moreover, we set $F(E) = E - TS$ in anticipation of its relation to the *Helmholtz free energy*. Note that instead of summing over the microstates, it follows from equation (2.15) that the normalization constant $\mathcal{Z}$ can also be found by summing over the energy states,

$$\mathcal{Z} = \sum_i \mathrm{e}^{-\beta E_i} = \sum_E \mathrm{e}^{-\beta F(E)} \approx \mathrm{e}^{-\beta F(E^*)}, \qquad (2.16)$$

since the terms in equation (2.15) must add up to unity. In the last step of equation (2.16) we used that the probability $p(E)$ is sharply peaked at the most probable energy E^*, which is the minimum of $F(E)$ with respect to E. From the definition of $\mathcal{Z}$ in equation (2.14), the average internal energy U can be computed as,

$$U = \langle E \rangle = \sum_i E_i \frac{\mathrm{e}^{-\beta E_i}}{\mathcal{Z}} = -\frac{1}{\mathcal{Z}} \frac{\partial}{\partial \beta} \sum_i \mathrm{e}^{-\beta E_i} = -\frac{\partial \ln \mathcal{Z}}{\partial \beta}, \qquad (2.17)$$

where the last step follows from the chain rule. In fact, the nth cumulant (which determine the moments) of the energy, can be calculated from,

$$\langle E^n \rangle_c = (-1)^n \frac{\partial^n \ln \mathcal{Z}}{\partial \beta^n}. \qquad (2.18)$$

From this it can be shown that the relative variance of the energy falls of in the thermodynamic limit as $1/\sqrt{N}$ and we can rightfully define

$$F \equiv U - TS = -\beta^{-1} \ln \mathcal{Z} \quad \text{and} \quad F = \mathbf{J} \cdot \mathbf{x} + \sum_k \mu_k N_k, \qquad (2.19)$$

after putting in the expression for U from equation (2.7). The Helmholtz free energy F represents the useful work obtainable from a closed thermodynamic system at a constant temperature and volume and note that it is constructed to be minimal at equilibrium. This is not to be confused with the *Gibbs free energy* G, which represents the useful work obtainable from a closed thermodynamic system at a constant temperature and pressure in the (N, p, T)

ensemble. In this ensemble, a system is forced to be at constant pressure and the energy of the system including the work done against the external forces is $E-\mathbf{J}\cdot\mathbf{x}$. Then the microstates occur with (canonical) probabilities,

$$p_{i,\mathbf{x}} = Z^{-1}\mathrm{e}^{-\beta(E_i-\mathbf{J}\cdot\mathbf{x})} \quad \text{where} \quad Z = \sum_{i,\mathbf{x}}\mathrm{e}^{-\beta(E_i-\mathbf{J}\cdot\mathbf{x})}, \qquad (2.20)$$

is the normalization constant which is called the *Gibbs partition function*. Similarly to equation (2.15), we search for the probability density in terms of energy, now using the probability terms from equation (2.20),

$$\begin{aligned} p(E,\mathbf{x}) &= \sum_{i,\mathbf{x}} p_i\delta(E_i-E) = Z^{-1}\mathrm{e}^{-\beta(E-\mathbf{J}\cdot\mathbf{x})}\sum_i \delta(E_i-E) \\ &= Z^{-1}\mathrm{e}^{-\beta(E-\mathbf{J}\cdot\mathbf{x})}\mathcal{Q}(E) = Z^{-1}\mathrm{e}^{-\beta(E-\mathbf{J}\cdot\mathbf{x}-TS)} = Z^{-1}\mathrm{e}^{-\beta G(E)}, \end{aligned} \qquad (2.21)$$

where we used in the third step the definition of the number of microstates corresponding to a certain energy, in the fourth step the definition of entropy equation (2.5), and in the last step we defined the Gibbs free energy as,

$$G \equiv E - \mathbf{J}\cdot\mathbf{x} - TS = -\beta^{-1}\ln Z. \qquad (2.22)$$

This definition also follows naturally from the characteristic that the probability distribution is sharply peaked around the equilibrium $(E^*,\mathbf{x}^*)$ in the *thermodynamic limit* of $N\to\infty$, similar to equation (2.16), i.e.,

$$Z = \sum_{i,\mathbf{x}}\mathrm{e}^{-\beta(E_i-\mathbf{J}\cdot\mathbf{x})} = \sum_{E,\mathbf{x}}\mathrm{e}^{-\beta G(E,\mathbf{x})} \approx \mathrm{e}^{-\beta G(E^*,\mathbf{x}^*)}. \qquad (2.23)$$

Substituting $E^*=U$ from equation (2.7) into the definition of G, gives an expression in terms of the chemical work only,

$$G = TS - \mathbf{x}\cdot\mathbf{J} + \sum_k \mu_k N_k + \mathbf{x}\cdot\mathbf{J} - TS = \sum_k \mu_k N_k. \qquad (2.24)$$

In order to obtain thermodynamic relations of the derivatives of G, we need to find its differential form. It can easily be obtained from the fundamental thermodynamic relation, equation (2.7), and with for example only volume as external parameter and a single species it becomes,

$$\mathrm{d}G = -\mathbf{x}\cdot\mathrm{d}\mathbf{J} - S\mathrm{d}T + \sum_k \mu_k \mathrm{d}N_k \quad \text{e.g.} \quad \mathrm{d}G = V\mathrm{d}p - S\mathrm{d}T + \mu\mathrm{d}N. \quad (2.25)$$

Since a chemical reaction is *isobaric*, i.e. at constant pressure, and the *total* number of particles is conserved, the differences of the displacements and

particles is zero and the change in Gibbs free energy is in the Gibbs canonical ensemble directly related to entropy. This in combination with the second law of thermodynamics, tells us that a chemical reaction can only spontaneously take place if $-T\Delta S = \Delta G \leq 0$, with equality in equilibrium. Since the free energy is minimal in equilibrium, clearly the species with the lowest chemical potential will acquire all the particles (see equation (2.24)). Actually even the definition for chemical potential is often taken as,

$$\mu \equiv \left.\frac{\partial G}{\partial N}\right|_{T,\mathbf{J},\{N_{i\neq j}\}} = \left.\frac{\partial F}{\partial N}\right|_{T,\mathbf{x},\{N_{i\neq j}\}}. \tag{2.26}$$

Following a similar procedure at constant temperature and volume leads to a similar expression for the Helmholtz free energy, as shown on the right-hand side of the above equation. The introduced quantities follow most intuitively from their relation with entropy. Pressure is by definition the force exerted on an area, but in generalized coordinates can it can also be thought of as an energy density, since from equation (2.7) follows that,

$$p = \left.\frac{\partial U}{\partial V}\right|_{S,\{N_i\}} = T\left.\frac{\partial S}{\partial V}\right|_{U,\{N_i\}} = -\left.\frac{\partial F}{\partial V}\right|_{T,\{N_i\}}, \tag{2.27}$$

where we have used the definition of temperature equation (2.10) and the chain rule for the second equality. So if the derivative of entropy S w.r.t volume V is large, the system will gain entropy by expanding and this is what we mean by pressure. The constant of proportionality has units of temperature and we have already established before (in equation (2.10)) that bodies in thermal equilibrium have equal temperature. Other thermodynamic relations can be derived from the differentials of the internal energy U and the free energies G and F, such as shown on the right hand side of equation (2.27). Equating the second derivatives, leads for example to the thermodynamic Maxwell relations.

We have now encountered the intrinsic properties: temperature, pressure and chemical potential, and the definitions of them can all be motivated by the equilibrium state of a system with maximal entropy, see table 2.2. For any finite system, the canonical and microcanonical properties are distinct. However, in the thermodynamic limit of $N\to\infty$, the canonical energy probability is so sharply peaked around the average density that the ensemble actually becomes indistinguishable from the microcanonical ensemble at that energy.

In the grand canonical (μ, V, T) ensemble, a systems can exchange energy and particles with the reservoir/environment. It can be shown that the

Table 2.2: The three main intrinsic thermodynamic quantities, their relation to entropy and the kind of equilibrium which is achieved when constant.

Intrinsic quantity	Exchanged quantity	Type of interaction	Relation to entropy
Temperature	energy	thermal	$\frac{1}{T}=\frac{\partial S}{\partial U}\big|_{V,\{N_i\}}$
Pressure	volume	mechanical	$p=T\frac{\partial S}{\partial V}\big|_{U,\{N_i\}}$
Chemical potential	particles	diffusive	$\mu_i=-T\frac{\partial S}{\partial N_i}\big|_{U,\{N_{i\neq j}\}}$

probability that the system is in a particular microstate i with energy level E_i and N_r particles is given by,

$$p_i = \Xi^{-1}\mathrm{e}^{-\beta(E_i-\mu N)} \qquad \text{with normalization constant}$$

$$\Xi = \sum_{N,i} \mathrm{e}^{-\beta(E_i(N)-\mu N)} = \sum_{N=0}^{\infty} \mathrm{e}^{\beta\mu N}\mathcal{Z}_N = \sum_{N=0}^{\infty} \mathrm{e}^{-\beta(F(N)-\mu N)}, \qquad (2.28)$$

where $\mathcal{Z}_N$ is the partition function for N particles which we have encountered in the canonical ensemble, $F(N)$ is the Helmholtz free energy with N particles in the system from equation (2.19) and Ξ is the *grand partition function* which sums over all possible energy states for all possible number of particles (up to infinity). Equating Ξ to the largest probability term in the sum leads to the definition of the grand potential,

$$\Omega \equiv F-\mu N = -\beta^{-1}\ln\Xi \qquad (2.29)$$

which, after putting in the expressions for F and U, simplifies to $\Omega=\mathbf{J}\cdot\mathbf{x}$ (e.g. $\Omega=-pV$). When there is a liquid vapor interface, the surface area A of the interface is another external parameter, besides volume, and the surface tension γ is the corresponding generalized force. In this case the work done by the system is $\delta W = p\,\mathrm{d}V - \gamma\,\mathrm{d}A$ and for instance the grand potential becomes,

$$\Omega = -pV + \gamma A. \qquad (2.30)$$

The characteristics for the ensembles and the thermodynamic energies are once more summarized in table 2.3.

Now we have encountered enough statistical physics to introduce classical density functional theory (classical DFT), in which thermodynamic quantities are written as functionals of the equilibrium probability densities. Classical DFT has its roots in quantum mechanical density functional theory,

Table 2.3: Comparison of statistical ensembles with different suppressed variables.

Ensemble	Suppressed	Microscopic features	Macroscopic function
Microcan.	(N, V, E)	# microstates $\mathcal{Q}$	$S= \quad k_B \ln \mathcal{Q}$
Canonical	(N, V, T)	part. function $\mathcal{Z}$	$F = -\beta^{-1} \ln \mathcal{Z} = \mathbf{J} \cdot \mathbf{x} + \boldsymbol{\mu} \cdot \mathbf{N}$
Gibbs can.	(N, p, T)	Gibbs part. func. Z	$G = -\beta^{-1} \ln Z = \boldsymbol{\mu} \cdot \mathbf{N}$
Grand can.	(μ, V, T)	Grand part. func. Ξ	$\Omega = -\beta^{-1} \ln \Xi = \mathbf{J} \cdot \mathbf{x}$

in which the energy of an electronic system is expressed as a functional of the total electron density. Density functional theory thus provides a unified framework for both quantum mechanical and classical systems. We will use it to describe molecular fluids.

2.3 Classical Density Functional Theory

We will continue in the grand canonical (μ, V, T) ensemble. Statistical results for physical quantities can be obtained by summing over all possible configurations (i.e. microstates) in phase space. For classical systems one needs to integrate over the continuous spectrum of all possible values of particle position $\mathbf{r}_i$ and momentum $\mathbf{p}_i$ for all particles i, as opposed to quantum systems for which only a discrete set of states is possible. The integral over phase space can be written as an operator called the 'classical' trace, i.e,

$$\mathrm{Tr}_{\mathrm{cl}} = \sum_{N=0}^{\infty} \frac{1}{N! h^{3N}} \int \cdots \int \mathrm{d}\mathbf{r}_1 \ldots \mathrm{d}\mathbf{r}_N \mathrm{d}\mathbf{p}_1 \ldots \mathrm{d}\mathbf{p}_N. \qquad (2.31)$$

Here Planck's constant h is used since the coordinates in phase space cannot precisely be defined because of the uncertainty principle (and we need it in order to get a dimensionless number) and we sum over all possible amounts of particles present in the system, each term with $6N$ integrals. Because the particles are *indistinguishable* we need the factor of $1/N!$, otherwise we would over-count the number of microstates (interchanging two particles does not lead to another microstate). The spatial integrals run over the entire fixed volume and the magnitude of the momentum integrals runs all the way up to infinity. If there were more degrees of freedom, for example spin, then we would need to integrate over those as well. Configuration averages of any physical quantity written as an operator $\hat{O}$ can then be obtained from,

$$\langle \hat{O} \rangle = \mathrm{Tr}_{\mathrm{cl}} f_0 \hat{O}, \qquad (2.32)$$

17

where $f_0 := f_0(\mathbf{r}^N, \mathbf{p}^N; N)$ denotes the equilibrium probability density function which carries the information of all possible microstates (so $\mathbf{r}^N := \{\mathbf{r}_1, \dots \mathbf{r}_N\}$ etc.) for the equilibrium density (i.e., the macrostate) when there are N particles in the system. In the grand canonical ensemble f_0 is given by,

$$f_0 = \Xi^{-1} e^{-\beta(\mathcal{H}_N - \mu N)} \quad \text{with} \quad \Xi = \text{Tr}_{\text{cl}} e^{-\beta(\mathcal{H}_N - \mu N)} = \sum_{N=0}^{\infty} \mathcal{Z}_N e^{\beta \mu N}. \quad (2.33)$$

Here $\mathcal{H}_N$ is the Hamiltonian when there are N particles present, $\beta \equiv 1/k_B T$ with the Boltzmann constant k_B, Ξ is the grand partition function which normalizes f_0 and $\mathcal{Z}_N$ is the partition function when there are N particles in the system, just like equation (2.28) (cf. eq. (2.31)). A Hamiltonian is an operator representing the total energy of a system and it is in the most general form written as,

$$\mathcal{H}_N = \mathcal{K} + \mathcal{U} + \mathcal{V}. \quad (2.34)$$

On the right-hand side of this equation we respectively have the total kinetic energy $\mathcal{K}$, the total potential energy due to interactions between particles $\mathcal{U}$ and the total energy of the external forces acting on the system $\mathcal{V}$,

$$\mathcal{K} = \sum_{i=1}^{N} \frac{p_i^2}{2m}, \quad \mathcal{U} = \mathcal{U}_N(\mathbf{r}^N), \text{ and } \mathcal{V} = \sum_{i=1}^{N} V_{\text{ext}}(\mathbf{r}_i), \quad (2.35)$$

where m is the mass of the particles. An external force on the system can be anything which adds energy from outside of the system into the system, for instance a wall or an electric field.

Next, consider the functional,

$$\Omega[f] = \text{Tr}_{\text{cl}} f (\mathcal{H}_N - \mu N + \beta^{-1} \ln f), \quad (2.36)$$

where we have used the statistical way to write the entropy term (2.5) (i.e., in terms of the microscopic probability density function). The functional maps the function f to a scalar and it reduces to the grand potential for the equilibrium density f_0,

$$\begin{aligned} \Omega[f_0] &= \text{Tr}_{\text{cl}}(f_0 \cdot (\mathcal{H}_N - \mu N + \beta^{-1} \ln f_0)) \\ &= \Xi^{-1} \text{Tr}_{\text{cl}} \, e^{-\beta(\mathcal{H}_N - \mu N)} (\mathcal{H}_N - \mu N) \\ &\quad + \Xi^{-1} \beta^{-1} \text{Tr}_{\text{cl}} \, e^{-\beta(\mathcal{H}_N - \mu N)} (-\ln \Xi - \beta(\mathcal{H}_N - \mu N)) \\ &= -\beta^{-1} \ln \Xi \equiv \Omega, \end{aligned} \quad (2.37)$$

where we substituted f_0 from (2.33) on the second line. Moreover, the equilibrium probability density function f_0 uniquely minimizes the functional,

$$\Omega[f_0] < \Omega[f] \quad \text{for any} \quad f \neq f_0, \quad (2.38)$$

since for all possible probability densities (i.e., the normalized ones with $\mathrm{Tr}_{\mathrm{cl}} f = 1$) we have,

$$\begin{aligned}
\Omega[f] &= \mathrm{Tr}_{\mathrm{cl}} f \cdot (\mathcal{H}_{\mathrm{N}} - \mu N) + \beta^{-1} \mathrm{Tr}_{\mathrm{cl}} f \ln f \\
&= \mathrm{Tr}_{\mathrm{cl}} f \cdot (\mathcal{H}_{\mathrm{N}} - \mu N) - \beta^{-1} (\ln \Xi - \mathrm{Tr}_{\mathrm{cl}} f \ln \Xi) + \beta^{-1} \mathrm{Tr}_{\mathrm{cl}} f \ln f \\
&= -\beta^{-1} \ln \Xi - \beta^{-1} \mathrm{Tr}_{\mathrm{cl}} f \cdot (\ln \Xi - \beta(\mathcal{H}_{\mathrm{N}} - \mu N)) + \beta^{-1} \mathrm{Tr}_{\mathrm{cl}} f \ln f \\
&= -\beta^{-1} (\ln \Xi + \mathrm{Tr}_{\mathrm{cl}} f \ln f_0) + \beta^{-1} \mathrm{Tr}_{\mathrm{cl}} f \ln f \\
&= \Omega[f_0] + \beta^{-1} (\mathrm{Tr}_{\mathrm{cl}} f \ln f - \mathrm{Tr}_{\mathrm{cl}} f \ln f_0).
\end{aligned}$$

The second term on the second line is zero since Ξ is a scalar and f is normalized and the last term on the last line is strictly positive if $f \neq f_0$ by Gibbs' inequality ($\sum f \ln f > \sum f \ln g$, for $f \neq g$). What this means is simply that any state other than the equilibrium state has lower entropy, which has to be the case by the second law of thermodynamics (2.11).

Next, suppose there exists another potential corresponding to the same equilibrium density $\rho_0(\mathbf{r})$. Let this potential $V'_{\mathrm{ext}}(\mathbf{r})$ correspond to the Hamiltonian $H'_N = K + U + \mathcal{V}'$. The corresponding equilibrium probability density f'_0 and the grand potential Ω' refer to the original temperature and chemical potential. Even if the two external potentials differ by only a constant, the grand canonical probability densities are different, i.e., $f'_0 \neq f_0$. We get

$$\begin{aligned}
\Omega' &= \mathrm{Tr}_{\mathrm{cl}} f'_0 (H'_{\mathrm{N}} - \mu N + \beta^{-1} \ln f'_0) \\
&< \mathrm{Tr}_{\mathrm{cl}} f_0 (H'_{\mathrm{N}} - \mu N + \beta^{-1} \ln f_0) \\
&= \Omega + \mathrm{Tr}_{\mathrm{cl}} f_0 (\mathcal{V}' - \mathcal{V}) \\
&= \Omega + \int \mathrm{d}\mathbf{r} \rho_0(\mathbf{r}) (V'_{\mathrm{ext}}(\mathbf{r}) - V_{\mathrm{ext}}(\mathbf{r})), \qquad (2.39)
\end{aligned}$$

because of equation (2.38) and since f_0 gives rise to $\rho_0(\mathbf{r})$. This reasoning remains valid when primed and unprimed quantities are interchanged, giving:

$$\Omega < \Omega' + \int \mathrm{d}\mathbf{r} \rho_0(\mathbf{r}) (V_{\mathrm{ext}}(\mathbf{r}) - V'_{\mathrm{ext}}(\mathbf{r})). \qquad (2.40)$$

Adding equations (2.39) and (2.40) gives the contradiction:

$$\Omega + \Omega' < \Omega + \Omega'.$$

Consequently there is a unique $V_{\mathrm{ext}}(\mathbf{r})$ which will determine a given equilibrium density, i.e., $V_{\mathrm{ext}}(\mathbf{r})$ is uniquely determined by $\rho_0(\mathbf{r})$. The resulting $V_{\mathrm{ext}}(\mathbf{r})$ then determines f_0, thus it follows that f_0 is a unique functional of $\rho_0(\mathbf{r})$.

Comparing equation (2.36) with equation (2.29) motivates to write another functional which is related to the Helmholtz free energy as,

$$\mathcal{F}[\rho] = \mathrm{Tr}_{\mathrm{cl}} f(\mathcal{K} + \mathcal{U} + \beta^{-1}\mathrm{ln}f), \tag{2.41}$$

where we have excluded the external potential $\mathcal{V}$ contribution to the energy and ρ is an average spatial density corresponding to a certain distribution f. The average equilibrium density $\rho_0(\mathbf{r})$ is given by,

$$\rho_0(\mathbf{r}) = \langle \hat{\rho}(\mathbf{r}) \rangle \quad \text{where} \quad \hat{\rho}(\mathbf{r}) = \sum_{i=1}^{N} \delta(\mathbf{r} - \mathbf{r}_i), \tag{2.42}$$

and the configuration average of any operator $\hat{O}$ is defined as in equation (2.32). For a given external potential V_{ext}, the equilibrium density ρ_0 is a unique functional of the equilibrium probability density f_0, which makes $\mathcal{F}$ a unique functional of the density ρ. Besides that, similarly to the derivation of equation (2.37), the functional $\mathcal{F}$ in equation (2.41) can be shown to be equivalent to the 'intrinsic' Helmholtz free energy,

$$
\begin{aligned}
\mathcal{F}[\rho_0] &= \mathrm{Tr}_{\mathrm{cl}}(f_0 \cdot (\mathcal{K} + \mathcal{U} + \beta^{-1}\mathrm{ln}f_0)) \\
&= \Xi^{-1}\mathrm{Tr}_{\mathrm{cl}}\, e^{-\beta(\mathcal{H}_{\mathrm{N}} - \mu N)}(\mathcal{K} + \mathcal{U}) \\
&\quad + \Xi^{-1}\beta^{-1}\mathrm{Tr}_{\mathrm{cl}}\, e^{-\beta(H_{\mathrm{N}} - \mu N)}(-\mathrm{ln}\Xi - \beta(\mathcal{H}_{\mathrm{N}} - \mu N)) \\
&= \mathrm{Tr}_{\mathrm{cl}}(f_0 \cdot (\mathcal{K} + \mathcal{U} - \mathcal{H}_N + \mu N - \beta^{-1}\mathrm{ln}\Xi)) \\
&= \mathrm{Tr}_{\mathrm{cl}}(f_0 \cdot (-\mathcal{V} + \mu N + \Omega)) \\
&= F - \int \rho_0(\mathbf{r}) V_{\mathrm{ext}}(\mathbf{r}) \mathrm{d}\mathbf{r},
\end{aligned}
\tag{2.43}
$$

where in the fourth step we put in the Hamiltonian $\mathcal{H}_N$ equation (2.34) and in the last step we used the definition of the grand potential ($\Omega \equiv F - \mu N$) and integrated out the degrees of freedom other than the spatial ones for the external potential V_{ext}. So by the intrinsic Helmholtz free energy $\mathcal{F}$ is meant the free energy which does not arise from external forces. Obviously,

$$
\begin{aligned}
\Omega[f] &= \mathrm{Tr}_{\mathrm{cl}} f \cdot (\mathcal{H}_N - \mu N + \beta^{-1}\mathrm{ln}f) \\
&= \mathrm{Tr}_{\mathrm{cl}} f \cdot (\mathcal{K} + \mathcal{U} + \beta^{-1}\mathrm{ln}f + \mathcal{V} - \mu N) \\
&= \mathcal{F}[\rho] + \int \rho(\mathbf{r})(V_{\mathrm{ext}}(\mathbf{r}) - \mu)\mathrm{d}\mathbf{r} = \Omega_V[\rho],
\end{aligned}
\tag{2.44}
$$

where naturally the integral of the number density $\rho(\mathbf{r})$ over the whole volume results in the number of particles in the system N. We have now shown that for a given external potential we can express the functional which results in

the grand potential Ω for the equilibrium density f_0, as a functional $\Omega_V[\rho]$ of the density in terms of an intrinsic free energy functional and an external potential term. Since the equilibrium probability density f_0 minimizes Ω, the equilibrium density ρ_0 minimizes Ω_V. We can summarize this important result as,

$$\left.\frac{\delta\Omega_V[\rho]}{\delta\rho}\right|_{\rho_0} = 0 \quad\text{and}\quad \Omega_V[\rho] = \Omega. \tag{2.45}$$

Taking a functional derivative of expression (2.44) gives us an expression for the chemical potential,

$$\mu = \left.\frac{\delta\mathcal{F}[\rho]}{\delta\rho}\right|_{\rho_0} + V_{\text{ext}}(\mathbf{r}). \tag{2.46}$$

The functional derivative of an arbitrary functional $F[u]$ can be defined as

$$\delta F = F[u+\delta u] - F[u] = \int \frac{\delta F}{\delta u(x)}\delta u(x)\mathrm{d}x. \tag{2.47}$$

More about functional derivatives can be read in section 4.2 of [5]. Equation (2.46) is the fundamental equation in the theory of non-uniform fluids. Given some means of determining $\mathcal{F}[\rho]$, this is an explicit equation for the equilibrium density. As a result of the classical approximation, the contribution to thermodynamic properties that arise from thermal motion can be separated from those due to interactions between particles. This important simplification can be shown as follows. When there are N particles in the system we have for the partition function (with $\mathbf{r}^N:=\{\mathbf{r}_1,\ldots,\mathbf{r}_N\}$ etc.),

$$\begin{aligned}
\mathcal{Z}_N &= \frac{1}{N!h^{3N}}\int \mathrm{e}^{-\beta\sum_{i=1}^N p_i^2/2m}\mathrm{e}^{-\beta U_N(\mathbf{r}^N)}\mathrm{d}\mathbf{r}^N\mathrm{d}\mathbf{p}^N \\
&= \frac{V^N}{N!}\left(\frac{2\pi mk_BT}{h^2}\right)^{3N/2}\int \frac{\mathrm{d}\mathbf{r}^N}{V^N}\mathrm{e}^{-\beta U_N(\mathbf{r}^N)} \\
&= \mathcal{Z}_{\text{ideal}}\mathcal{Z}_c,
\end{aligned} \tag{2.48}$$

where the term before the integral on the second line is the partition function of an ideal system $\mathcal{Z}_{\text{ideal}}$ with no interactions ($U{=}0$) and the integral itself is a *configuration integral* (because it involves an integral over all configurations, or positions, of the particles) and will be written as $\mathcal{Z}_c$. This means that the momenta $\mathbf{p}_i$ are uncorrelated with positions $\mathbf{r}_i$ (and orientations ω_i). Note that, since the external potential is accounted for in a different term (see equation (2.44)), they are *intrinsic* partition functions. From the multiplicative form of the partition function terms, we find that the intrinsic Helmholtz

free energy is additive in terms of the ideal and excess contribution to the intrinsic partition function,

$$\mathcal{F}[\rho] = -\beta^{-1}\ln\mathcal{Z}_{\text{ideal}} - \beta^{-1}\ln\mathcal{Z}_{\text{c}}. \qquad (2.49)$$

The ideal part of the intrinsic free energy can from (2.48) shown to be,

$$\beta\mathcal{F}_{\text{ideal}}[\rho] = \int \rho(\mathbf{r})(\ln(\Lambda^3\rho(\mathbf{r})) - 1)\mathrm{d}\mathbf{r}, \qquad (2.50)$$

where we defined the thermal wavelength $\Lambda \equiv \sqrt{h^2/2\pi k_B T m}$, used the spatial varying averaged number density $\rho_0(\mathbf{r})$ and Stirling's approximation ($\ln n! = n\ln n - n$). From this we cannot proceed until we assume an explicit formula for the interactions. For a *pairwise* inter-molecular potential $\phi(\mathbf{r}, \mathbf{r}')$ we can write the grand partition function as,

$$\Xi = \sum_{N=0}^{\infty} \frac{1}{N!\Lambda^N} \int \mathrm{d}\mathbf{r}^N \exp\left(\beta\int\mathrm{d}\mathbf{r}u(\mathbf{r})\hat{\rho}(\mathbf{r}) - \frac{\beta}{2}\int\mathrm{d}\mathbf{r}\mathrm{d}\mathbf{r}'\hat{I}(\mathbf{r},\mathbf{r}')\phi(\mathbf{r},\mathbf{r}')\right), \quad (2.51)$$

where we defined,

$$u(\mathbf{r}) \equiv \mu - V_{\text{ext}}(\mathbf{r}), \qquad \hat{I}(\mathbf{r},\mathbf{r}') \equiv \sum_{i\neq j}\delta(\mathbf{r}-\mathbf{r}_i)\delta(\mathbf{r}-\mathbf{r}_j)$$

$$\text{and used} \qquad U(\mathbf{r}^N) = \frac{1}{2}\sum_{i\neq j}\phi(\mathbf{r}_i,\mathbf{r}_j) = \sum_{i<j}\phi(\mathbf{r}_i,\mathbf{r}_j), \qquad (2.52)$$

where the factor $^1/_2$ in the last expression is there to avoid double counting of the interactions. From this we find that,

$$\frac{\delta\Omega_V[\rho_0]}{\delta\phi(\mathbf{r},\mathbf{r}')} = \frac{\delta\Omega}{\delta\phi(\mathbf{r},\mathbf{r}')} = \frac{-1}{\beta}\frac{\delta\ln\Xi}{\delta\phi(\mathbf{r},\mathbf{r}')} = \frac{\langle\hat{I}(\mathbf{r},\mathbf{r}')\rangle}{2} \equiv \frac{\rho^{(2)}(\mathbf{r},\mathbf{r}')}{2} = \frac{\delta\mathcal{F}[\rho_0]}{\delta\phi(\mathbf{r},\mathbf{r}')}, \quad (2.53)$$

where we used for the last equality that Ω only depends on the interaction potential through $\mathcal{F}$. In this expression, $\rho^{(2)}(\mathbf{r},\mathbf{r}')$ is the pairwise distribution function for a system of density $\rho_0(\mathbf{r})$. It is a measure for the correlations of particles located at $\mathbf{r}$ and $\mathbf{r}'$ respectively and practically this is difficult to obtain and more approximations are necessary. Next we will evaluate a general approximation for state properties of interacting particles in terms of pairwise interaction terms.

2.4 Interacting Particles

Many physical systems are non ideal. Interactions between particles give rise to interesting phenomena, such as thermodynamic instability, metastability, phase transition and phase separation. The virial expansion is the simplest and most general theory addressing these effects. The standard way of calculating interactions is to find a reference state which is not very different from the real system, after which a perturbation theory around this state can be used to get a better approximation (of course, this approach is doomed to fail if the interactions are too strong or the density too high). The virial expansion is such a perturbation theory. It is used when the interactions are dominated by two-body interactions, whereas many-body ones are rare. The virial expansion is thus suited for modeling real gases, but not for saturated liquid. Our results will be compared with molecular dynamic (MD) simulations in which the movement of particles is simulated by numerically solving the Newton's equations of motion for a system of pair-interacting particles. Therefore we will still use the virial expansion to describe liquids in our field approximation, since the pairwise interacting approach is also used in our benchmark solution.

We will assume not only that the particles interact only in pairs, but also that the interactions are short ranged, i.e., $\lim |\mathbf{r}_i - \mathbf{r}_j|^3 \phi_{ij} = 0$ as $|\mathbf{r}_i - \mathbf{r}_j| \to \infty$, where $\phi(\mathbf{r}_i, \mathbf{r}_j) \equiv \phi_{ij}$. Therefore the Boltzmann factor will be close to 1 and instead we will work with the *deviation* of each Boltzmann factor from 1, by writing,

$$\mathrm{e}^{-\beta u_{ij}} \equiv 1 + f_{ij}. \tag{2.54}$$

Here f_{ij} is called the *Mayer f-function*. In this notation we can write the configuration integral as,

$$
\begin{aligned}
\mathcal{Z}_c &= \frac{1}{V^N} \int \mathrm{d}\mathbf{r}_1 \ldots \mathrm{d}\mathbf{r}_N \prod_{i<j} \mathrm{e}^{-\beta u_{ij}} \\
&= \frac{1}{V^N} \int \mathrm{d}\mathbf{r}_1 \ldots \mathrm{d}\mathbf{r}_N \left(1 + \sum_{i<j} f_{ij} + \sum_{i<j,k<l} f_{ij} f_{kl} + \ldots \right),
\end{aligned}
\tag{2.55}
$$

where on the last line we put in equation (2.54) worked out the brackets. Since it doesn't matter which particles are labeled which number, all the terms in a sum are equal. Thus each term between the large brackets can be represented by products of connected diagrams, for instance three such

terms are,

$$\bullet - \bullet = \frac{1}{2}\frac{N(N{-}1)}{V^2}\int d\mathbf{r}_1 d\mathbf{r}_2 f_{12}$$

$$\bullet - \bullet - \bullet = \frac{1}{2}\frac{N(N{-}1)(N{-}2)}{V^3}\int d\mathbf{r}_1 d\mathbf{r}_2 d\mathbf{r}_3 f_{12}f_{23} \qquad (2.56)$$

$$\bullet - \bullet \quad + \quad \bullet - \bullet = \frac{1}{8}\frac{N(N{-}1)(N{-}2)(N{-}3)}{V^4}\int d\mathbf{r}_1 d\mathbf{r}_2 d\mathbf{r}_3 d\mathbf{r}_4 f_{12}f_{34}.$$

Two particles i and j are connected if the term contains f_{ij} or if both of them are connected to another particle k. Terms in the expansion belonging to different connected diagrams are separable, and the variables within a connected diagram are not separable. Therefore we need just to consider the integration of the connected terms, also called *linked clusters*. The value of each complete graph is the product of the contributions from its linked clusters. An example of a graph with independent linked clusters is,

$$\left(\int d\mathbf{r}_1\right)\left(\int d\mathbf{r}_2 d\mathbf{r}_3 f_{23}\right)\left(\int d\mathbf{r}_4 d\mathbf{r}_5 d\mathbf{r}_6 f_{45} f_{56}\right)\cdots\left(\int d\mathbf{r}_N\right). \qquad (2.57)$$

Since the interaction potential is short-ranged, f_{ij} decays quickly with the relative distance between the two particles and is invariant with translation of the center-of-mass coordinate. Therefore we can change variables such that there is always one independent parameter which can be integrated out to become V. Integration over the other coordinates yield a constant independent of the volume of the system and therefore all connected terms are proportional to the volume of the system regardless of how many coordinates are included in the connected diagram. This motivates us to define a quantity b_l equal to the sum over all l-particle linked clusters, independent of the coordinates and the volume,

$$b_l \equiv \frac{1}{V}\frac{1}{l!}\int d\mathbf{r}_1 d\mathbf{r}_2 \ldots d\mathbf{r}_l f_{1,2,\ldots,l} = \frac{1}{l!}\int d\mathbf{r}_2 d\mathbf{r}_3 \ldots d\mathbf{r}_l f_{1,2,\ldots,l}, \qquad (2.58)$$

where the connected terms involving the same group of coordinates are concisely written as $f_{1,2,\ldots,l}$. For instance,

$$f_{1,2,3} \equiv f_{12}f_{23} + f_{23}f_{31} + f_{31}f_{12} + f_{12}f_{23}f_{31} = 3f_{12}f_{23} + f_{12}f_{23}f_{31}. \qquad (2.59)$$

A given N-particle graph can be decomposed into n_1 1-clusters, n_2 2-clusters, $\ldots$, n_{l-1} $l{-}1$-clusters and n_l l-clusters. In order to find an expression for the grand partition function we need to sum over all possible clusters. The number of possible clusters $W(\{n_l\})$, i.e., the number of ways of grouping

the labels $1, \ldots, N$ into bins of n_l l-clusters, is equal to the total number of permutations, $N!$, divided by the number of equivalent assignments. Within each bin of ln_l particles, equivalent assignments are obtained by (i) permuting the l labels in each subgroup in $l!$ ways, for a total of $(l!)^{n_l}$ permutations; and (ii) the $n_l!$ arrangements of the n_l subgroups. Hence,

$$W(\{n_l\}) = \frac{N!}{\displaystyle\prod_{l=1}^{N} n_l!(l!)^{n_l}} = \frac{N!}{n_1!(1!)^{n_1} n_2!(2!)^{n_2} n_3!(3!)^{n_3} \cdot \ldots \cdot n_N!(N!)^{n_N}}. \quad (2.60)$$

Now we can write the *total* partition function from equation (2.48) as,

$$\mathcal{Z}_N = \frac{1}{N!\Lambda^{3N}} \sum_{n_1+2n_2+\ldots+Nn_n=N} \frac{N!}{\displaystyle\prod_{k=1}^{N} n_k!(k!)^{n_k}} \prod_{l=1}^{N} V^{n_l} b_l^{n_l}. \quad (2.61)$$

The restriction in the sum (next denoted as $\{n_l\}$) can for the grand partition function be removed by noting that we can sum over the number of l n_l-clusters instead of over the total number of particles N (i.e., $\sum_{N=0}^{\infty} \sum_{\{n_l\}} \delta_{\sum_l ln_l, N} = \sum_{\{n_l\}}$), showing here,

$$\Xi = \sum_{N=0}^{\infty} e^{\beta\mu N} \mathcal{Z}_N = \sum_{\{n_l\}} \left(\frac{e^{\beta\mu}}{\Lambda^3}\right)^{\sum_l ln_l} \prod_{l=1}^{N} \frac{V^{n_l} b_l^{n_l}}{n_l!(l!)^{n_l}} = \sum_{\{n_l\}} \prod_{l=1}^{N} \frac{1}{n_l!} \left(\frac{e^{\beta\mu l} V b_l}{\Lambda^{3l} l!}\right)^{n_l}. \quad (2.62)$$

Changing summations (all of the l bins can contain up to N particles) and products leads to,

$$\begin{aligned}
\Xi &= \prod_{l=1}^{N} \sum_{n_l=0}^{\infty} \frac{1}{n_l!} \left[\left(\frac{e^{\beta\mu}}{\Lambda^3}\right)^l \frac{V b_l}{l!}\right]^{n_l} = \prod_{l=1}^{N} \exp\left[\left(\frac{e^{\beta\mu}}{\Lambda^3}\right)^l \frac{V b_l}{l!}\right] \\
&= \exp\left[\sum_{l=1}^{\infty} \left(\frac{e^{\beta\mu}}{\Lambda^3}\right)^l \frac{V b_l}{l!}\right].
\end{aligned} \quad (2.63)$$

The above result means that the sum over all graphs, connected or not, equals the exponent of the sum over the *connected* clusters. The grand potential follows from this,

$$\ln\Xi = -\beta\Omega = \frac{pV}{kT} = \sum_{l=1}^{\infty} \left(\frac{e^{\beta\mu}}{\Lambda^3}\right)^l \frac{V b_l}{l!}. \quad (2.64)$$

We want an expansion in terms of particle density $\rho = N/V$ and we want to eliminate $x \equiv e^{\beta\mu}/\Lambda^3$. This can be done by using the following thermodynamic

relation,

$$N = \frac{\partial \Omega}{\partial \mu} = \sum_{l=1}^{\infty} l \left(\frac{x^l}{l!} \right)^l V b_l. \qquad (2.65)$$

Since we know that $b_1=1$, we can recursively rewrite $N/V=\rho=x+b_2x^2+b_3x^3/2!$ $+\ldots$, to obtain an expression for x in terms of ρ and b_l. This results after some steps in an expansion in powers of ρ. The result is called the *virial expansion*,

$$\beta p = \rho - \frac{b_2}{2}\rho^2 + \left(b_2^2 - \frac{b_3}{3} \right)\rho^3 + \mathcal{O}(\rho^4) = \rho + \sum_{l=2}^{\infty} B_l(T)\rho^l, \qquad (2.66)$$

where we defined the temperature dependent virial coefficients $B_l(T)$. The first term yields the ideal gas result. After putting in the terms b_l in the coefficients B_l, one will find that only the one-particle irreducible clusters remain, i.e. the ones in which all l dots are connected to each other, for instance,

$$B_3 = b_2^2 - \frac{b_3}{3} = \left[\int \mathrm{d}\mathbf{r}_{12}f_{12}(\mathbf{r}_{12}) \right]^2 - \frac{1}{3}\left[3\int \mathrm{d}\mathbf{r}_{12}\mathrm{d}\mathbf{r}_{13}f_{12}(\mathbf{r}_{12})f_{13}(\mathbf{r}_{13}) \right.$$

$$\left. + \int \mathrm{d}\mathbf{r}_{12}\mathrm{d}\mathbf{r}_{13}f_{12}(\mathbf{r}_{12})f_{13}(\mathbf{r}_{13})f_{13}(\mathbf{r}_{23}) \right] \qquad (2.67)$$

$$= -\frac{1}{3}\int \mathrm{d}\mathbf{r}_{12}\mathrm{d}\mathbf{r}_{13}f_{12}(\mathbf{r}_{12})f_{13}(\mathbf{r}_{13})f_{13}(\mathbf{r}_{23}).$$

Generally $B_l(T)=-(l-1)d_l/l!$, where d_l is the sum over all one-particle irreducible clusters of l points. From the expression for pressure p we can obtain an expression for the free energy via thermodynamic relations.

$$-p = \frac{\partial F}{\partial V} \rightarrow F = F_{\mathrm{ideal}} + N\beta^{-1}\sum_{l=2}^{\infty} B_l(T)\frac{\rho^{l-1}}{l-1} \qquad (2.68)$$

The over-ideal contributions give rise to interesting behavior such as phase transitions. In the next section we will discuss liquid-gas systems and consider a typical mathematical model.

2.5 Phase Transitions

The transition from one state to another can be a first or a second order phase transition. For liquid vapor transitions, the latter occurs above a critical temperature and a system changes gradually from a liquid- like behavior
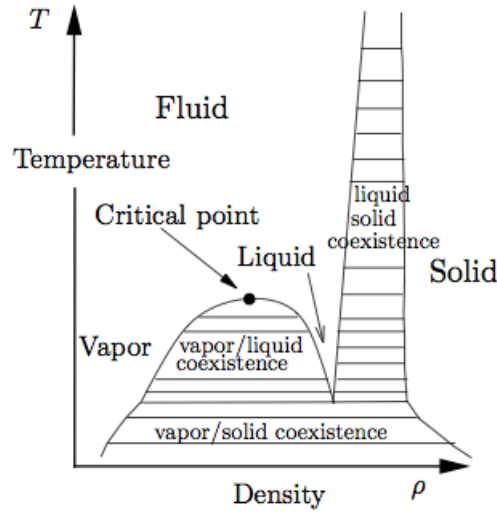
Figure 2.3: A sketch of a typical temperature−density (T, ρ) diagram, illustrating coexistence phases.[38]

to a gas-type behavior or vice versa. Below the critical temperature, a liquid and vapor state can coexist and a phase transition from one pure state to another requires latent heat to be overcome or released. We will study the region where this can occur, the so-called liquid-vapor coexistence region. In figure 2.3 a typical coexistence diagram is shown. The transitions involving latent heat can equivalently be characterized by a discontinuity of the first derivatives of the free energy with respect to temperature or pressure, hence also called first order phase transitions. The continuous phase transitions have continuous first derivatives of free energy, but discontinuous second derivatives, hence the name second order phase transitions. The free energy itself is always continuous.

The free energy is the amount of work that a thermodynamic system can perform. The Gibbs free energy G is the energy that can be converted into work at a uniform temperature and pressure throughout a system. For G the following thermodynamic relations hold,

$$\left.\frac{\partial G}{\partial T}\right|_p = -S \quad \text{and} \quad \left.\frac{\partial G}{\partial p}\right|_T = V, \tag{2.69}$$

where T is temperature, S is entropy, p is pressure and V is volume. So both of the above relations are discontinuous at a first order phase transition as sketched in figure 2.4. The discontinuity of the first expresses the latent heat $Q = T_{\text{trs}}\Delta S$ needed to be overcome or released in a transition from a liquid
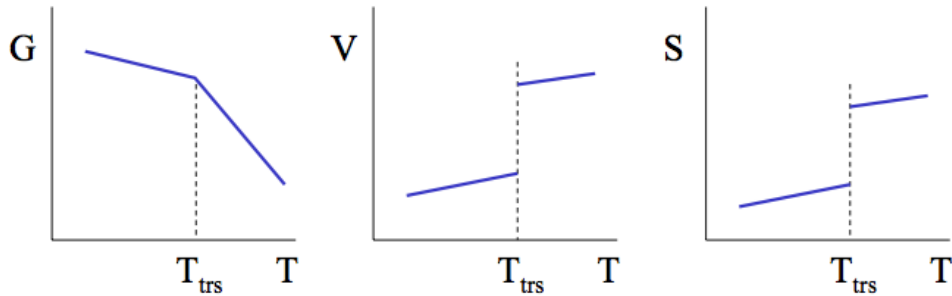
27

Figure 2.4: A sketch of the behavior of the Gibbs free energy G, the volume of the system V and the entropy of the system S as a function of temperature with transition temperature T_{trs} at a first order phase transition.[39]

state to a vapor state or vice versa. The second expresses the discontinuity in density of the pure liquid and vapor states.

In order to show that the discontinuities arise from a minimization of the free energy, we will examine a specific mathematical model. For liquid-vapor systems, the most famous model is the *Van der Waals equation*,

$$\left(P + \frac{aN^2}{V^2}\right)(V - Nb) = Nk_BT, \tag{2.70}$$

and although its simple form, it predicts *all* of the qualitative properties of real fluids (liquid-vapor phase transition, general shape of the boundary phase curve and the critical point). The equation makes two modifications to the ideal gas law: adding aN^2/V^2 to P and subtracting Nb from V. The second modification means that we cannot compress a fluid all the way to zero volume; it is limited to a value of Nb. The first modification takes the short ranged attractive forces into account. The potential energy around a particle is for an isotropic fluid proportional to the density of particles N/V. The *total* potential energy associated with the interactions of *all* molecules must then be proportional to N^2/V. The contribution to the pressure follows from differentiating this to volume ($dU=-PdV$). This model shows no good quantitative results, since for instance a gas becomes inhomogeneous on microscopic scale as it becomes more dense and clusters of molecules begin to form. Some pressure curves for a constant temperature as a function of volume are shown in figure 2.5. The strange local minima for some of the isotherms, which would indicate a region where decreasing the volume would lead to a decrease in pressure, is discussed next.

In order to explain phase separation, we consider the Gibbs free energy G which determines the equilibrium state at a given temperature and pressure.
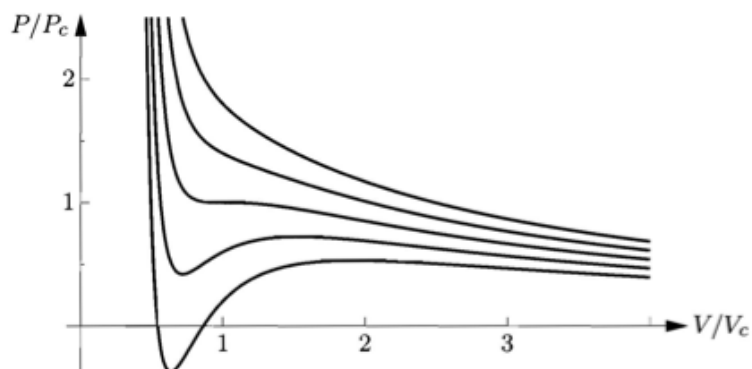
Figure 2.5: Isotherms for a Van der Waals fluid. From bottom to top, the lines are 0.8, 0.9, 1.0, 1.1 and 1.2 times T_c, the temperature at the critical point. The axes are labeled in units of the critical pressure and volume.[37]

We can find the Gibbs free energy from the Helmholtz free energy, which can in turn be obtained by integrating the pressure over volume (see equation (2.27)),

$$G = F + pV = -\int p\mathrm{d}V + pV \qquad \text{leading with eq. (2.70) to,}$$

$$G = -Nk_BT\ln(V-Nb) + \frac{Nk_BTV}{V-Nb} - \frac{2aN^2}{V}, \tag{2.71}$$

where we omitted an integration constant, which is unimportant for the purpose of a qualitative picture. Figure 2.6 shows an example of a free energy curve as a function of pressure, for a temperature whose isotherm is shown also. Although the Van der Waals equation associates some pressures with more than one volume, the thermodynamic stable state is the one with the lowest Gibbs free energy. This means that the triangular loop in the graph of G (points 2-3-4-5-6) correspond to unstable states. In fact, the states at 3-2 or 6-5 are metastable (stable for small perturbations) since $\partial P/\partial V < 0$ (a mechanical stability condition); this means that increasing the volume along the curves does still lower the free energy, although there is a state with less free energy. Eventually, however, a large fluctuation will occur and the system will make a transition to the true equilibrium state. As the pressure is gradually increased, the system will go straight from point 2 to point 6, with an abrupt decrease in volume: a phase transformation.

At point 2 we call the fluid a gas, because its volume decreases rapidly with increasing pressure. At point 6 the fluid is a liquid, because its volume decreases only slightly under a large increase in pressure. At intermediate volumes between these points, the thermodynamic stable state is actually a
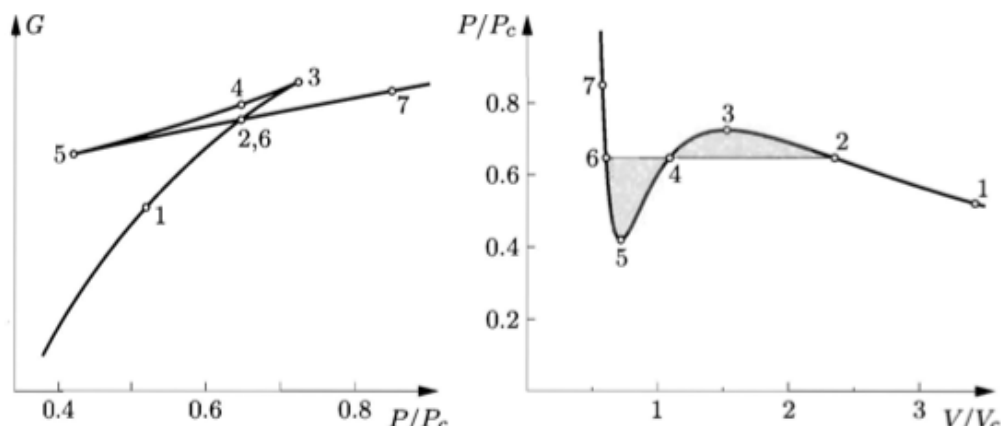
29

Figure 2.6: Gibbs free energy as a function of pressure for a Van der Waals fluid at $T=0.9T_c$. The corresponding isotherm is shown at the right. States in the range 2-3-4-5-6 are unstable.[37]

combination of gas and liquid, still at the transition pressure, as indicated by the straight horizontal line in the $P-V$ diagram. The curved parts of the isotherm that are cut off by this straight line correctly indicates what the allowed states *would* be if the fluid was in a pure phase, but these states are unstable since there is always another state (a liquid-vapor mixture) at the same pressure with lower free energy.

An interesting side remark is that the two shaded areas in the $P-V$ plane have the same area. This is the case, since traversing the $G-P$ diagram along the loop 2-3-4-5-6 leads to a net change in G of exactly zero,

$$0 = \int_{\text{loop}} \mathrm{d}G = \int_{\text{loop}} \left.\frac{\partial G}{\partial P}\right|_T \mathrm{d}P = \int_{\text{loop}} V \mathrm{d}P. \tag{2.72}$$

For higher temperatures there is no first order phase transformation involving discontinuous first derivatives in G as the isotherms have no local maxima or minima anymore. This happens for temperatures above a critical value and there are second order phase transitions, where the second derivatives of G are discontinuous. From figure 2.5 it can be seen that this is a unique value and both the first and second derivatives of P with respect to V are zero (it is not only a stationary point but also an inflection point, hence a saddle point). It can be shown that $V_c=3Nb$, $P_c=a/27b^2$ and $k_BT_c=8a/27b$. In terms of reduced units (i.e., T/T_c, P/P_c and V/V_c) the constants a and b disappear.

Now having seen the importance of the description of the free energy, we will try to find an appropriate description for the over-ideal part using a theory called fundamental measure theory.

2.6 Fundamental Measure Theory

In order to describe any over-ideal contribution to a thermodynamic quantity requires information about the long ranged (spatially varying) correlations $\rho^2(\mathbf{r}, \mathbf{r}')$ between the particles as in equation (2.53). Fundamental measure theory (FMT) can provide in a way to obtain these correlations. FMT was originally developed to describe inhomogeneous density profiles of mixtures of hard particles. The physics of inhomogeneous systems is not fully understood. An inhomogeneous system is a system with fluctuating density profiles $\rho(\mathbf{r})$, i.e., it is anisotropic. This in contrast to an isotropic homogeneous system where $\rho(\mathbf{r}){=}\rho_{\text{bulk}}$. A homogeneous system, has therefore bulk properties and is also called a bulk system. Having bulk properties makes it able to describe thermodynamic energies by their densities, since the total value of the system can simply be obtained by multiplying by the volume of the system. Expressions for free energy densities of homogeneous systems therefore had already been obtained before. FMT is a powerful tool to numerically calculate inhomogeneous density characteristics and the equations simplify in homogeneous systems to the known expressions.

For now we will consider a ν component mixture of hard spheres (i.e., particles which cannot overlap and have no other interactions). For mixtures the functional introduced in equation (2.44) in section 2.3 becomes

$$\Omega[\{\rho_i\}] = \mathcal{F}[\{\rho_i\}] + \sum_{i=1}^{\nu} \int \mathrm{d}\mathbf{r}\rho_i(\mathbf{r})(V_{\text{ext}}^i(\mathbf{r}) - \mu_i). \qquad (2.73)$$

which reduces for the equilibrium density profiles $\{\rho_{0,i}(\mathbf{r})\}$ to the grand potential Ω which is also the minimal value of the above functional,

$$\frac{\delta\Omega[\{\rho_i\}]}{\delta\rho_i(\mathbf{r})}\bigg|_{\rho_i=\rho_{0,i}} = 0. \qquad (2.74)$$

Here ρ_i is the number density of species i. For mixtures we can still write the Helmholtz free energy in functional notation as a sum of the ideal and excess contribution as in the former sections, i.e. $\mathcal{F}{=}\mathcal{F}_{\text{ideal}}{+}\mathcal{F}_{\text{excess}}$, where

$$\beta\mathcal{F}_{\text{ideal}}[\{\rho_i\}] = \sum_{i=1}^{\nu} \int \mathrm{d}\mathbf{r}\rho_i(\mathbf{r})(\ln\Lambda_i^3\rho_i(\mathbf{r}) - 1). \qquad (2.75)$$

where Λ_i is the thermal wavelength of species i. For hard particles i and j interacting via pair interactions $\phi(r_{ij})$ where r_{ij} is the particle separation distance, the excess free energy functional can be expanded for low densities

using the virial expansion as in equation (2.68). In functional notation we can write,

$$\beta \mathcal{F}_{\text{excess}}[\{\rho_i\}] = -\sum_{i,j} \frac{1}{2} \int d\mathbf{r}_1 d\mathbf{r}_2 \rho_i(\mathbf{r}_1)\rho_j(\mathbf{r}_2)f(r_{12}) \tag{2.76}$$

$$-\frac{1}{6}\sum_{i,j,k} \int d\mathbf{r}_1 d\mathbf{r}_2 d\mathbf{r}_3 \rho_i(\mathbf{r}_1)\rho_j(\mathbf{r}_2)\rho_k(\mathbf{r}_3)f(r_{12})f(r_{13})f(r_{23}) + \mathcal{O}(\rho^4),$$

with $r_{ij}=|\mathbf{r}_i-\mathbf{r}_j|$, $f(r)$ is the Mayer-f function and the spatially varying density $\rho(\mathbf{r})$. In the case of the hard-sphere model, the Mayer function reduces to:

$$f_{ij}(r) = e^{-\beta\phi_{ij}(r)} - 1 = -\Theta(R_i+R_j-r), \tag{2.77}$$

where $\Theta(r)$ is the Heaviside step function, since the interaction potential ϕ_{ij} is infinite when the spheres overlap and zero otherwise, and R_i is the radius of particle i. So the excluded volume for particle i in the neighborhood of particle j, is given by a volume of a sphere of radius $R_{i+j}=R_i+R_j$. FMT starts with writing the pair exclusion function (2.77) into single particle characteristics (intuitively like $V_{i+j}=V_i+S_iR_j+R_iS_j+V_j$, where V_i, S_i and R_i are respectively the volume, surface area and radius of particle i). It is convenient to do this in Fourier space where the function can be uniquely factored in multiplicative terms of single particle functions, which are transforms of the Heaviside step function and its derivatives. In real space we obtain (see appendix A.2),

$$\begin{aligned}
\Theta(R_i+R_j-|\mathbf{r}_i-\mathbf{r}_j|) = \omega_i^{(0)} \otimes \omega_j^{(3)} &+ \omega_i^{(3)} \otimes \omega_j^{(0)} \\
&+ \omega_i^{(1)} \otimes \omega_j^{(2)} + \omega_i^{(2)} \otimes \omega_j^{(1)} \\
&- \boldsymbol{\omega}_i^{(V1)} \otimes \boldsymbol{\omega}_j^{(V2)} - \boldsymbol{\omega}_i^{(V2)} \otimes \boldsymbol{\omega}_j^{(V1)}.
\end{aligned} \tag{2.78}$$

Here '$\otimes$' denotes a convolution product defined as:

$$\omega_i^{(\alpha)} \otimes \omega_j^{(\gamma)} = \int \omega_i^{(\alpha)}(\mathbf{r}-\mathbf{r}_i) \cdot \omega_j^{(\gamma)}(\mathbf{r}-\mathbf{r}_j)d\mathbf{r}, \tag{2.79}$$

where the dot stands for the usual product for the scalar weight functions and the scalar product for the vector weight functions. From the definition of a Fourier transform

$$\mathcal{T}\omega^{(q)} = \widetilde{\omega}^{(q)}(\mathbf{k}) = \int \omega^{(q)}(\mathbf{r})e^{i\mathbf{k}\cdot\mathbf{r}}d\mathbf{r}, \tag{2.80}$$

it can be shown that (see appendix A.2)

$$\mathcal{T}(\omega_i^{(\alpha)} \otimes \omega_j^{(\gamma)}) = \widetilde{\omega}_i^{(\alpha)}(-\mathbf{k})\widetilde{\omega}_j^{(\gamma)}(\mathbf{k}). \tag{2.81}$$

32

With this property we find from equation (2.78) the transforms of the weights,

$$\widetilde{\omega}_j^{(q)}(\mathbf{k}) = R_j^{(q)}\frac{\sin(kR_j)}{kR_j} \qquad \text{for q = 0,1,2,} \tag{2.82}$$

$$\widetilde{\omega}_j^{(3)}(\mathbf{k}) = 4\pi\frac{\sin(kR_j) - kR_j\cos(kR_j)}{k^3} \quad \text{and} \quad \widetilde{\boldsymbol{\omega}}_j^{(V2)}(\mathbf{k}) = -\sqrt{-1}\mathbf{k}\widetilde{\omega}_j^{(3)}(\mathbf{k}),$$

where $k=|\mathbf{k}|$ and $R_j^{(q)}=1, R_j, S_j$ for $q=0,1,2$. The weights then become,

$$\omega_j^{(2)}(\mathbf{r}) = |\nabla\Theta(R_j-|\mathbf{r}|)| = \delta(R-|\mathbf{r}|) = 4\pi R_j\,\omega_j^{(1)}(\mathbf{r}) = 4\pi R_j^2\,\omega_j^{(0)}(\mathbf{r}),$$

$$\boldsymbol{\omega}_i^{(V2)}(\mathbf{r}) = \nabla\Theta(R_j-|\mathbf{r}|) = \frac{\mathbf{r}}{r}\delta(R_j-|\mathbf{r}|) = 4\pi R_j\,\boldsymbol{\omega}_j^{(V1)}(\mathbf{r}), \tag{2.83}$$

$$\omega_j^{(3)}(\mathbf{r}) = \Theta(R_j-|\mathbf{r}|),$$

where $\delta(x)$ is the Dirac delta function. Note that there are only three linear independent weights. The scalar transforms obey $\widetilde{\omega}_j^{(q)}(k\to0)=R_j^{(q)}=1, R_j, S_j, V_j$ for $q=0,1,2,3$, while the transforms of the vector types obey the relation $\widetilde{\boldsymbol{\omega}}_j^{(Vq)}(k\to0)=0$ for $q=1,2$. From the weights we define the *weighted* densities,

$$n_\alpha(\mathbf{r}) = \sum_{i=1}^\nu \int \rho_i(\mathbf{r}')\omega_i^{(\alpha)}(\mathbf{r}-\mathbf{r}')\mathrm{d}\mathbf{r}', \tag{2.84}$$

which have dimensions of $[n_q]=[\mathbf{n}_q]=(\text{volume})^{(q-3)/3}$. In the limit of uniform densities this approach reduces to the scaled particle theory (SPT), i.e., the scalars obey $n_q(\mathbf{r})\to\xi_q=\sum\rho_{i,\text{bulk}}R_i^{(q)}$, while the vectors vanish, $\mathbf{n}_{Vq}(\mathbf{r})\to0$. Through this construction we can write the first term in the virial expansion in equation (2.76) as,

$$\lim_{\rho\to0}\beta\mathcal{F}_\text{excess}[\rho]=\sum_{i,j}\int \mathrm{d}\mathbf{r}_1\mathrm{d}\mathbf{r}_2\rho_i(\mathbf{r}_1)\rho_j(\mathbf{r}_2)\sum_{\alpha,\gamma}\omega_i^{(\alpha)}(\mathbf{r}_1)\otimes\omega_j^{(\gamma)}(\mathbf{r}_2)$$

$$= \int \mathrm{d}\mathbf{r}(n_0(\mathbf{r})n_3(\mathbf{r})+n_1(\mathbf{r})n_2(\mathbf{r})-\mathbf{n}_{V1}(\mathbf{r})\cdot\mathbf{n}_{V2}(\mathbf{r})), \tag{2.85}$$

where we add the terms in the sum which have the right dimension $[\omega^{(\alpha)}]\times[\omega^{(\gamma)}]=(\text{volume})^{-1}$. The 3-body term in equation (2.76) however cannot be reproduced exactly in this way, because the structure of the integrals are not simple convolutions. Equation (2.85) suggests that we can write the general excess free energy functional in general as

$$\beta\mathcal{F}_\text{excess}[\rho] = \int \Phi(\{n_\alpha(\mathbf{r})\})\mathrm{d}\mathbf{r}, \tag{2.86}$$

33

where the excess free energy density Φ is a function of the weighted densities. Note that $n_0, n_1 n_2, n_2^3, \mathbf{n}_{V1} \cdot \mathbf{n}_{V2}$ and $n_2(\mathbf{n}_{V2} \cdot \mathbf{n}_{V2})$ are the only five combinations of the weighted densities that are scalars of dimension $[\Phi] = (\text{volume})^{-1}$, making the quantities in equation (2.86) dimensionless. Therefore Φ should be of the form:

$$
\begin{aligned}
\Phi(\{n_\alpha\}) =& f_1(n_3)n_0 + f_2(n_3)n_1 n_2 + f_3(n_3)\mathbf{n}_{V1} \cdot \mathbf{n}_{V2} \\
& + f_4(n_3)n_2^3 + f_5(n_3)n_2 \mathbf{n}_{V2} \cdot \mathbf{n}_{V2},
\end{aligned}
\tag{2.87}
$$

where the coefficients are functions of the dimensionless weighted density n_3. To determine these coefficients we extrapolate the known low-density result for Φ to higher densities using thermodynamic arguments. We consider the case of a homogeneous hard-sphere mixture where the density distributions $\rho_i(\mathbf{r}) = \rho_i = N_i/V$ are constant. We can obtain an expression for Φ by equating two expressions for the pressure. From the thermodynamic relation we have,

$$
\begin{aligned}
\beta p_{\text{TD}} = -\beta \frac{\partial \mathcal{F}}{\partial V} &= -\beta \frac{\partial \mathcal{F}_{\text{ideal}}}{\partial V} - \beta \frac{\partial \mathcal{F}_{\text{excess}}}{\partial V} = \rho - \frac{\partial(\Phi V)}{\partial V} \\
&= n_0 - \Phi - V \frac{-\rho}{V} \frac{\partial \Phi}{\partial \rho} = n_0 - \Phi + \rho \frac{\partial \Phi}{\partial \rho}.
\end{aligned}
\tag{2.88}
$$

Another expression follows from scaled particle theory (SPT),

$$
\begin{aligned}
\beta p_{\text{SP}} = \lim_{R_i \to \infty} \frac{\beta \mu_{\text{ex}}}{V} &= \lim_{R_i \to \infty} \frac{\beta}{V} \left. \frac{\delta \mathcal{F}_{\text{excess}}}{\delta N_i} \right|_{T,V} \\
&= \lim_{R_i \to \infty} \frac{\beta}{V} \frac{\partial \Phi}{\partial \rho_i} = \lim_{R_i \to \infty} \sum_\alpha \frac{\partial \Phi}{\partial n_\alpha} \frac{\delta n_\alpha}{\delta \rho_i} = \frac{\partial \Phi}{\partial n_3},
\end{aligned}
\tag{2.89}
$$

where due to the geometrical meaning of the weight functions we have $\partial n_q / \partial \rho_i = R_i^{(q)}$ for $q = 0, 1, 2, 3$ and in the limit of $R_i \to \infty$ all but $\partial n_3 / \partial \rho_i$ vanish. This equation relates the excess chemical potential for the insertion of a sphere with radius R_i into a hard-sphere fluid to the leading order term pV_i of the reversible work necessary to create a cavity big enough to hold this particle. A semi empirical expression for pressure (put in scaled particle variables) is the Mansoori-Carnahan-Starling-Leland (MCSL) equation of state,

$$
\beta p_{\text{MCSL}} = \frac{n_0}{1-n_3} + \frac{n_1 n_2}{(1-n_3)^2} + \frac{n_2^3}{12\pi(1-n_3)^3} - \frac{n_2^3 n_3}{36\pi(1-n_3)^3}.
\tag{2.90}
$$

This equation of state follows from a proposed recursive relation of the virial coefficients of the hard sphere virial expansion. Equating (2.88) and (2.89)

34

with Φ as in equation (2.87) leads to a set of differential equations. By requiring that the low density limit (2.85) is obtained the integration constants can be obtained and the result is the Rosenfeld free energy density,

$$\Phi_{\mathrm{RF}} = -n_0\ln(1-n_3) + \frac{n_1n_2 - \mathbf{n}_{V1}\cdot\mathbf{n}_{V2}}{1-n_3} + \frac{n_2^3 - 3n_2\mathbf{n}_{V2}\cdot\mathbf{n}_{V2}}{24\pi(1-n_3)^2}. \qquad (2.91)$$

Similarly equating (2.88) and (2.90) leads to what is called the White Bear (WB) free energy density,

$$\begin{aligned}\Phi_{\mathrm{WB}} = {}& -n_0\ln(1-n_3) + \frac{n_1n_2 - \mathbf{n}_{V1}\cdot\mathbf{n}_{V2}}{1-n_3}\\ & + (n_2^3 - 3n_2\mathbf{n}_{V2}\cdot\mathbf{n}_{V2})\frac{n_3 + (1-n_3)^2\ln(1-n_3)}{36\pi n_3^2(1-n_3)^2}.\end{aligned} \qquad (2.92)$$

In bulk the two above expressions simplify to respectively the Percus-Yevick (PY) and Carnahan-Starling (CS) formulas is scaled particle variables,

$$\Phi_{\mathrm{PY}} = -\rho\ln(1-\xi) + \rho\frac{6\xi - 9\xi^2 + 3\xi^3}{2(1-\xi)^3} \quad \text{and} \quad \Phi_{\mathrm{CS}} = \rho\frac{4\xi - 3\xi^2}{(1-\xi)^2}. \qquad (2.93)$$

where $\xi = \xi_3 = \sum_i \pi\sigma^3\rho_i/6$ is the packing fraction. The latter is generally more accurate since it has an empirical background whereas the former has a theoretical background. We will only examine single species. In this section we have shown the general derivation of the FMT, since a single component derivation would do no justice to the theory.

We will continue to describe the mathematical model in which this FMT is used. Note that for the repulsive forces in bulk, we don't need FMT but only the bulk limits, i.e., equation (2.93). We will use FMT to obtain the only thing that is still missing: the pairwise distribution function, equation (2.53).

2.7   Particle Distribution Functions

In equation (2.48) we saw that a factorization of the equilibrium phase-space (the space of all possible microstates) probability density function f_0 into kinetic and potential terms leads to a separation of thermodynamic properties into into ideal and excess parts. A similar factorization can be made of the reduced phase-space distribution

$$f^{(n)}(\mathbf{r}^n, \mathbf{p}^n) = \frac{n!h^{3n}}{N!h^{3N}}\frac{N!}{(N-n)!}\iint f^{(N)}(\mathbf{r}^N, \mathbf{p}^N)\mathrm{d}\mathbf{r}^{(N-n)}\mathrm{d}\mathbf{p}^{(N-n)}, \qquad (2.94)$$

where $\mathbf{r}^N := \{\mathbf{r}_1, \dots \mathbf{r}_N\}$, $\mathbf{r}^{(N-n)} := \{\mathbf{r}_{n+1}, \dots \mathbf{r}_N\}$, etc. For the moment we have fixed the number of particles N, so $f^{(N)} := f^{(N)}(\mathbf{r}^N, \mathbf{p}^N)$ is the probability density function of the *canonical* ensemble. In equilibrium that is

$$f_0^{(N)} = \mathcal{Z}_N^{-1} \mathrm{e}^{-\beta \mathcal{H}_N} \quad \text{where} \quad \mathcal{Z}_N = \frac{1}{N! h^{3N}} \iint \mathrm{e}^{-\beta \mathcal{H}_N} \mathrm{d}\mathbf{r}^N \mathrm{d}\mathbf{p}^N \qquad (2.95)$$

normalizes $f_0^{(N)}$ to one. Expression (2.94) means that $f^{(n)}(\mathbf{r}^n, \mathbf{p}^n) \mathrm{d}\mathbf{r}^n \mathrm{d}\mathbf{p}^n / n! h^{3n}$ is the probability of finding *any* subset of n particles in the reduced phase space element $\mathrm{d}\mathbf{r}^n \mathrm{d}\mathbf{p}^n$, irrespective of the coordinates and momenta of the remaining $N-n$ particles. The factor $N!/(N-n)!$ is the number of ways of choosing $n < N$ particles out of N. From the particle *distribution* function we arrive at the particle *density* function, which is in the canonical ensemble defined as

$$\begin{aligned}
\rho_N^{(n)}(\mathbf{r}^n) &\equiv \frac{N!}{(N-n)!} \frac{1}{N! h^{3N}} \iint f_0^{(N)}(\mathbf{r}^N, \mathbf{p}^N) \mathrm{d}\mathbf{r}^{(N-n)} \mathrm{d}\mathbf{p}^N \\
&= \frac{N!}{(N-n)!} \frac{1}{N! h^{3N}} \iint \mathcal{Z}_N^{-1} \mathrm{e}^{-\beta \mathcal{H}_N} \mathrm{d}\mathbf{r}^{(N-n)} \mathrm{d}\mathbf{p}^N \qquad (2.96) \\
&= \frac{N!}{(N-n)!} \frac{1}{N! \Lambda^{3N} \mathcal{Z}_N} \int \mathrm{e}^{-\beta \mathcal{U}_N(\mathbf{r}^N)} \mathrm{d}\mathbf{r}^{(N-n)}.
\end{aligned}$$

Here $\rho_N^{(n)}(\mathbf{r}^n) \mathrm{d}\mathbf{r}^n$ is the probability of finding n particles of the system with coordinates in the element $\mathrm{d}\mathbf{r}^n$ of coordinate space, irrespective of the coordinates of the remaining particles and irrespective of the momenta of all the particles. The particle densities provide a complete but compact description of the (spatial) structure of a fluid. Moreover, the low-order particle distribution is often sufficient to calculate the equation of state and other thermodynamic properties of the system (see the end of this section). From equation (2.95) it follows that the n-particle density in equation (2.96) is normalized such that

$$\int \rho_N^{(n)}(\mathbf{r}^n) \mathrm{d}\mathbf{r}^n = \frac{N!}{(N-n)!}. \qquad (2.97)$$

The particle density function has dimensions of ρ^n (i.e., [volume^{-n}]). We can define the dimensionless *n-particle distribution* function $g_N^{(n)}(\mathbf{r}^N)$ in terms of the corresponding particle density by

$$g_N^{(n)}(\mathbf{r}^n) \equiv \frac{\rho_N^{(n)}(\mathbf{r}^n)}{\displaystyle\prod_{i=1}^{n} \rho_N^{(1)}(\mathbf{r}_i)}, \qquad (2.98)$$

36

which for a homogeneous system becomes

$$g_N^{(n)}(\mathbf{r}^n) = \frac{\rho_N^{(n)}(\mathbf{r}^n)}{\rho^n}. \tag{2.99}$$

The particle distribution functions measure the extent to which the structure of a fluid deviates from complete randomness. If the system is isotropic as well as homogeneous, the pair distribution function $g_N^{(2)}(\mathbf{r}_1, \mathbf{r}_2)$ is a function of the inter-particle separation $r_{12}=|\mathbf{r}_1-\mathbf{r}_2|$ only and it is then usually called the *radial distribution function* $g(r)$. In advancing to the grand canonical ensemble, the n-particle density is defined, in terms of the n-particle density for the canonical ensemble $\rho_N^{(n)}$, as

$$\rho^{(n)}(\mathbf{r}^n) \equiv \sum_{N=n}^{\infty} P(N)\rho_N^{(n)}(\mathbf{r}^n), \tag{2.100}$$

where $P(N)$ is the probability that the system actually has N particles, irrespective of their coordinates and momenta. Naturally the system cannot contain less than n particles for the n-particle density to exist. The probability $P(N)$ is obtained by integrating f_0 over all phase space, that is

$$
\begin{aligned}
P(N) &\equiv \frac{1}{N!h^{3N}} \iint f_0(\mathbf{r}^N, \mathbf{p}^N; N)\mathrm{d}\mathbf{r}^N\mathrm{d}\mathbf{p}^N \\
&= \frac{1}{N!h^{3N}} \iint \Xi^{-1}\mathrm{e}^{-\beta(\mathcal{H}_N-\mu N)}\mathrm{d}\mathbf{r}^N\mathrm{d}\mathbf{p}^N \\
&= \frac{\mathrm{e}^{\beta\mu N}}{\Xi}\mathcal{Z}_N = \frac{\mathrm{e}^{-\beta(\mathcal{H}_N-N\mu)}}{\Xi}\frac{\mathcal{Z}_N}{\mathrm{e}^{-\beta\mathcal{H}_N}} = \frac{f_0(\mathbf{r}^N, \mathbf{p}^N; N)}{f_0^{(N)}(\mathbf{r}^N, \mathbf{p}^N)}.
\end{aligned}
\tag{2.101}
$$

For the second equality we used equation (2.33) for the expression of f_0; for the third equality we wrote the integral over the probability distribution function of the grand canonical ensemble f_0 in terms of the partition function $\mathcal{Z}_N$ as in equation (2.95) and for the fifth equality we used both equations again for the definition of f_0 respectively $f_0^{(N)}$. Clearly $\sum P(N)=1$ by the above equation, since $\mathrm{Tr}_{\mathrm{cl}}f_0(\mathbf{r}^N, \mathbf{p}^N; N)=1$. Putting $\rho_N^{(n)}$ and $P(N)$ from respectively equation (2.96) and (2.101) in the definition of $\rho^{(n)}$ (equation

(2.100)) gives

$$
\rho^{(n)}(\mathbf{r}^n) = \sum_{N=n}^{\infty} \frac{e^{\beta\mu N}}{\Xi} \mathcal{Z}_N \cdot \frac{N!}{(N-n)!} \frac{1}{N! h^{3N}} \iint \mathcal{Z}_N^{-1} e^{-\beta\mathcal{H}_N} \mathrm{d}\mathbf{r}^{(N-n)} \mathrm{d}\mathbf{p}^N
$$

$$
= \sum_{N=n}^{\infty} \frac{1}{N! h^{3N}} \iint \frac{N!}{(N-n)!} \Xi^{-1} e^{-\beta(\mathcal{H}_N - \mu N)} \mathrm{d}\mathbf{r}^{(N-n)} \mathrm{d}\mathbf{p}^N
$$

$$
= \frac{1}{\Xi} \sum_{N=n}^{\infty} \frac{1}{(N-n)!} \left(\frac{e^{\beta\mu}}{\Lambda^3}\right)^N \int e^{-\beta\mathcal{U}_N(\mathbf{r}^N)} \mathrm{d}\mathbf{r}^{(N-n)}. \tag{2.102}
$$

When equation (2.102) is integrated over the coordinates $\mathbf{r}_1, \ldots, \mathbf{r}_n$ we find that $\rho^{(n)}(\mathbf{r}^n)$ is normalized such that

$$
\int \rho^{(n)}(\mathbf{r}^n) \mathrm{d}\mathbf{r}^n = \left\langle \frac{N!}{(N-n)!} \right\rangle. \tag{2.103}
$$

(Cf. the second line of equation (2.102) with equation (2.31) and (2.32)). It follows in particular that for a homogeneous system

$$
\rho^{(1)} = \frac{\langle N \rangle}{V} = \rho. \tag{2.104}
$$

For an ideal gas there are no interactions (i.e. $\mathcal{U}_N = 0$). This means that the integrals for $\rho^{(n)}$ in equation (2.102) over $N-n$ spatial variables $\mathbf{r}_i$ result in $N-n$ powers of the volume: V^{N-n}. The integrals over the momenta $\mathbf{p}_i$ result in the thermal wavelength cubed (Λ^3). We obtain for the ideal gas

$$
\rho^{(n)} = \frac{\displaystyle\sum_{N=n}^{\infty} \frac{1}{(N-n)!} \left(\frac{e^{\beta\mu}}{\Lambda^3}\right)^N V^{N-n}}{\displaystyle\sum_{N=0}^{\infty} \frac{1}{N!} \left(\frac{e^{\beta\mu}}{\Lambda^3}\right)^N V^N} = \left(\frac{e^{\beta\mu}}{\Lambda^3}\right)^n \equiv z^n. \tag{2.105}
$$

Here the denominator after the first equality is the grand partition function Ξ for the ideal case and the second equality is the result of a change of the summation index ($N \to N-n$). In the last equality we defined the *fugacity* z (an effective pressure). It can be shown that for an ideal gas $z = \rho$ and therefore

$$
\rho^{(n)} = \rho^n \qquad \text{(ideal gas)}. \tag{2.106}
$$

Now we see that the particle distribution function in the grand canonical ensemble, defined as

$$
g^{(n)}(\mathbf{r}^n) \equiv \frac{\rho^{(n)}(\mathbf{r}^n)}{\displaystyle\prod_{i=1}^{n} \rho^{(1)}(\mathbf{r}_i)}, \tag{2.107}
$$

(cf. equation (2.98)), approaches one as the separations of all pairs of particles becomes sufficiently large and the ideal approximation holds (i.e., $g^{(n)}(\mathbf{r}^n) \to 1$ as $\mathbf{r}^n \to \infty$ componentwise). Moreover from equation (2.102) and (2.104) we find that for homogeneous densities we can write $g^{(n)}$ as

$$
\begin{aligned}
g^{(n)}(\mathbf{r}^n) &= \frac{1}{\rho^n} \sum_{N=n}^{\infty} \frac{1}{(N-n)!} \left(\frac{e^{\beta\mu}}{\Lambda^3} \right)^N \int \Xi^{-1} e^{-\beta \mathcal{U}_N(\mathbf{r}^N)} d\mathbf{r}^{(N-n)} \\
&= \frac{1}{\Xi} \frac{z^n}{\rho^n} \sum_{N=0}^{\infty} \frac{z^N}{N!} \int e^{-\beta \mathcal{U}_{N+n}(\mathbf{r}^{N+n})} d\mathbf{r}^N \\
&= \frac{1}{\Xi} \frac{z^n}{\rho^n} \left(e^{-\beta \mathcal{U}_n(\mathbf{r}^n)} + \sum_{N=1}^{\infty} \frac{z^N}{N!} \int e^{-\beta \mathcal{U}_{N+n}(\mathbf{r}^{N+n})} d\mathbf{r}^N \right).
\end{aligned}
\tag{2.108}
$$

On the second line we changed the summation index again ($N \to N-n$) and substituted for the fugacity z from equation (2.105); on the third line we excluded the first term in the summation. In the low density limit, $\rho \to 0$, $z \to 0$, $z/\rho \to 1$ and $\Xi \to 1$, so only the first term in the above expression would remain,

$$
g^{(n)}(\mathbf{r}^n) \overset{\rho \to 0}{=} e^{-\beta \mathcal{U}_n \cdot (\mathbf{r}^n)}
\tag{2.109}
$$

In particular

$$
g(r) \overset{\rho \leftarrow \rho(\mathbf{r})}{=} g^{(2)}(\mathbf{r}_1, \mathbf{r}_2) \overset{\rho \to 0}{=} e^{-\beta \phi(r)}
\tag{2.110}
$$

where $r = |\mathbf{r}_1 - \mathbf{r}_2|$ and ϕ is the pair potential as in equation (2.52) (taken to be only dependent of the inter-particle separation r).

In the canonical ensemble we would calculate expectation values of an operator $\hat{O}$ via

$$
\langle \hat{O} \rangle = \frac{1}{N! h^{3N}} \iint \hat{O} f_0^{(N)} d\mathbf{r}^N d\mathbf{p}^N.
\tag{2.111}
$$

Compare this to the expressions for the grand canonical ensemble in equations (2.31) and (2.32). From equation (2.111) we find

$$
\begin{aligned}
\langle \delta(\mathbf{r} - \mathbf{r}_1) \rangle &= \frac{1}{N! h^{3N}} \iint \delta(\mathbf{r} - \mathbf{r}_1) \mathcal{Z}_N^{-1} e^{-\beta \mathcal{H}_N} d\mathbf{r}^N d\mathbf{p}^N \\
&= \frac{1}{N! \Lambda^{3N}} \frac{1}{\mathcal{Z}_N} \int e^{-\beta \mathcal{U}_N(\mathbf{r}, \mathbf{r}^{(N-1)})} d\mathbf{r}^{(N-1)}.
\end{aligned}
\tag{2.112}
$$

The statistical average in this expression is a function of the coordinate $\mathbf{r}$, but it is independent of the particle label (here taken to be 1). Therefore we can write

$$
\left\langle \sum_{i=1}^{N} \delta(\mathbf{r} - \mathbf{r}_i) \right\rangle = N \langle \delta(\mathbf{r} - \mathbf{r}_1) \rangle = \rho_N^{(1)}(\mathbf{r}),
\tag{2.113}
$$

39

where the last step follows directly from the definition of $\rho_N^{(1)}$ in equation (2.96) with $n=1$ and equation (2.112). Similarly, the statistical average of a product of two delta-functions δ is

$$
\begin{aligned}
\langle \delta(\mathbf{r}-\mathbf{r}_1)\delta(\mathbf{r}'-\mathbf{r}_2)\rangle &= \frac{1}{N!h^{3N}}\iint \delta(\mathbf{r}-\mathbf{r}_1)\delta(\mathbf{r}'-\mathbf{r}_2)\mathcal{Z}_N^{-1}\mathrm{e}^{-\beta\mathcal{H}_N}\mathrm{d}\mathbf{r}^N\mathrm{d}\mathbf{p}^N \\
&= \frac{1}{N!\Lambda^{3N}}\frac{1}{\mathcal{Z}_N}\int \mathrm{e}^{-\beta\mathcal{U}_N(\mathbf{r},\mathbf{r}',\mathbf{r}^{(N-2)})}\mathrm{d}\mathbf{r}^{(N-2)}.
\end{aligned}
\tag{2.114}
$$

From this and the definition of $\rho_N^{(2)}$ in equation (2.96) (with $n=2$) it follows that

$$
\left\langle \sum_{i\neq j}\delta(\mathbf{r}-\mathbf{r}_i)\delta(\mathbf{r}'-\mathbf{r}_j)\right\rangle = N(N-1)\langle\delta(\mathbf{r}-\mathbf{r}_1)\delta(\mathbf{r}'-\mathbf{r}_2)\rangle = \rho_N^{(2)}(\mathbf{r},\mathbf{r}').
\tag{2.115}
$$

This is consistent with equation (2.53), because both (2.113) and (2.115) also hold in the grand canonical ensemble. Showing here,

$$
\begin{aligned}
\left\langle \sum_{i=1}^N \delta(\mathbf{r}-\mathbf{r}_i)\right\rangle &= \mathrm{Tr}_{\mathrm{cl}}\sum_{i=1}^N \delta(\mathbf{r}-\mathbf{r}_i)f_0(\mathbf{r}^N,\mathbf{p}^N;N) \\
&= \sum_{N=1}^{\infty}\frac{1}{N!h^{3N}}\sum_{i=1}^N \iint \delta(\mathbf{r}-\mathbf{r}_i)\Xi^{-1}\mathrm{e}^{-\beta(\mathcal{H}_N-\mu N)}\mathrm{d}\mathbf{r}^N\mathrm{d}\mathbf{p}^N \\
&= \sum_{N=1}^{\infty}\frac{\mathrm{e}^{\beta\mu N}}{N!\Lambda^{3N}}\frac{N}{\Xi}\int \mathrm{e}^{-\beta\mathcal{U}_N(\mathbf{r},\mathbf{r}^{(N-1)})}\mathrm{d}\mathbf{r}^{(N-1)} \\
&= \sum_{N=1}^{\infty}\frac{\mathrm{e}^{\beta\mu N}}{\Xi}\mathcal{Z}_N\rho_N^{(1)}(\mathbf{r}) = \sum_{N=1}^{\infty}P(N)\rho_N^{(1)}(\mathbf{r}) \equiv \rho^{(1)}(\mathbf{r}).
\end{aligned}
\tag{2.116}
$$

For the first and second equality we used the definitions for the grand canonical ensemble as in equations (2.32), (2.31) and (2.33) respectively. For the third equality we integrated the momenta out, resulting in the factor Λ, as well as the integral involving the delta function. Besides that, we used the fact that all terms in the (inner) sum are the same (as we used in equation (2.113)). For the fourth equality we used the definition of $\rho_N^{(1)}$ as in equation (2.96) and for the fifth step we used the definition of $P(N)$ from equation (2.101). The last step follows from the definition of $\rho^{(1)}$ in equation (2.100) (naturally $P(N)=0$ for $N<n$, here $n=1$).

Similarly for the 2-particle density function,

$$
\begin{aligned}
\left\langle \sum_{i \neq j} \delta(\mathbf{r}-\mathbf{r}_i)\delta(\mathbf{r}'-\mathbf{r}_j) \right\rangle &= \mathrm{Tr}_{\mathrm{cl}} \sum_{i \neq j} \delta(\mathbf{r}-\mathbf{r}_i)\delta(\mathbf{r}'-\mathbf{r}_j) f_0(\mathbf{r}^N, \mathbf{p}^N; N) \\
&= \sum_{N=2}^{\infty} \frac{1}{N! h^{3N}} \sum_{i \neq j} \iint \delta(\mathbf{r}-\mathbf{r}_i)\delta(\mathbf{r}'-\mathbf{r}_j) \Xi^{-1} \mathrm{e}^{-\beta(\mathcal{H}_N - \mu N)} \mathrm{d}\mathbf{r}^N \mathrm{d}\mathbf{p}^N \\
&= \sum_{N=2}^{\infty} \frac{\mathrm{e}^{\beta \mu N}}{N! \Lambda^{3N}} \frac{N(N-1)}{\Xi} \int \mathrm{e}^{-\beta \mathcal{U}_N(\mathbf{r}, \mathbf{r}', \mathbf{r}^{(N-2)})} \mathrm{d}\mathbf{r}^{(N-2)} \\
&= \sum_{N=1}^{\infty} \frac{\mathrm{e}^{\beta \mu N}}{\Xi} \mathcal{Z}_N \rho_N^{(2)}(\mathbf{r}, \mathbf{r}') = \sum_{N=2}^{\infty} P(N) \rho_N^{(2)}(\mathbf{r}, \mathbf{r}') \equiv \rho^{(2)}(\mathbf{r}, \mathbf{r}'),
\end{aligned}
\tag{2.117}
$$

where we used the same steps as in equation (2.116). The regularity for higher particle densities are straightforward. Finally, for homogeneous systems we obtain for the radial distribution function,

$$
\begin{aligned}
\left\langle \frac{1}{N} \sum_{i \neq j} \delta(\mathbf{r}+\mathbf{r}_i-\mathbf{r}_j) \right\rangle &= \left\langle \int \frac{1}{N} \sum_{i \neq j} \delta(\mathbf{r}+\mathbf{r}'-\mathbf{r}_j)\delta(\mathbf{r}'-\mathbf{r}_i) \mathrm{d}\mathbf{r}' \right\rangle \\
&= \frac{1}{N} \int \rho_N^{(2)}(\mathbf{r}', \mathbf{r}+\mathbf{r}') \mathrm{d}\mathbf{r}' = \rho g_N(r),
\end{aligned}
\tag{2.118}
$$

where we used equation (2.115) for the second equality and the last step follows for homogeneous densities and equation (2.107). It follows via the same steps as in equations (2.116) and (2.117) that this also holds in the grand canonical ensemble.

The importance of the particle density functions is that thermodynamic properties can be obtained from them. Since most interactions can be approximated via (sequences of) pairwise interactions, the radial distribution function $g=g^{(2)}$ is in particular important (because for example the triplet distribution function $g^{(3)}$ arises only in the presence of three body forces). For instance the average excess potential energy in the grand canonical ensemble is

$$
\frac{\langle \mathcal{U}_N(\mathbf{r}^N) \rangle}{\langle N \rangle} = \frac{1}{2\langle N \rangle} \iint \rho^{(2)}(\mathbf{r}_1, \mathbf{r}_2) = 2\pi\rho \int_0^{\infty} \phi(r)g(r)r^2 \mathrm{d}r, \tag{2.119}
$$

see equation (A.9). The result can intuitively be understood by realizing that the mean number of particles at a distance r and $r+\mathrm{d}r$ from a reference particle is given by $n(r)\mathrm{d}r=4\pi r^2 \rho g(r)\mathrm{d}r$; the total potential energy of

interaction with the reference particle is $\phi(r)n(r)\mathrm{d}r$, and the excess internal energy per particle follows by integrating between $r{=}0$ and $r{=}\infty$ and dividing by 2, to avoid counting every interaction twice. The equation also holds for the canonical ensemble, with simply N particles, by the same reasoning. Another important equation involving g is the *pressure equation*

$$\frac{\beta P}{\rho} = 1 - \frac{2\pi\beta\rho}{3} \int \frac{\mathrm{d}\phi(r)}{\mathrm{d}r} g(r) r^3 \mathrm{d}r. \qquad (2.120)$$

It follows from the virial equation and the ergodic property, see equation (A.10), and it again also holds in the canonical ensemble. However the *compressibility equation* can only be derived in the grand canonical ensemble, since it is related to particle fluctuations,

$$
\begin{aligned}
\rho k_B T \chi_T &= \frac{\langle N^2 \rangle - \langle N \rangle^2}{\langle N \rangle} = 1 + \frac{\langle N^2 \rangle - \langle N \rangle - \langle N \rangle^2}{\langle N \rangle} \\
&= 1 + \frac{\iint [\rho^{(2)}(\mathbf{r}_1, \mathbf{r}_2) - \rho^{(1)}(\mathbf{r}_1)\rho^{(1)}(\mathbf{r}_2)] \mathrm{d}\mathbf{r}_1 \mathrm{d}\mathbf{r}_2}{\int \rho^{(1)}(\mathbf{r}) \mathrm{d}\mathbf{r}} \\
&= 1 + \rho \int [g(\mathbf{r}) - 1] \mathrm{d}\mathbf{r} = 1 + 4\pi\rho \int [g(r) - 1] r^2 \mathrm{d}r. \qquad (2.121)
\end{aligned}
$$

The first equality is shown in appendix (A.3) (because the *isothermal compressibility* χ_T is defined as minus the change in pressure due to a change in volume of the system, divided by the volume). The third step follows from equation (2.103) and the fourth results for homogeneous densities (cf. equations (2.104) and (2.107)).

Now we have learned about what particle density functions are and why they are important, we will continue to find an expression for the excess free energy. The earlier discussed FMT will play an essential role in this.

2.7.1   The λ-expansion

We will assume that the interactions between particles are pairwise additive. The basis of the perturbation theory we will use here, is to write the pair potential as

$$\phi(\mathbf{r}, \mathbf{r}') = \phi_0(\mathbf{r}, \mathbf{r}') + \phi_\mathrm{p}(\mathbf{r}, \mathbf{r}'). \qquad (2.122)$$

Here $\phi_0(\mathbf{r}, \mathbf{r}')$ is the pair potential of what will be the reference system and $\phi_\mathrm{p}(\mathbf{r}, \mathbf{r}')$ is the pair potential of the (small) perturbation. The λ-expansion uses a path with parameter λ from the reference system (with λ_0) to the system of interest (with λ_1). We will write

$$\phi_\lambda(\mathbf{r}, \mathbf{r}') = \phi_0(\mathbf{r}, \mathbf{r}') + \lambda\phi_p(\mathbf{r}, \mathbf{r}'), \qquad (2.123)$$

where λ varies from the reference system ($\lambda_0=0$) to the system of interest (with $\lambda_1=1$). We obtain the total pair interaction for λ_1 (i.e., $\phi_{\lambda_1}=\phi_0+1\phi_p = \phi$). Physical quantities are calculated from ϕ_λ by integrating from the initial to the final state, that is, integrate λ from 1 to 0. The total energy due to interactions, as a function of λ, becomes

$$\mathcal{U}_N(\mathbf{r}^N;\lambda) = \sum_{i\neq j}\phi_\lambda(\mathbf{r}_i,\mathbf{r}_j). \tag{2.124}$$

From equation (2.95) it follows that we can write

$$\beta\frac{\partial\mathcal{F}}{\partial\lambda} = \frac{-1}{\mathcal{Z}_N}\frac{1}{N!\Lambda^{3N}}\int(-\beta\mathcal{U}_N'(\lambda))\mathrm{e}^{-\beta\mathcal{U}_N(\mathbf{r}^N;\lambda)}\mathrm{d}\mathbf{r}^N = \langle\mathcal{U}_N'(\lambda)\rangle_\lambda, \tag{2.125}$$

where $\mathcal{U}_N'=\partial\mathcal{U}_N/\partial\lambda$ and $\langle\ldots\rangle_\lambda$ denotes the canonical ensemble average for the system characterized by the potential ϕ_λ. Since the complete potential ϕ_λ depends only on λ through the perturbation potential, we can write

$$\mathcal{W}_N(\mathbf{r}^N) := \mathcal{U}_N'(\mathbf{r}^N;\lambda) = \sum_{i\neq j}\phi_p(\mathbf{r}_i,\mathbf{r}_j) \tag{2.126}$$

Integrating equation (2.125) with respect to the coupling parameter λ gives

$$\beta\mathcal{F} = \beta\mathcal{F}_0 + \beta\int_0^1\langle\mathcal{U}_N'(\lambda)\rangle_\lambda\mathrm{d}\lambda$$

$$= \beta\mathcal{F}_0 + \beta\int_0^1\mathrm{d}\lambda\sum_{i\neq j}\frac{1}{\mathcal{Z}_N N!\Lambda^{3N}}\int\mathrm{e}^{-\beta\mathcal{U}_N(\mathbf{r}^N;\lambda)}\phi_p(\mathbf{r}_i,\mathbf{r}_j)\mathrm{d}\mathbf{r}^N$$

$$= \beta\mathcal{F}_0 + \beta\int_0^1\mathrm{d}\lambda\iint\left(\frac{N(N-1)/2}{\mathcal{Z}_N N!\Lambda^{3N}}\int\mathrm{e}^{-\beta\mathcal{U}_N(\mathbf{r}^N;\lambda)}\mathrm{d}\mathbf{r}^{(N-2)}\right)\phi_p(\mathbf{r}_1,\mathbf{r}_2)\mathrm{d}\mathbf{r}_1\mathrm{d}\mathbf{r}_2$$

$$= \beta\mathcal{F}_0 + \frac{\beta}{2}\int_0^1\mathrm{d}\lambda\iint\rho_{N,\lambda}^{(2)}(\mathbf{r}_1,\mathbf{r}_2)\phi_p(\mathbf{r}_1,\mathbf{r}_2)\mathrm{d}\mathbf{r}_1\mathrm{d}\mathbf{r}_2. \tag{2.127}$$

For the second equality we put in the definition of the average as in equation (2.125) and the derivative of the total interaction energy with respect to the coupling parameter (2.126). For the third equality we recognize that all the terms in the sum are equal and for the fourth we used definition (2.96), where $\rho_{N,\lambda}^{(2)}$ is the pair density function in the canonical ensemble for the system with interaction potential ϕ_λ. So we need to know the pairwise

43

correlation function as a function of the potential $\rho_{N,\lambda}^{(2)}$. This is in principle unknown, but we can expand it in powers of λ around a known reference system,

$$\rho_{N,\lambda}^{(2)}(\mathbf{r}_1, \mathbf{r}_2) = \rho_{N,0}^{(2)}(\mathbf{r}_1, \mathbf{r}_2) + \left.\frac{\partial \rho_{N,\lambda}^{(2)}}{\partial \lambda}\right|_{\lambda=0} \lambda + \mathcal{O}(\lambda^2). \tag{2.128}$$

(We wil not use an expansion around the reference system, but this is what it looks like.) Putting the zeroth order term in λ back in equation (2.127) yields the first order term in the free energy,

$$\beta \mathcal{F}_1 = \frac{\beta}{2} \iint \rho_{N,0}^{(2)}(\mathbf{r}_1, \mathbf{r}_2)\phi_p(\mathbf{r}_1, \mathbf{r}_2)\mathrm{d}\mathbf{r}_1 \mathrm{d}\mathbf{r}_2. \tag{2.129}$$

In this approximation (up to first order), the structure of the fluid is unaltered by the perturbation. At second order in λ, however, the derivative of the pair density function with respect to λ is involved. It becomes

$$\beta \mathcal{F}_2 = \frac{\beta}{2} \iint \frac{1}{2} \left.\frac{\partial \rho_{N,\lambda}^{(2)}}{\partial \lambda}\right|_{\lambda=0} \phi_p(\mathbf{r}_1, \mathbf{r}_2)\mathrm{d}\mathbf{r}_1 \mathrm{d}\mathbf{r}_2 \tag{2.130}$$

$$= -\frac{\beta^2}{4} \iint \phi_p(\mathbf{r}_1, \mathbf{r}_2) \bigg\{ \phi_p(\mathbf{r}_1, \mathbf{r}_2)\rho_{N,0}^{(2)}(\mathbf{r}_1, \mathbf{r}_2)$$

$$+ \int \rho_{N,0}^{(3)}(\mathbf{r}_1, \mathbf{r}_2, \mathbf{r}_3)(\ \phi_p(\mathbf{r}_1, \mathbf{r}_3) + \phi_p(\mathbf{r}_2, \mathbf{r}_3)\ )\mathrm{d}\mathbf{r}_3$$

$$+ \frac{1}{2} \int [\rho_{N,0}^{(4)}(\mathbf{r}_1, \mathbf{r}_2, \mathbf{r}_3, \mathbf{r}_4) - \rho_{N,0}^{(2)}(\mathbf{r}_1, \mathbf{r}_2)\rho_{N,0}^{(2)}(\mathbf{r}_3, \mathbf{r}_4)]\phi_p(\mathbf{r}_3, \mathbf{r}_4)\mathrm{d}\mathbf{r}_3 \mathrm{d}\mathbf{r}_4 \bigg\}\mathrm{d}\mathbf{r}_1 \mathrm{d}\mathbf{r}_2,$$

however some care must be taken in the thermodynamic limit, see [42]. The derivation of equation (2.127) from equation (2.125) can also be done in the grand canonical ensemble, by taking derivatives of the grand potential Ω with respect to λ. Then the reference system also contains the external potential and chemical potential terms, see equation (2.73), but the perturbation terms are the same since λ is only apparent in $\mathcal{U}_N$. The derivation of equation (2.130) (done in the grand canonical ensemble) can be found in appendix A.4.

It is important that the perturbation potential is small compared to the potential of the reference system. Usually the reference is chosen to be a system of hard spheres, because the interaction potential is easy. However, special care must be taken if we want to treat soft cores asdiscussed in the next section.
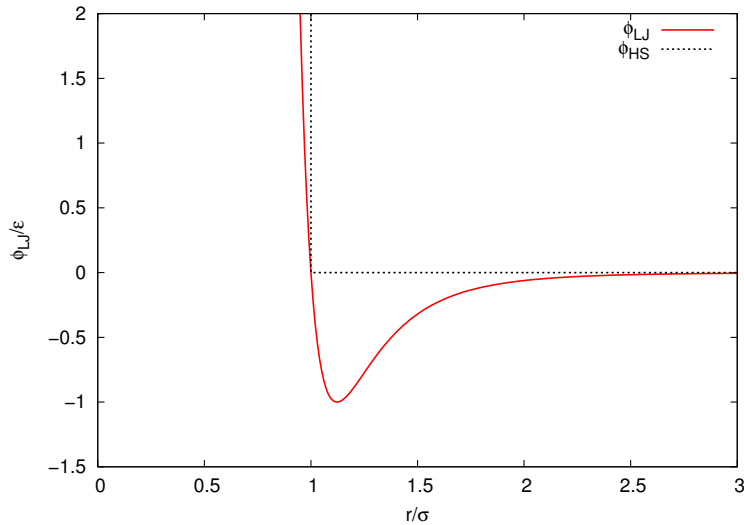
Figure 2.7: The LJ potential and the hard-sphere reference potential as a function of r. Note that the axis are normalized.

2.7.2 Soft-Core Reference Systems

Realistic inter-molecular potentials do not have an infinitely steep repulsive core. Therefore there is no natural separation into a hard-sphere part and a weak perturbation. Instead, one can arbitrarily separate the potential. The properties of the reference system, with potential ϕ_{ref}, can then be related to those of hard spheres independently of the way the perturbation is treated. The relation between the reference system and the hard sphere system is usually taken into account by choosing an effective diameter for the hard sphere system. This diameter may in principle depend on density and temperature and on the reference potential. An expression which does not depend on density is [45],

$$d = \int_0^\infty (1 - \mathrm{e}^{-\beta\phi_0(r)})\mathrm{d}r. \tag{2.131}$$

We are still free to separate our potential in the reference and the perturbation. The interaction potential we shall use here is the Lennard-Jones potential,

$$\phi_{\mathrm{LJ}}(r) = 4\varepsilon\left(\frac{\sigma^{12}}{r^{12}} - \frac{\sigma^6}{r^6}\right), \tag{2.132}$$

see figure 2.7. In this expression, σ is the particle diameter and the minimum of the potential is $-\varepsilon$. The potential energy of the long ranged attractions scale as r^{-6} where r is the inter-particle separation. This is a dispersion
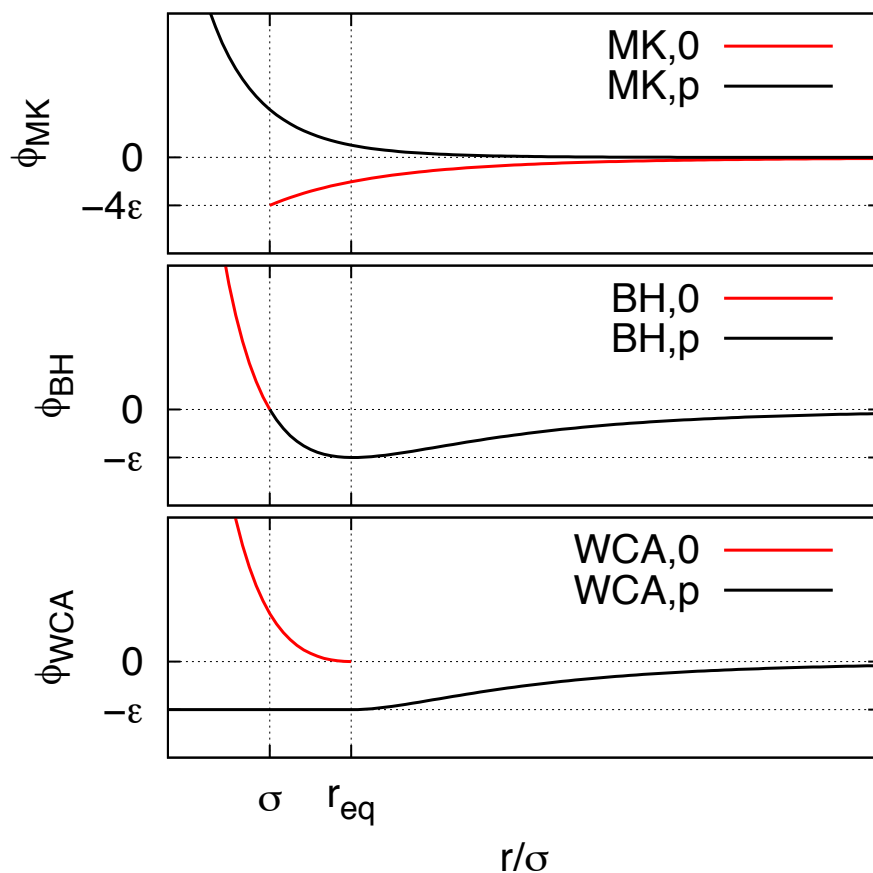
Figure 2.8: The splitting of the LJ potential into a reference part and a perturbation, by three methods MK, BH and WCA.

force; it arises from a rearrangement of the internal distribution of electrons in non-polar particles due to interactions with other particles. Phase separation cannot occur without attractive forces since particles will never cluster and form, for example, liquids. The scaling of the repulsive forces, which arise from overlapping electron clouds, are less important and the corresponding potential energy is taken to scale as $r^{-12} = (r^{-6})^2$ out of computational convenience. The result is the Lennard Jones (LJ) potential.

It may seem that the softness of the sphere makes it more difficult to obtain satisfactory results by perturbation theory, compared to hard particles with an attractive tail. This is not necessarily true, due to the extra flexibility provided by the separation of the potential into a reference part and a perturbation. Three ways to do this are shown in figure 2.8. They are given

by

$$\phi_{\mathrm{MK,0}}(r) = 4\varepsilon\frac{\sigma^{12}}{r^{12}} \qquad\qquad \phi_{\mathrm{MK,p}}(r) = -4\varepsilon\frac{\sigma^6}{r^6}, \qquad (2.133)$$

$$\phi_{\mathrm{BH,0}}(r) = \begin{cases} \phi_{\mathrm{LJ}}(r) \\ 0 \end{cases} \quad , \qquad \phi_{\mathrm{BH,p}}(r) = \begin{cases} 0 & r \le \sigma \\ \phi_{\mathrm{LJ}}(r) & r > \sigma \end{cases}, \qquad (2.134)$$

$$\phi_{\mathrm{WCA,0}}(r) = \begin{cases} \phi_{\mathrm{LJ}}(r)+\varepsilon \\ 0 \end{cases} \quad , \qquad \phi_{\mathrm{WCA,p}}(r) = \begin{cases} -\varepsilon & r \le r_{\mathrm{eq}} \\ \phi_{\mathrm{LJ}}(r) & r > r_{\mathrm{eq}} \end{cases}, \qquad (2.135)$$

where $r_{\mathrm{eq}}=2^{1/6}\sigma$ is the lowest point of the LJ potential. The method of Mc-Quarrie and Katz (MK) works well for high temperatures ($kT/\varepsilon\approx3$), way above the critical temperature ($kT/\varepsilon=1.35$) but is much less satisfactory at lower temperatures. This is understandable, since the reference system is considerably softer than the full potential in the positive (repulsive) region. The separation used by Barker and Henderson (BH) gives better results, however, the perturbation still contains the rapidly fluctuating part between $r=\sigma$ and $r=r_{\mathrm{eq}}$. Often better results are found due the WCA split of potentials. Although the reference part is softer than the normal potential, the perturbation is strictly attractive and varies more slowly over the range of r.

2.8 Liquid-vapor saturation curves

Once the radial distribution function is known, state properties can be calculated, for example the internal energy via equation (2.119), from which an equation of state can be determined. For all equilibrium systems the chemical potential must be constant on the whole domain, otherwise the particles will shift to locations with a lower chemical potential (for mixtures the changes in $N_i\mu_i$ for all species i across the domain must add up to zero). We also realize from figure 2.6 that the pressure for both a saturated liquid and a saturated vapor system must be the same in order to coexist. This means that for the saturation curves we have the set of equations,

$$p(\rho_l) = p(\rho_v) \quad \text{and} \quad \mu(\rho_l) = \mu(\rho_v), \qquad (2.136)$$

with liquid and vapor density ρ_l respectively ρ_v. Pressure and chemical potential can both be found from the free energy density via the thermodynamic relations,

$$\mu = \left.\frac{\partial\mathcal{F}}{\partial N}\right|_V = \frac{\partial\Phi}{\partial\rho} \text{ and } -p = \left.\frac{\partial\mathcal{F}}{\partial V}\right|_N = \frac{\partial V\Phi}{\partial V} = \Phi - \rho\frac{\partial\Phi}{\partial\rho} = \Phi - \mu\rho. \quad (2.137)$$

Here we used that $\rho = N/V$ and in bulk $\mathcal{F} = V\Phi$. Since we work with bulk systems to obtain phase diagrams, it is easier to work with the free energy *densities* Φ instead of the total free energy $\mathcal{F}$ in the system. We can write the equations of state (now denoting the free energies with a small 'f') as,

$$-p = f_{\text{ideal}}(\rho_{\text{bulk}}) + f_{\text{hs}}(\rho_{\text{bulk}}) + f_{\text{lr}}(\rho_{\text{bulk}}) - \mu\rho_{\text{bulk}},$$
$$\mu = \left.\frac{\mathrm{d}f_{\text{ideal}}}{\mathrm{d}\rho}\right|_{\rho_{\text{bulk}}} + \left.\frac{\mathrm{d}f_{\text{hs}}}{\mathrm{d}\rho}\right|_{\rho_{\text{bulk}}} + \left.\frac{\mathrm{d}f_{\text{lr}}}{\mathrm{d}\rho}\right|_{\rho_{\text{bulk}}}. \tag{2.138}$$

For the ideal part we have,

$$\beta f_{\text{ideal}}(\rho) = \rho(\ln(\Lambda^3\rho)-1), \quad \frac{\mathrm{d}\beta f_{\text{ideal}}}{\mathrm{d}\rho} = \ln(\Lambda^3\rho), \quad \frac{\mathrm{d}^2\beta f_{\text{ideal}}}{\mathrm{d}\rho^2} = \rho^{-1}, \tag{2.139}$$

and for the Percus-Yevick hard sphere equation,

$$\beta f_{\text{hs}}(\rho) = -\rho\ln(1-\xi) + \rho\frac{6\xi-9\xi^2+3\xi^3}{2(1-\xi)^3}, \quad \frac{\mathrm{d}\beta f_{\text{hs}}}{\mathrm{d}\rho} = -\ln(1-\xi) + \frac{14\xi-13\xi^2+5\xi^3}{2(1-\xi)^3},$$
$$\frac{\mathrm{d}^2\beta f_{\text{hs}}}{\mathrm{d}\rho^2} = \frac{\pi\sigma^3}{6}\frac{8-2\xi+4\xi^2-\xi^3}{(1-\xi)^4}. \tag{2.140}$$

and for the Carnahan-Starling hard sphere equation,

$$\beta f_{\text{hs}}(\rho) = \rho\frac{4\xi-3\xi^2}{(1-\xi)^2}, \quad \frac{\mathrm{d}\beta f_{\text{hs}}}{\mathrm{d}\rho} = \frac{8\xi-9\xi^2+3\xi^3}{(1-\xi)^3}, \quad \frac{\mathrm{d}^2\beta f_{\text{hs}}}{\mathrm{d}\rho^2} = \frac{\pi\sigma^3}{6}\frac{4-\xi}{(1-\xi)^4}, \tag{2.141}$$

where $\xi = \pi\sigma^3\rho/6$ is the packing fraction. The real problem is calculating the contribution due to long ranged interactions given by,

$$f_{\text{lr}}(\rho) = \frac{1}{2}\rho^2\int g(r,\rho)\phi_{\text{LJ}}(r)4\pi r^2\mathrm{d}r$$
$$\frac{\mathrm{d}f_{\text{lr}}(\rho)}{\mathrm{d}\rho} = \rho\int g(r,\rho)\phi_{\text{LJ}}(r)4\pi r^2\mathrm{d}r + \frac{1}{2}\rho^2\int\frac{\mathrm{d}g(r,\rho)}{\mathrm{d}\rho}\phi_{\text{LJ}}(r)4\pi r^2\mathrm{d}r$$
$$\frac{\mathrm{d}^2 f_{\text{lr}}(\rho)}{\mathrm{d}\rho^2} = \int g(r,\rho)\phi_{\text{LJ}}(r)4\pi r^2\mathrm{d}r + 2\rho\int\frac{\mathrm{d}g(r,\rho)}{\mathrm{d}\rho}\phi_{\text{LJ}}(r)4\pi r^2\mathrm{d}r \tag{2.142}$$
$$+ \frac{1}{2}\rho^2\int\frac{\mathrm{d}^2 g(r,\rho)}{\mathrm{d}\rho^2}\phi_{\text{LJ}}(r)4\pi r^2\mathrm{d}r,$$

where we need the derivatives because we can solve the set of equations in equation (2.136) with the Newton-Raphson method, a gradient descent method.

Chapter 3

Research Formulation

3.1   Test-particle method

What we want is to numerically obtain the radial distribution function for the corresponding interaction potential, i.e., we want to find $\rho^{(2)}(r; \phi_{\mathrm{LJ}})$ for the LJ interactions as in equation (2.132). We will do so, using Percus' test-particle method, which means that we fix a particle in the origin and let the other particles move in the force field of that particle acting as a (weak) external potential V_{ext}. If we label the fixed particle as '0', we can write the excess internal energy as

$$\mathcal{U}_N(\mathbf{r}^N) + \sum_{i=1}^{N} V_{\mathrm{ext}}(\mathbf{r}_i) = \sum_{i=1}^{N} \sum_{j>i}^{N} \phi_{\mathrm{LJ}}(\mathbf{r}_i, \mathbf{r}_j) + \sum_{j=1}^{N} \phi_{\mathrm{LJ}}(\mathbf{r}_0, \mathbf{r}_j) = \mathcal{U}_{N+1}(\mathbf{r}^{N+1}),$$

(3.1)

where $\mathbf{r}_0 = 0$. The grand potential with the external potential $\Xi[\phi_{\mathrm{LJ}}]$ becomes after integrating out the kinetic part

$$\begin{aligned}
\Xi[\phi_{\mathrm{LJ}}] &= \sum_{N=0}^{\infty} \frac{z^N}{N!} \int \cdots \int \mathrm{e}^{-\beta \mathcal{U}_{N+1}(\mathbf{r}^{N+1})} \mathrm{d}\mathbf{r}_1 \ldots \mathrm{d}\mathbf{r}_N \\
&= \frac{\Xi_0}{z} \left(\frac{1}{\Xi_0} \sum_{N=0}^{\infty} \frac{z^{N+1}}{N!} \int \cdots \int \mathrm{e}^{-\beta \mathcal{U}_{N+1}(\mathbf{r}^{N+1})} \mathrm{d}\mathbf{r}_1 \ldots \mathrm{d}\mathbf{r}_N \right) \\
&= \frac{\Xi_0}{z} \left(\frac{1}{\Xi_0} \sum_{N=1}^{\infty} \frac{z^N}{(N-1)!} \int \cdots \int \mathrm{e}^{-\beta \mathcal{U}_N(\mathbf{r}^N)} \mathrm{d}\mathbf{r}_1 \ldots \mathrm{d}\mathbf{r}_{N-1} \right) = \frac{\Xi_0 \rho}{z},
\end{aligned}$$

(3.2)

where Ξ_0 is the grand canonical potential in the absence of an external potential. In the third step we shifted the summation index and then we recognize the single-particle density in the *absence* of an external potential from

equation (2.102) between the large brackets. In the absence of any external potential the single particle density $\rho^{(1)}$ is constant (ρ). For a general external potential V_{ext} we would arrive at

$$\rho^{(n)}(\mathbf{r}^n; V_{\text{ext}}) = \frac{1}{\Xi[V_{\text{ext}}]} \sum_{N=n}^{\infty} \frac{1}{(N-n)!} \int e^{-\beta \mathcal{U}_N(\mathbf{r}^N)} \left(\prod_{i=1}^{N} \frac{e^{\beta \psi(\mathbf{r}_i)}}{\Lambda^3} \right) d\mathbf{r}^{(N-n)}. \quad (3.3)$$

where

$$\psi(\mathbf{r}) = \mu - V_{\text{ext}}(\mathbf{r}) \quad (3.4)$$

is called the *intrinsic chemical potential* and

$$\Xi[V_{\text{ext}}] = \sum_{N=0}^{\infty} \frac{1}{N!} \int e^{-\beta \mathcal{U}_N(\mathbf{r}^N)} \left(\prod_{i=1}^{N} \frac{e^{\beta \psi(\mathbf{r}_i)}}{\Lambda^3} \right) d\mathbf{r}^N \quad (3.5)$$

is the grand canonical potential in the presence of external forces. The single particle density in the presence of the test particle can be written as

$$\begin{aligned}
\rho^{(1)}(\mathbf{r}_1; \phi_{\text{LJ}}) &= \frac{1}{\Xi[\phi_{\text{LJ}}]} \sum_{N=1}^{\infty} \frac{1}{(N-1)!} \int e^{-\beta \mathcal{U}_N(\mathbf{r}^N)} \left(\prod_{i=1}^{N} \frac{e^{\beta \psi(\mathbf{r}_i)}}{\Lambda^3} \right) d\mathbf{r}^{(N-1)} \\
&= \frac{z}{\Xi_0 \rho} \sum_{N=1}^{\infty} \frac{z^N}{(N-1)!} \int e^{-\beta \mathcal{U}_{N+1}(\mathbf{r}^{N+1})} d\mathbf{r}^{(N-1)} \quad (3.6) \\
&= \frac{1}{\rho} \left(\frac{z}{\Xi_0} \sum_{N=2}^{\infty} \frac{z^{N-1}}{(N-2)!} \int e^{-\beta \mathcal{U}_N(\mathbf{r}^N)} d\mathbf{r}^{(N-2)} \right) = \frac{\rho^{(2)}(\mathbf{r}_1, \mathbf{r}_2; 0)}{\rho},
\end{aligned}$$

where we used in the second step the equations (3.1) and (3.2) to substitute $\Xi[\phi_{\text{LJ}}]$ for Ξ_0 and the internal energy $\mathcal{U}_N$ for $\mathcal{U}_{N+1}$ respectively. For the third equality we change the summation index and recognize the second-particle density function in the absence of an external potential from equation (2.102). Because the system is spatially uniform in the absence of external forces we arrive with equation (2.107) at

$$\rho^{(1)}(r; \phi_{\text{LJ}}) = \rho g^{(2)}(0, r) = \rho g(r) \quad (3.7)$$

So now we have shown that the single-particle density is proportional to the radial distribution function. From equation (2.127) we see that the functional which needs to be minimized with respect to $\rho(r)$, where the ideal part of the free energy of the reference system follows from equation (2.75) and the hard-sphere part from equation(2.86), is then given by (see also equation

(2.44) and (2.107)),

$$\Omega[\rho(r)] = \mathcal{F}_{\text{ideal}}[\rho(r)] + \beta^{-1} \int \Phi(\rho(r))\mathrm{d}\mathbf{r}$$
$$+ \frac{1}{2} \int_0^1 \iint \rho(\mathbf{r}_1)\rho(\mathbf{r}_2)g_\lambda^{(2)}(\mathbf{r}_1, \mathbf{r}_2; \phi_\lambda)\phi_{\text{LJ}}(r_{12})\mathrm{d}\mathbf{r}_1\mathrm{d}\mathbf{r}_2\mathrm{d}\lambda \qquad (3.8)$$
$$+ \int \rho(r)(V_{\text{ext}}(r)-\mu)\mathrm{d}\mathbf{r}$$

Here $r_{12}=|\mathbf{r}_1-\mathbf{r}_2|$, and we now take $V_{\text{ext}}(r)=\phi_{\text{LJ}}(r)$. Now only a choice has to be made for $g_\lambda^{(2)}$ in this integral equation. That is, we need to know how the particles, with long ranged attractions, interact in the presence of an external potential, as the attractions are turned 'on' as λ is integrated. Next we will discuss the possibilities.

3.2   Model Descriptions

We can substitute $g_\lambda^{(2)}$ in equation (3.8) by an ideal approximation

$$g_\lambda^{(2)}(\mathbf{r}_1, \mathbf{r}_2; \phi_\lambda) \approx 1 \qquad (3.9)$$

or the low density approximation

$$g_\lambda^{(2)}(\mathbf{r}_1, \mathbf{r}_2; \phi_\lambda) \approx \mathrm{e}^{-\beta\phi(r_{12})}, \qquad (3.10)$$

from equation (2.110), both for $r_{12}=|\mathbf{r}_1-\mathbf{r}_2|>\sigma$ and zero otherwise. Alternatively, the profile that is solved for can be used:

$$g_\lambda^{(2)}(\mathbf{r}_1, \mathbf{r}_2; \phi_\lambda) \approx g_1^{(2)}(\mathbf{r}_1, \mathbf{r}_2; \phi_\lambda) = \frac{\rho(|\mathbf{r}_1-\mathbf{r}_2|; \phi_\lambda)}{\rho_{\text{bulk}}}, \qquad (3.11)$$

where ρ_{b} is the single-particle (bulk) density function in the absence of an external field, compare this to equation (3.7). The disadvantage of the last choice, which would be exact for homogeneous systesm, is that it loses a degree of freedom. The first two choices are namely completely analytic and we can integrate out two spatial dimensions which is not possible for the latter. Even an expansion around the bulk value of 1 does not prevent that, because it is a numerical approximation as well,

$$g_\lambda^{(2)}(\mathbf{r}_1, \mathbf{r}_2) = 1 + \left.\frac{\partial g_\lambda^{(2)}(\mathbf{r}_1, \mathbf{r}_2)}{\partial\rho}\right|_{\rho=\rho_{\text{b}}} \frac{\rho(\mathbf{r}_1)-\rho_b+\rho(\mathbf{r}_2)-\rho_b}{2\rho_b^2}$$
$$+ \left.\frac{1}{2!}\frac{\partial^2 g_\lambda^{(2)}(\mathbf{r}_1, \mathbf{r}_2)}{\partial\rho_b^2}\right|_{\rho=\rho_{\text{b}}} \big(\rho(\mathbf{r}_1)-\rho_b\big)(\rho(\mathbf{r}_2)-\rho_b) + \ldots, \qquad (3.12)$$

51

unless we can make a guess for the value of the derivative for the bulk density as a function of space.

The equation that we need to solve for, (i.e., the minimum of equation (3.8) with respect to $\rho(r)$) is in general (see appendix B)

$$0 = \frac{\mathrm{d}f_{\mathrm{id}}(\rho(r))}{\mathrm{d}\rho} + \frac{1}{\beta}\sum_{\alpha}\frac{\partial\Phi}{\partial n_{\alpha}}\frac{\delta n_{\alpha}}{\delta\rho(\mathbf{r})} + \int_{0}^{\infty}\rho(r')\frac{g(|\mathbf{r}-\mathbf{r}'|)}{\rho_{\mathrm{bulk}}}\phi_{\mathrm{LJ}}(|\mathbf{r}-\mathbf{r}'|)\mathrm{d}\mathbf{r}'$$

$$+ \frac{1}{2}\iint\rho(r)\rho(r')\frac{\delta g(|\mathbf{r}-\mathbf{r}'|)}{\delta\rho(r)}\phi_{\mathrm{LJ}}(|\mathbf{r}-\mathbf{r}'|)\mathrm{d}\mathbf{r}\mathrm{d}\mathbf{r}' + V_{\mathrm{ext}}(r)-\mu. \qquad (3.13)$$

(The integral over λ is assumed to be already done in here.) Note that the choices presented at the beginning of this section (eqs. (3.9), (3.10) and (3.11)) are not expansions around the hard-sphere reference system as in eq. (2.128), but merely judicious guesses of what the function looks like under certain circumstances. The last term vanishes when the choice for effective radial distribution function g does not depend on the density $\rho(r)$. The bulk chemical potential μ can be found by examining a point far from the external potential where the density profile is constant, that is $\rho = \rho_{\mathrm{bulk}}$,

$$\mu = \frac{\mathrm{d}f_{\mathrm{id}}(\rho_{\mathrm{bulk}})}{\mathrm{d}\rho} + \frac{\mathrm{d}f_{\mathrm{hs}}(\rho_{\mathrm{bulk}})}{\mathrm{d}\rho} + \rho_{\mathrm{bulk}}\int\frac{\rho(r)}{\rho_{\mathrm{bulk}}}\phi_{\mathrm{LJ}}(r)\mathrm{d}\mathbf{r} \quad . \qquad (3.14)$$

Where the last term in the equations again drops out if g does not depend on the density $\rho(r)$ and the second term comes from equation (2.140) or (2.141).

All the above integrals in equation (3.13) are still done over a 3D space, no matter what choice for g. We will seek to reduce these to integrals over a single dimension by exploiting the radial symmetry of the integrand, that is, we take $\rho(\mathbf{r}):=\rho(r)$. Then the stencils n_{α} and the third term in equation (3.8) are of convolution type and can be simplified if we put the 'free' coordinate along the z-axis. So when we write $\mathbf{r}:=r\hat{\mathbf{z}}$, then

$$\int\rho(r')w(|\mathbf{r}-\mathbf{r}'|)\mathrm{d}\mathbf{r}' = \int\rho(r')\left(\int w(|r\hat{\mathbf{z}}-\mathbf{r}'|)\sin\theta\mathrm{d}\theta'\mathrm{d}\phi'\right)r'^{2}\mathrm{d}r', \qquad (3.15)$$

for a general function w and the term between brackets can be calculated analytically. The 1D (radial) 'stencils' or 'weights' for both the short ranged repulsions and the long ranged attractions are discussed next.

For the short ranged repulsions the expression for weighted densities can be simplified to a single integral, by integrating out the polar (θ) and azimuth
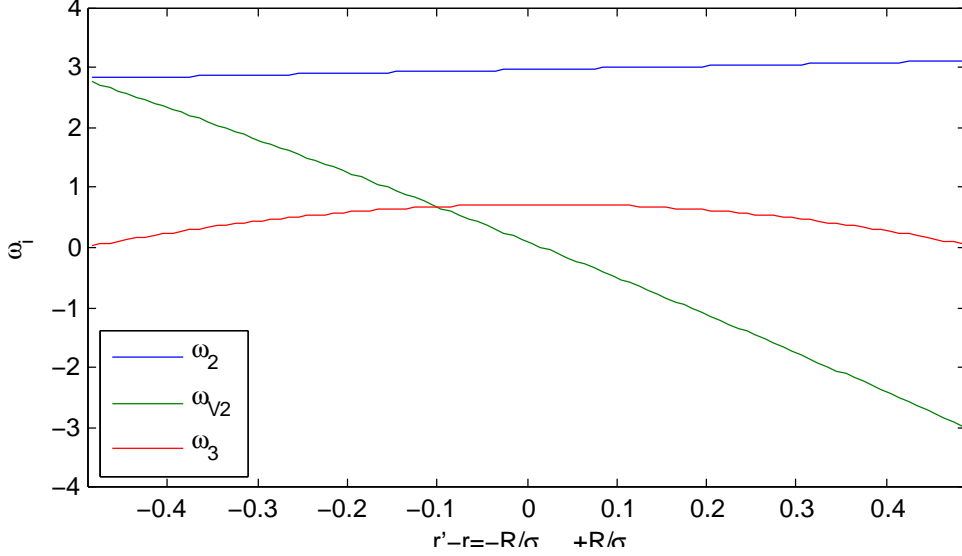
Figure 3.1: The stencils $\omega^{(\alpha)}(r,r')$ for the weighted densities $n_\alpha(r)$ as a function of r' in units of $\sigma=2R$ for $r=10\sigma$. The norms are $\int \omega^{(2)}(r,r')r'^2\mathrm{d}r'=\pi\sigma^2$, $\int \omega^{(V2)}(r,r')r'^2\mathrm{d}r'=0$ and $\int \omega^{(3)}(r,r')r'^2\mathrm{d}r'=\pi\sigma^3/6$. The limiting weights (i.e., for large r) become respectively constant, linear and quadratic in r' for $\omega^{(2)}$, $\omega^{(V2)}$ and $\omega^{(3)}$ independent of r.

(ϕ) angles. They are derived in appendix A.5 and given in [40],

$$n_2(r) = \frac{2\pi R}{r} \int\limits_{|r-R|}^{r+R} \rho(r')r'\mathrm{d}r', \quad n_{V2}(r)\hat{\mathbf{r}} = \frac{\pi}{r^2} \int\limits_{|r-R|}^{r+R} \rho(r')r'(r^2-r'^2+R^2)\mathrm{d}r'\hat{\mathbf{r}}$$

$$n_3(r) = 4\pi \int\limits_{0}^{R-r} \rho(r')r'^2\mathrm{d}r'\Theta(R-r) + \frac{\pi}{r} \int\limits_{|r-R|}^{r+R} \rho(r')r'(R^2-(r-r')^2)\mathrm{d}r', \quad (3.16)$$

where $R=\sigma/2$ and the other weighted densities are proportional to these, see equation (2.83). Note that the weights are different for each r and that they are properly normalized in bulk for all r, i.e. $n_2=4\pi R^2\rho_b$, $n_{V2}=0$ and $n_3=4\pi R^3\rho_b/3$ as noted on page 33. See figure 3.1 for a plot of the $\omega^{(i)}$ for a particular r. The stencils approach a limit as r becomes large. For $r>R$ the stencils are centered around r with a total length of σ and for $r<R$ the stencils are centered around R and have a length of $2r$ (but $R+r$ for $\omega^{(3)}$ due to the integral over a volume instead of a surface).

3.2.1 Model 1A: ideal case (BH)

Next we will evaluate the long ranged attractions for the ideal approximation, $g(r)=1$ for $r>\sigma$ and zero otherwise. The integral over the coupling parameter results in

$$\boxed{\int_0^1 \phi_p \mathrm{d}\lambda = \frac{1}{2}\phi_p} \tag{3.17}$$

The perturbation ϕ_p is the LJ potential for $r>\sigma$ and zero otherwise. This is the BH way to split the potential, see equation (2.134). The above integral is the integral over λ in equation (3.8) and substituted for $g\phi_{\mathrm{LJ}}$ in the third term of equation (3.13). First write the vector $\mathbf{r}'$ in Euclidean coordinates $\mathbf{r}'=r'\sin\theta'\cos\varphi'\hat{\mathbf{x}}+r'\sin\theta'\sin\varphi'\hat{\mathbf{y}}+r'\cos\theta'\hat{\mathbf{z}}$ and without loss of generality we can choose the $\mathbf{r}$ to be along the $z-$axis, i.e. $\mathbf{r}=r\hat{\mathbf{z}}$. Then

$$\begin{aligned}
|\mathbf{r}-\mathbf{r}'|^2 &= (r'\sin\theta'\cos\varphi')^2 + (r'\sin\theta'\sin\varphi')^2 + (r-r'\cos\theta')^2 \\
&= r'^2 + r^2 - 2rr'\cos\theta'.
\end{aligned} \tag{3.18}$$

The angular part of the integral we are evaluating is

$$\begin{aligned}
\int_0^{2\pi} \int g_{\mathrm{id}}(|\mathbf{r}-\mathbf{r}'|)&\phi_{\mathrm{LJ}}(|\mathbf{r}-\mathbf{r}'|)\sin\theta\mathrm{d}\theta'\mathrm{d}\varphi' \\
&= 8\pi\varepsilon \int g_{\mathrm{id}}(|\mathbf{r}-\mathbf{r}'|)\left(\frac{\sigma^{12}}{|\mathbf{r}-\mathbf{r}'|^{12}}-\frac{\sigma^6}{|\mathbf{r}-\mathbf{r}'|^6}\right)\sin\theta\mathrm{d}\theta'.
\end{aligned} \tag{3.19}$$

We must distinguish two cases for the limits of the integral. When $|r-r'|>\sigma$ then $g_{\mathrm{id}}(|\mathbf{r}-\mathbf{r}'|)=1$ for all θ. But when $|r-r'|<\sigma$ we must exclude a part of the integral over the azimuth angle, see figure 3.2. Here we see that in the second case we need to adjust the lower bound to γ, which depends on r and r'. It follows from the law of cosines that this bound is,

$$\sigma^2 = r^2 + r'^2 - 2rr'\cos\gamma \quad \text{or} \quad \cos\gamma = \frac{r^2+r'^2-\sigma^2}{2rr'}. \tag{3.20}$$

This holds for both the case that $0\leq r-r'\leq\sigma$ (as shown in figure 3.2) and for $0\leq r'-r\leq\sigma$. However, the case that $r<\sigma$ must be treated with special care, since we then also have a constraint on the lower bound of r', that is $r'>\sigma-r$, since otherwise there is only overlap possible (see figure A.1 for a sketch which makes this clear).

For the first case ($|r-r'|>\sigma$), the first term in equation (3.19) becomes, upon
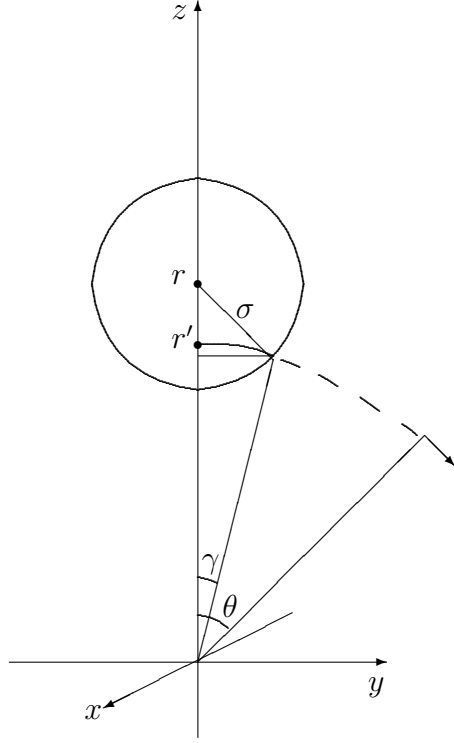
Figure 3.2: A sketch of a particle with radius $R=\sigma/2$ on a $z-$axis located at r. For cases when $|r-r'|<2R=\sigma$, we must exclude a part of the integral over θ' in equation (3.19) since the hard particles overlap for certain angles. We have to adjust the lower bound '0' of the integral over the polar angle θ' to 'γ' as shown in the picture.

substituting $u := \cos\theta'$,

$$
\int_0^\pi \frac{8\pi\sigma^{12}\varepsilon\sin\theta}{(r'^2+r^2-2rr'\cos\theta')^6}\mathrm{d}\theta' = \int_{-1}^1 \frac{8\pi\sigma^{12}\varepsilon}{(r'^2+r^2-2rr'\mathrm{u}\ )^6}\mathrm{d}u
$$

$$
= \frac{4\pi\sigma^{12}\varepsilon}{5rr'(r'^2+r^2-2rr'\mathrm{u})^5}\Bigg|_{-1}^1 = \frac{4\pi\sigma^{12}\varepsilon}{5rr'}\left(\frac{1}{(r'-r)^{10}}-\frac{1}{(r'+r)^{10}}\right),
$$

(3.21)

and the second term becomes,

$$
\int_0^\pi \frac{8\pi\sigma^6\varepsilon\sin\theta}{(r'^2+r^2-2rr'\cos\theta')^3}\mathrm{d}\theta' = \int_{-1}^1 \frac{8\pi\sigma^6\varepsilon}{(r'^2+r^2-2rr'\mathrm{u}\ )^3}\mathrm{d}u
$$

$$
= \frac{2\pi\sigma^6\varepsilon}{rr'(r'^2+r^2-2rr'\mathrm{u})^2}\Bigg|_{-1}^1 = \frac{2\pi\sigma^6\varepsilon}{rr'}\left(\frac{1}{(r'-r)^4}-\frac{1}{(r'+r)^4}\right).
$$

(3.22)

55

Together this can be written, with $\mathrm{d}\omega' = \sin\theta\mathrm{d}\theta'\mathrm{d}\varphi'$, as

$$\int g_{\mathrm{id}}(|\mathbf{r}-\mathbf{r}'|)\phi_{\mathrm{LJ}}(|\mathbf{r}-\mathbf{r}'|)\mathrm{d}\omega' = \frac{16\pi\sigma^6\varepsilon}{5rr'}\left[\frac{\sigma^6}{4}\left(\frac{1}{(r-r')^{10}}-\frac{1}{(r+r')^{10}}\right)\right. \quad (3.23)$$
$$\left.-\frac{5}{8}\left(\frac{1}{(r-r')^4}-\frac{1}{(r+r')^4}\right)\right] =: \zeta_{\mathrm{LJ}}^{(1)}(r,r').$$

For the second case ($|r-r'|<\sigma$) we have to use the lower bound γ from eq. (3.20) for the polar angle. This gives powers of $1/\sigma^2$ as lower bounds in the integral, since $r'^2+r^2-2rr'\cos\gamma=\sigma^2$. The total integral becomes in this case,

$$\int g_{\mathrm{id}}(|\mathbf{r}-\mathbf{r}'|)\phi_{\mathrm{LJ}}(|\mathbf{r}-\mathbf{r}'|)\mathrm{d}\omega' = \frac{16\pi\sigma^6\varepsilon}{5rr'}\left[\frac{\sigma^6}{4}\left(\frac{1}{\sigma^{10}}-\frac{1}{(r+r')^{10}}\right)\right. \quad (3.24)$$
$$\left.-\frac{5}{8}\left(\frac{1}{\sigma^4}-\frac{1}{(r+r')^4}\right)\right] =: \zeta_{\mathrm{LJ}}^{(1)}(r,r').$$

In figure 3.3 a contour plot of $\zeta_{\mathrm{LJ}}^{(1)}(r,r')$ is shown. Note that $\zeta_{\mathrm{LJ}}^{(1)}(r,r')$ is continuous at $|r-r'|=\sigma$ and that it is symmetric in both coordinates, i.e. $\zeta_{\mathrm{LJ}}^{(1)}(r,r') = \zeta_{\mathrm{LJ}}^{(1)}(r',r)$. The stencil $\zeta_{\mathrm{LJ}}^{(1)}$ is largest when r and r' are close together, but the region where both $r<\sigma$ and $r'-r<\sigma$ is excluded. For large r the stencil approaches 0, since *on average* the separation between r and r' on the surface of all possible θ' and φ', is large.

Some curves with constant r are shown in figure 3.4. Note that the curves are not symmetric around r, i.e. $\zeta_{\mathrm{LJ}}^{(1)}(r,r'-\delta)\neq\zeta_{\mathrm{LJ}}^{(1)}(r,r'+\delta)$, but the interactions are larger when closer to zero, i.e. $\zeta_{\mathrm{LJ}}^{(1)}(r,r'-\delta)>\zeta_{\mathrm{LJ}}^{(1)}(r,r'+\delta)$. This is due to the prefactor before the square brackets in equations (3.23) and (3.24). The physical explanation is that points on the surface $\{r'=r-\sigma, \theta\in[0,\pi], \forall\varphi\}$ are on average closer to r than points on the surface $\{r'=r+\sigma, \theta\in[0,\pi], \forall\varphi\}$; this difference gets smaller as r gets larger. Essentially we now have a one dimensional weight (in the radial direction) for all r and r' in equations (3.23) and (3.24). The local chemical potential due to long ranged interactions becomes $\int \rho(r')\zeta_{\mathrm{LJ}}^{(1)}(r,r')r'^2\mathrm{d}r'$. We conclude with some remarks.

- Firstly, the interactions along the line $r+r'=\sigma$ are weaker than the interactions along the curve $r^2+r'^2=r_{\mathrm{eq}}^2=2^{1/3}\sigma^2$ as can be seen in the figure 3.3. This is due to the shape of the LJ potential (see figure 2.8).

- Secondly, if one substitutes $r'=\alpha r$ with $\alpha>0$ into $\zeta_{\mathrm{LJ}}^{(1)}(r,r')$, then the 12-6 structure of the LJ potential is retrieved when $r\geq\sigma$ and $|1-\alpha|r\geq\sigma$,

$$\frac{\zeta_{\mathrm{LJ}}^{(1)}(r,\alpha r)}{8\pi\varepsilon} = \frac{(1+\alpha)^{10}-(1-\alpha)^{10}}{10\alpha(1-\alpha^2)^{10}}\frac{\sigma^{12}}{r^{12}} - \frac{(1+\alpha)^4-(1-\alpha)^4}{4\alpha(1-\alpha^2)^4}\frac{\sigma^6}{r^6}, \quad (3.25)$$
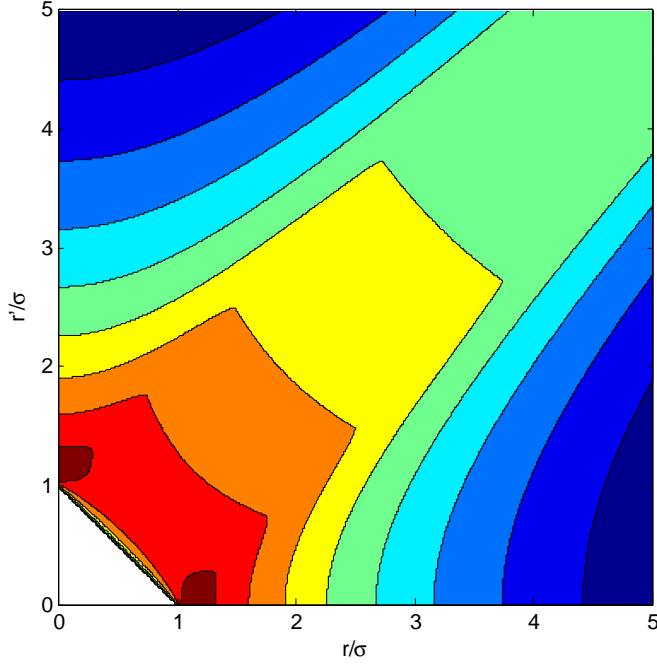
Figure 3.3: A contour plot of the resulting weight $\zeta_{\mathrm{LJ}}^{(1)}(r, r')$ of the long ranged interactions after integration over the polar angle and the azimuth angle in units of σ. Note that $\zeta_{\mathrm{LJ}}^{(1)}$ is large in *magnitude* when r and r' are close together, i.e., along the diagonal $r=r'$. The interactions go to zero as the particles are far apart. The part where both $r<\sigma$ and $r'-r<\sigma$ is excluded since there is no non-overlapping part.

but otherwise (when $|1-\alpha|r<\sigma$) we get an r^{-2} term,

$$\frac{\zeta_{\mathrm{LJ}}^{(1)}(r, \alpha r)}{8\pi\varepsilon} = -\frac{1}{10\alpha(1+\alpha)^{10}}\frac{\sigma^{12}}{r^{12}} + \frac{1}{4\alpha(1+\alpha)^4}\frac{\sigma^6}{r^6} - \frac{3}{20\alpha}\frac{\sigma^2}{r^2}. \qquad (3.26)$$

This extra term becomes a constant after putting in the Jacobian $(\alpha^2 r^2)$. Putting in $\alpha=1\pm\sigma/r$ shows again that $\zeta_{\mathrm{LJ}}^{(1)}$ is continuous (at $|r-r'|=\sigma$).

- Thirdly, just as for the FMT stencils we can look at the normalization for each r. The integrals we get are of the form

$$\int \frac{r'}{(r\pm r')^n}\mathrm{d}r' = \frac{\mp(n-1)r'-r}{(n-1)(n-2)(r\pm r')^{n-1}}. \qquad (3.27)$$

For $r>\sigma$ we split the integrals in the parts $(0...r-\sigma)$, $(r-\sigma...r+\sigma)$ and

57
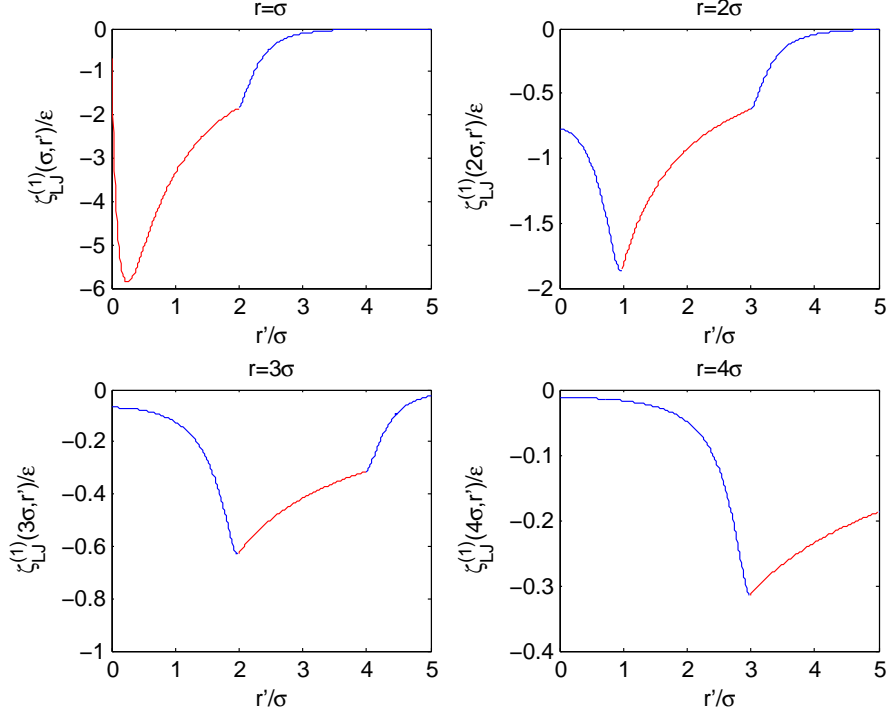
Figure 3.4: Four plots of $\zeta_{\mathrm{LJ}}^{(1)}(r, r')$ with constant r. The blue part shows the case that $|r-r'|>\sigma$ and the red part the other case. The lines are continuous and the interactions are maximal (in magnitude) when r' is approximately $r-\sigma$.

$(r+\sigma...\infty)$. The result is,

$$\int\limits_0^\infty \zeta_{\mathrm{LJ}}^{(1)}(r, r')r'^2\mathrm{d}r' = \frac{16\pi\sigma^6\varepsilon}{5r}\left(\frac{-10r}{9\sigma^3}\right) = -\frac{32\pi\sigma^3\varepsilon}{9} = \int\limits_\sigma^\infty \phi_{\mathrm{LJ}}(r)4\pi r^2\mathrm{d}r,$$

(3.28)

as should be. For the case that $0<r<\sigma$ we split the integrals in the parts $(\sigma-r...\sigma+r)$ and $(\sigma+r...\infty)$ which yields the same result.

- Fourthly, for the special case that $r=0$ we obtain the Lennard-Jones potential in the usual form,

$$\zeta_{\mathrm{LJ}}^{(1)}(0, r') = 16\pi\varepsilon\left(\frac{\sigma^{12}}{r'^{12}} - \frac{\sigma^6}{r'^6}\right), \qquad r' \geq \sigma.$$

(3.29)

3.2.2 Model 1B: ideal case (WCA)

In the former model we essentially used the BH way to split the LJ potential (see equation (2.134)). As argued in section 2.7.2 better results might be found from the WCA way to split the potential (see equation (2.135)). Now we separate the integral over the azimuth when

$$r_{\text{eq}}^2 = r^2 + r'^2 - 2rr'\cos\gamma' \quad \text{or} \quad \cos\gamma' = \frac{r^2 + r'^2 - r_{\text{eq}}^2}{2rr'}, \qquad (3.30)$$

where $r_{\text{eq}}=2^{1/6}\sigma$ is the equilibrium position (minimum) of the LJ potential. The part when $|r-r'|<r_{\text{eq}}$ is nonzero, namely $-\varepsilon$. The total result in for the region where $|r-r'|<r_{\text{eq}}$ and $r>r_{\text{eq}}$ case becomes

$$
\begin{aligned}
\zeta_{\text{WCA}}(r,r') :=\ & 2\pi\int_0^{\gamma'}(-\varepsilon)\sin\theta'\mathrm{d}\theta' + 2\pi\int_{\gamma'}^{\pi}g_{\text{id}}(|\mathbf{r}-\mathbf{r}'|)\phi_{\text{LJ}}(|\mathbf{r}-\mathbf{r}'|)\sin\theta'\mathrm{d}\theta' \\
=\ & -2\pi\varepsilon\left(\frac{r_{\text{eq}}^2 - (r-r')^2}{2rr'}\right) \\
& + \frac{16\pi\sigma^6\varepsilon}{5rr'}\left[\frac{\sigma^6}{4}\left(\frac{1}{r_{\text{eq}}^{10}}-\frac{1}{(r+r')^{10}}\right)-\frac{5}{8}\left(\frac{1}{r_{\text{eq}}^4}-\frac{1}{(r+r')^4}\right)\right].
\end{aligned}
\qquad (3.31)
$$

When $r+r'<r_{\text{eq}}$, we have $|\mathbf{r}-\mathbf{r}'|<r_{\text{eq}}$ for all $\theta'\in[0,\pi)$, so then $\zeta_{\text{WCA}}(r,r') = -4\pi\varepsilon$. In the case that $|r-r'|>r_{\text{eq}}$, ζ_{WCA} is the same as in model 1A (i.e., equation (3.23)). For the special case that $r=0$ the function becomes

$$
\zeta_{\text{WCA}}(0,r') = \begin{cases} -4\pi\varepsilon & r' < r_{\text{eq}} \\ 16\pi\varepsilon\left(\dfrac{\sigma^{12}}{r'^{12}} - \dfrac{\sigma^6}{r'^6}\right) & r' > r_{\text{eq}} \end{cases}. \qquad (3.32)
$$

In order to calculate the norm of the stencil we can use equation (3.27) again (the other integrals are straightforward polynomials). For $r>r_{\text{eq}}$ we split the integrals in the parts $(0...r-r_{\text{eq}})$, $(r-r_{\text{eq}}...r+r_{\text{eq}})$ and $(r+r_{\text{eq}}...\infty)$. The result is,

$$
\begin{aligned}
\int_0^{\infty}\zeta_{\text{WCA}}(r,r')r'^2\mathrm{d}r' =\ & \frac{16\pi\sigma^6\varepsilon}{5r}\left(\frac{5\sigma^6 r}{9r_{\text{eq}}^9} - \frac{5r}{3r_{\text{eq}}^3}\right) - \frac{4\pi r_{\text{eq}}^3\varepsilon}{3} \\
=\ & -\frac{4\pi r_{\text{eq}}^3\varepsilon}{3}\left(1 + 4\frac{\sigma^6}{r_{\text{eq}}^6} - \frac{4}{3}\frac{\sigma^{12}}{r_{\text{eq}}^{12}}\right) = \frac{4\pi r_{\text{eq}}^3}{3}(-\varepsilon) + \int_{r_{\text{eq}}}^{\infty}\phi_{\text{LJ}}(r)4\pi r^2\mathrm{d}r,
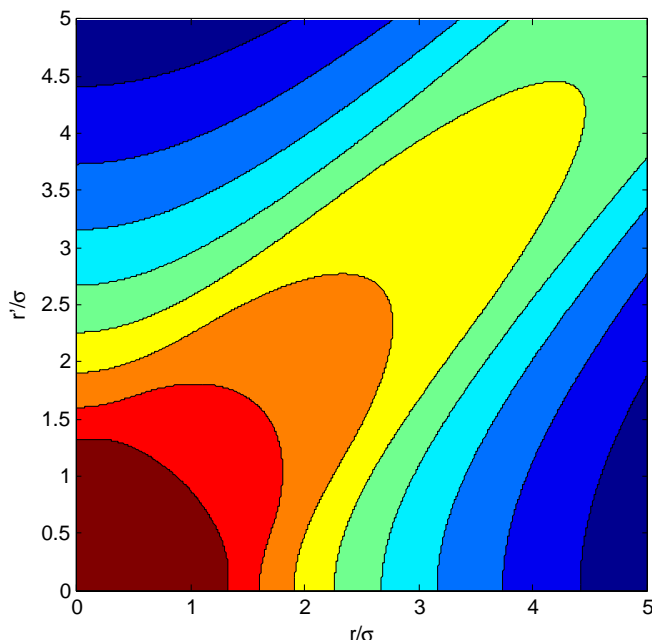\end{aligned}
\qquad (3.33)
$$

Figure 3.5: A contour plot of the *magnitude* of the resulting weight $\zeta_{\text{WCA}}(r, r')$ of the long ranged interactions after integration over the polar angle and the azimuth angle in units of σ. Note that in contrast to figure 3.3 the function is also defined for small arguments of r and r' and that the isolines are more smooth. The color-bar is the same as in figure 3.3.

as should be. For $r < r_{\text{eq}}$ we also must take the region with $r + r' < r_{\text{eq}}$ into account, We split the integrals in the parts $(0...r_{\text{eq}} - r)$, $(r_{\text{eq}} - r...r_{\text{eq}} + r)$ and $(r_{\text{eq}} + r...\infty)$ which yields the same result.

Note that the first term on the most right-hand side of equation (3.33) is simply the volume of a sphere of radius r_{eq} times the value of the potential $(-\varepsilon)$. In figure 3.5 we show a contour plot of $\zeta_{\text{WCA}}(r, r')$. Note that the function is continuous at $|r - r'| = r_{\text{eq}}$ and that it is symmetric in both coordinates, just as for $\zeta_{\text{LJ}}^{(1)}$. In contrast to the latter, the former is also defined for small values of the arguments. This is because the perturbation potential is also defined for small values of the argument, due to equation (2.135). Note that the isolines in figure 3.5 are more smooth than the isolines in figure 3.3. This is once more exemplified in figure 3.6. This was the intention, since this way to split the potential should give a smaller perturbation. The result is that the perturbation is more attractive, see also equation (2.135) and figure 2.8. The perturbation due to separation of the LJ potential with the WCA method has no repulsive part, whereas it does with the BH method (see again figure 2.8).
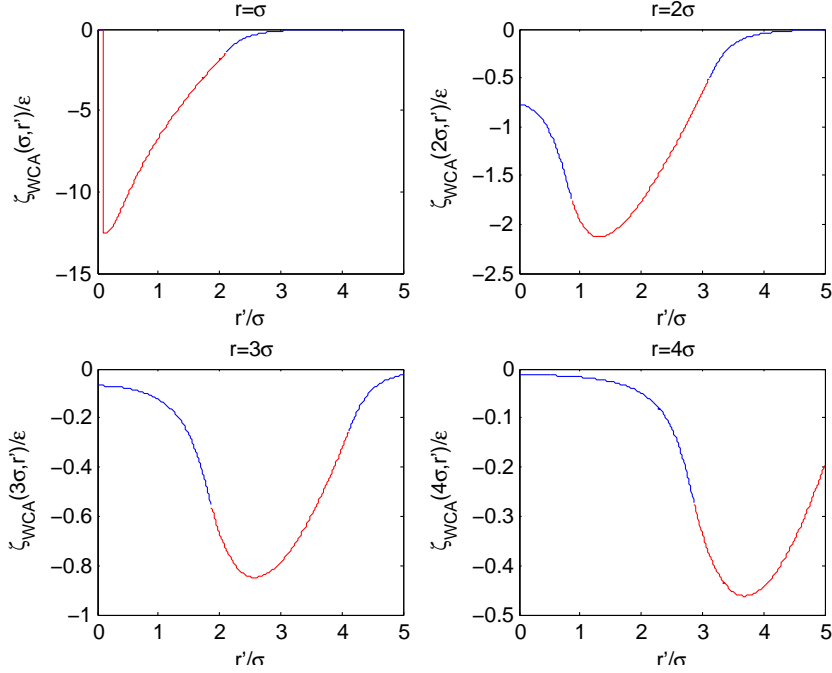
Figure 3.6: Four plots of $\zeta_{\mathrm{WCA}}(r, r')$ with constant r. The blue part shows the case that $|r-r'|>r_{\mathrm{eq}}$ and the red part the other case. The attractions are stronger than for $\zeta_{\mathrm{LJ}}^{(1)}(r, r')$ (see figure 3.8) because of the way the perturbed potential is defined, see figure 2.8 and equation (2.135). The curves can also be seen to be more smooth.

3.2.3 Model 2: modified mean field case (MMF)

The integral over the coupling parameter for the low density approximation from equation (3.10) becomes

$$\int_0^1 \phi_{\mathrm{p}} e^{-\beta(\phi_0+\lambda\phi_{\mathrm{p}})} \mathrm{d}\lambda = \frac{-e^{-\beta\phi_0}}{\beta}(e^{-\beta\phi_p}-1) \approx e^{-\beta\phi_0}(\phi_p - \beta\phi_p^2/2) \qquad (3.34)$$

see equation (2.123). The reference potential is a hard sphere potential, see equation (2.77), and the perturbation ϕ_p is the LJ potential for $r>\sigma$ and zero otherwise. This is the integral over λ in equation (3.8) and substituted for $g\phi_{\mathrm{LJ}}$ in the third term of equation (3.13). This is called the modified mean field approximation [41]. It involves the square of the interaction potential.

The angular part of the integral we need to evaluate for this is

$$\int_0^{2\pi}\int g_{\text{id}}(|\mathbf{r}-\mathbf{r}'|)\phi_{\text{LJ}}^2(|\mathbf{r}-\mathbf{r}'|)\sin\theta\mathrm{d}\theta'\mathrm{d}\varphi'$$

$$= 4\pi16\varepsilon^2\int g_{\text{id}}(|\mathbf{r}-\mathbf{r}'|)\left(\frac{\sigma^{12}}{|\mathbf{r}-\mathbf{r}'|^{12}}-\frac{\sigma^6}{|\mathbf{r}-\mathbf{r}'|^6}\right)^2\sin\theta\mathrm{d}\theta'. \tag{3.35}$$

For the first case ($|r-r'|>\sigma$), the first term in equation (3.35) becomes, upon substituting $u:=\cos\theta'$,

$$\int_0^\pi\frac{32\pi\sigma^{24}\varepsilon^2\sin\theta}{(r'^2+r^2-2rr'\cos\theta')^{12}}\mathrm{d}\theta' = \int_{-1}^1\frac{32\pi\sigma^{24}\varepsilon^2}{(r'^2+r^2-2rr'u)^{12}}\mathrm{d}u$$

$$= \left.\frac{16\pi\sigma^{24}\varepsilon^2}{11rr'(r'^2+r^2-2rr'u)^{11}}\right|_{-1}^1 = \frac{16\pi\sigma^{24}\varepsilon^2}{11rr'}\left(\frac{1}{(r'-r)^{22}}-\frac{1}{(r'+r)^{22}}\right), \tag{3.36}$$

and the cross term becomes,

$$2\int_0^\pi\frac{32\pi\sigma^{18}\varepsilon^2\sin\theta}{(r'^2+r^2-2rr'\cos\theta')^9}\mathrm{d}\theta' = \int_{-1}^1\frac{64\pi\sigma^{18}\varepsilon^2}{(r'^2+r^2-2rr'u)^9}\mathrm{d}u$$

$$= \left.\frac{32\pi\sigma^{18}\varepsilon^2}{8rr'(r'^2+r^2-2rr'u)^8}\right|_{-1}^1 = \frac{4\pi\sigma^{18}\varepsilon^2}{rr'}\left(\frac{1}{(r'-r)^{16}}-\frac{1}{(r'+r)^{16}}\right). \tag{3.37}$$

The last term becomes,

$$\int_0^\pi\frac{32\pi\sigma^{12}\varepsilon^2\sin\theta}{(r'^2+r^2-2rr'\cos\theta')^6}\mathrm{d}\theta' = \int_{-1}^1\frac{32\pi\sigma^{12}\varepsilon^2}{(r'^2+r^2-2rr'u)^6}\mathrm{d}u$$

$$= \left.\frac{16\pi\sigma^{12}\varepsilon^2}{5rr'(r'^2+r^2-2rr'u)^5}\right|_{-1}^1 = \frac{16\pi\sigma^{12}\varepsilon^2}{5rr'}\left(\frac{1}{(r'-r)^{10}}-\frac{1}{(r'+r)^{10}}\right). \tag{3.38}$$

Together this can be written, with $\mathrm{d}\omega'=\sin\theta\mathrm{d}\theta'\mathrm{d}\varphi'$, as

$$\int g_{\text{id}}(|\mathbf{r}-\mathbf{r}'|)\phi_{\text{LJ}}^2(|\mathbf{r}-\mathbf{r}'|)\mathrm{d}\omega' = \frac{4\pi\sigma^{12}\varepsilon^2}{rr'}\left[\frac{4\sigma^{12}}{11}\left(\frac{1}{(r-r')^{22}}-\frac{1}{(r+r')^{22}}\right)\right. \tag{3.39}$$

$$\left.-\sigma^6\left(\frac{1}{(r-r')^{16}}-\frac{1}{(r+r')^{16}}\right)+\frac{4}{5}\left(\frac{1}{(r-r')^{10}}-\frac{1}{(r+r')^{10}}\right)\right] =: \zeta_{\text{LJ}}^{(2)}(r,r').$$

For the second case ($|r-r'|<\sigma$) we have to use the lower bound γ from eq. (3.20) for the polar angle. This gives powers of $1/\sigma^2$ as lower bounds in the

integral, since $r'^2 + r^2 - 2rr' \cos\gamma = \sigma^2$. The total integral becomes in this case,

$$\int g_{\text{id}}(|\mathbf{r}-\mathbf{r}'|)\phi_{\text{LJ}}^2(|\mathbf{r}-\mathbf{r}'|)\mathrm{d}\omega' = \frac{4\pi\sigma^{12}\varepsilon^2}{rr'}\left[\frac{4\sigma^{12}}{11}\left(\frac{1}{\sigma^{22}}-\frac{1}{(r+r')^{22}}\right)\right. \qquad (3.40)$$

$$\left. - \sigma^6\left(\frac{1}{\sigma^{16}}-\frac{1}{(r+r')^{16}}\right)+\frac{4}{5}\left(\frac{1}{\sigma^{10}}-\frac{1}{(r+r')^{10}}\right)\right] =: \zeta_{\text{LJ}}^{(2)}(r,r').$$

For the special case that $r=0$ we arrive at

$$\zeta_{\text{LJ}}^{(2)}(0,r') = 64\pi\varepsilon^2\left(\frac{\sigma^{24}}{r'^{24}}-2\frac{\sigma^{18}}{r'^{18}}+\frac{\sigma^{12}}{r'^{12}}\right), \qquad r' \geq \sigma. \qquad (3.41)$$

We can also check the norm again. The integrals that appear are the same as in equation (3.27). For $r>\sigma$ we split the integrals in the parts $(0...r-\sigma)$, $(r-\sigma...r+\sigma)$ and $(r+\sigma...\infty)$. The result is (see equation (3.27)),

$$\int_0^\infty \zeta_{\text{LJ}}^{(2)}(r,r')r'^2\mathrm{d}r' = \frac{4\pi\sigma^{12}\varepsilon^2}{r}\left(\frac{128r}{315\sigma^9}\right) = \frac{512\pi\sigma^3\varepsilon^2}{315} = \int_\sigma^\infty \phi_{\text{LJ}}^2(r)4\pi r^2\mathrm{d}r,$$

$$(3.42)$$

as should be. For the case that $0<r<\sigma$ we split the integrals in the parts $(\sigma-r...\sigma+r)$ and $(\sigma+r...\infty)$ which yields the same result.

The local chemical potential due to long ranged interactions becomes now (in the modified mean field case) $\int \rho(r')\zeta_{\text{MMF}}(r,r')r'^2\mathrm{d}r'$, where $\zeta_{\text{MMF}} = \zeta_{\text{LJ}}^{(1)}-\beta\zeta_{\text{LJ}}^{(2)}/2$. The attractive forces are stronger compared to model 1, see figures 3.7 and 3.8.
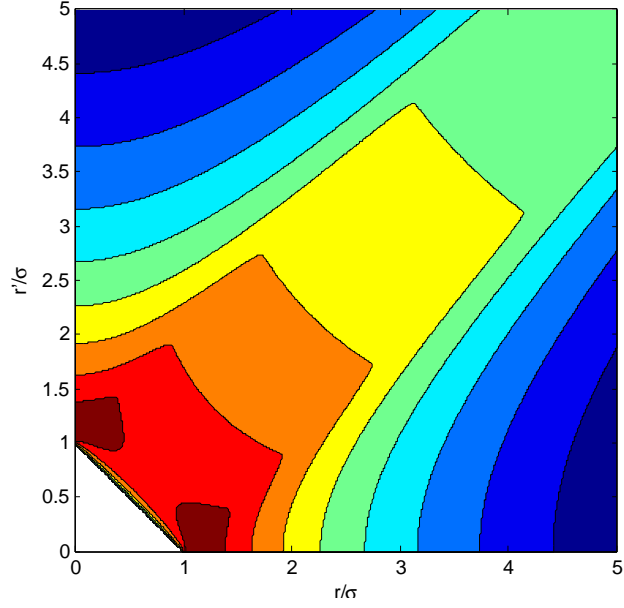
Figure 3.7: A contour plot of the resulting weight $\zeta_{\mathrm{MMF}}(r,r')$ of the long ranged interactions after integration over the polar angle and the azimuth angle in units of σ. Note the difference with figure 3.3 near $r=\sigma=r'$; the color-bar is the same.
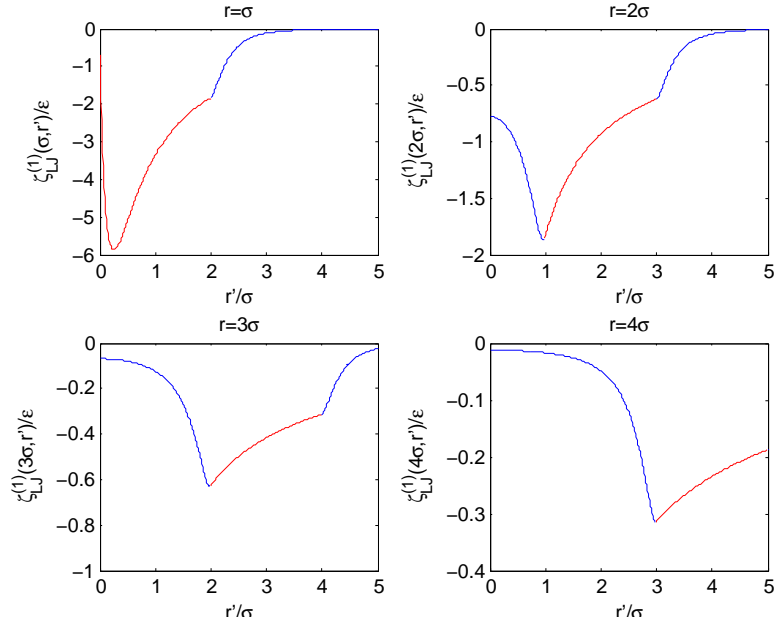

Figure 3.8: Four plots of $\zeta_{\mathrm{MMF}}(r,r')$ with constant r with $\beta=1$. The blue part shows the case that $|r-r'|>\sigma$ and the red part the other case. The attractions are stronger than for $\zeta_{\mathrm{LJ}}^{(1)}(r,r')$, see figure 3.8.

3.3 Overview

Summarized we want to find the solution of the following equation w.r.t $\rho(r)$ for a given bulk density ρ_b and temperature T,

$$\boxed{\frac{\ln(\Lambda^3\rho(r))}{\beta}+\int\limits_0^\infty\left(\frac{1}{\beta}\frac{\partial\Phi(r')}{\partial n_\alpha}\omega^{(\alpha)}(r,r')+\rho(r')\zeta(r,r')\right)r'^2\mathrm{d}r'+V_{\text{ext}}(r)=\mu}\quad (3.43)$$

with $\Lambda=h/\sqrt{2\pi mk_BT}$, where h is Planck's constant, m is the mass of the particles, k_B is Boltzmann's constant, $\beta=1/k_BT$. The α indicates a sum written in the Einstein summation convention ($\alpha=n_2,n_{V2},n_3$). The constant on the right-hand side is given by $\mu=\mu_{\text{id}}+\mu_{\text{hs}}+\mu_{\text{lr}}$, where $\beta\mu_{\text{id}}=\ln\Lambda^3\rho_b$, and, with $\xi=\pi\sigma^3\rho_b/6$ with bulk density ρ_b and particle diameter $\sigma=2R$,

$$\beta\mu_{\text{hs}}^{\text{PY}}=\ln(1-\xi)+\frac{14\xi-13\xi^2+5\xi^3}{2(1-\xi)^3}\text{ or }\beta\mu_{\text{hs}}^{\text{CS}}=\frac{8\xi-9\xi^2+3\xi^3}{(1-\xi)^3},$$

and μ_{lr} depends on the choice for ζ. There are two appropriate physical expressions available for the hard sphere part (PY and CS). The fundamental measure theory (FMT) provides two expressions for Φ (resp. RF and WB) which respectively reduce to these expressions in bulk. For single species:

$$\Phi_{\text{RF}}=-\frac{n_2}{\pi\sigma^2}\ln(1-n_3)+\frac{n_2^2-n_{V2}^2}{2\pi\sigma(1-n_3)}+\frac{n_2^3-3n_2n_{V2}^2}{24\pi(1-n_3)^2}\quad\text{or}$$

$$\Phi_{\text{WB}}=-\frac{n_2}{\pi\sigma^2}\ln(1-n_3)+\frac{n_2^2-n_{V2}^2}{2\pi\sigma(1-n_3)}+(n_2^3-3n_2n_{V2}^2)\frac{n_3+(1-n_3)^2\ln(1-n_3)}{36\pi n_3^2(1-n_3)^2}.$$

The weighted densities n_α are given by

$$n_2(r)=\frac{2\pi R}{r}\int_{|r-R|}^{r+R}\rho(r')r'\mathrm{d}r',\quad n_{V2}(r)=\frac{\pi}{r^2}\int_{|r-R|}^{r+R}\rho(r')r'(r^2-r'^2+R^2)\mathrm{d}r'$$

and $n_3(r)=4\pi\int_0^{R-r}\rho(r')r'^2\mathrm{d}r'\Theta(R-r)+\frac{\pi}{r}\int_{|r-R|}^{r+R}\rho(r')r'(R^2-(r-r')^2)\mathrm{d}r',$

where Θ is the Heaviside step function. The effective 1D radial weights (without the Jacobian r'^2) can then be written as

$$\omega^{(2)}(r,r')=2\pi R\mathbb{1}/(rr'),\quad\omega^{(V2)}(r,r')=\pi(r^2-r'^2+R^2)\mathbb{1}/(r^2r')$$
$$\text{and }\omega^{(3)}(r,r')=4\pi\Theta(R-r)+\pi(R^2-(r-r')^2)\mathbb{1}/(rr'),$$

where the indicator function $\mathbb{1}:=\mathbb{1}_{r'\in(|r-R|,r+R)}$ restricts r' to the specified interval ($\mathbb{1}$ is one when $r'\in(|r-R|,r+R)$ and zero elsewhere). There are three

weights, so there are three terms in the summation over α. The derivatives of the RF functional are

$$\frac{\partial \Phi_{\mathrm{RF}}}{\partial n_2} = -\frac{\ln(1-n_3)}{\pi\sigma^2} + \frac{n_2}{\pi\sigma(1-n_3)} + \frac{n_2^2-n_{V2}^2}{8\pi(1-n_3)^2}$$

$$\frac{\partial \Phi_{\mathrm{RF}}}{\partial n_{V2}} = -\frac{n_{V2}}{\pi\sigma(1-n_3)} - \frac{n_2 n_{V2}}{4\pi(1-n_3)^2}$$

$$\frac{\partial \Phi_{\mathrm{RF}}}{\partial n_3} = \frac{n_2}{\pi\sigma^2(1-n_3)} + \frac{n_2^2-n_{V2}^2}{2\pi\sigma(1-n_3)^2} + \frac{n_2^3-3n_2 n_{V2}^2}{12\pi(1-n_3)^3}.$$

And the derivatives of the WB functional are

$$\frac{\partial \Phi_{\mathrm{WB}}}{\partial n_2} = -\frac{\ln(1-n_3)}{\pi\sigma^2} + \frac{n_2}{\pi\sigma(1-n_3)} + (n_2^2-n_{V2}^2)\frac{n_3+(1-n_3)^2\ln(1-n_3)}{12\pi n_3^2(1-n_3)^2}$$

$$\frac{\partial \Phi_{\mathrm{WB}}}{\partial n_{V2}} = -\frac{n_{V2}}{\pi\sigma(1-n_3)} - n_2 n_{V2}\frac{n_3+(1-n_3)^2\ln(1-n_3)}{6\pi n_3^2(1-n_3)^2}$$

$$\frac{\partial \Phi_{\mathrm{WB}}}{\partial n_3} = \frac{n_2}{\pi\sigma^2(1-n_3)} + \frac{n_2^2-n_{V2}^2}{2\pi\sigma(1-n_3)^2}$$
$$+ (n_2^3-3n_2 n_{V2}^2)\frac{-n_3^3+5n_3^2-2n_3 n_3-2(1-n_3)^3\ln(1-n_3)}{36\pi n_3^3(1-n_3)^3}.$$

The effective weight for the long ranged interactions in the mean field with the BH split (Model 1A) is given by $\zeta(r,r')=\zeta_{\mathrm{LJ}}^{(1)}(r,r')=$

$$\begin{cases} \dfrac{16\pi\sigma^6\varepsilon}{5rr'}\left[\dfrac{\sigma^6}{4(r-r')^{10}} - \dfrac{\sigma^6}{4(r+r')^{10}} - \dfrac{5}{8(r-r')^4} + \dfrac{5}{8(r+r')^4}\right], & |r-r'|>\sigma \\[2ex] \dfrac{16\pi\sigma^6\varepsilon}{5rr'}\left[\dfrac{\sigma^6}{4\sigma^{10}} - \dfrac{\sigma^6}{4(r+r')^{10}} - \dfrac{5}{8\sigma^4} + \dfrac{5}{8(r+r')^4}\right], & |r-r'|<\sigma \end{cases}.$$

(The function is zero when $r+r'<\sigma$ and equal to 4π times the LJ potential (see equation (3.44)) when $r=0$ and $r'>\sigma$.) Here ε is a measure for the strength of the interaction between the particles. The local chemical potential due to long ranged interactions becomes in bulk $\mu_{\mathrm{lr}}=\mu_{\mathrm{lr}}^{\mathrm{LJ1}}=-32\pi\sigma^3\rho_b\varepsilon/9$.
For the mean field with the WCA split (Model 1B) the effective weight for the long ranged interactions is $\zeta(r,r')=\zeta_{\mathrm{WCA}}(r,r')=$

$$\begin{cases} \dfrac{16\pi\sigma^6\varepsilon}{5rr'}\left[\dfrac{\sigma^6}{4(r-r')^{10}} - \dfrac{\sigma^6}{4(r+r')^{10}} - \dfrac{5}{8(r-r')^4} + \dfrac{5}{8(r+r')^4}\right], & |r-r'|>r_{\mathrm{eq}} \\[2ex] -2\pi\varepsilon\dfrac{r_{\mathrm{eq}}^2-(r-r')^2}{2rr'} \\[2ex] \quad + \dfrac{16\pi\sigma^6\varepsilon}{5rr'}\left[\dfrac{\sigma^6}{4r_{\mathrm{eq}}^{10}} - \dfrac{\sigma^6}{4(r+r')^{10}} - \dfrac{5}{8r_{\mathrm{eq}}^4} + \dfrac{5}{8(r+r')^4}\right], & |r-r'|<r_{\mathrm{eq}} \end{cases}.$$

(The function is $-4\pi\varepsilon$ when $r+r'<r_{\mathrm{eq}}$ and equal to 4π times the LJ potential (see equation (3.44)) when $r=0$ and $r'>r_{\mathrm{eq}}$.) The local chemical potential due to long ranged interactions becomes in bulk $\mu_{\mathrm{lr}}=\mu_{\mathrm{lr}}^{\mathrm{WCA}}=-4\pi r_{\mathrm{eq}}^3\rho_b\varepsilon/3$ $\cdot(1+4\sigma^6/r_{\mathrm{eq}}^6-4\sigma^{12}/3r_{\mathrm{eq}}^{12})$.

The square of the LJ potential in these coordinates is given by $\zeta_{\mathrm{LJ}}^{(2)}(r,r')=$

$$
\begin{cases}
\dfrac{4\pi\sigma^{12}\varepsilon^2}{rr'}\left[\dfrac{4\sigma^{12}}{11(r-r')^{22}}-\dfrac{4\sigma^{12}}{11(r+r')^{22}}-\dfrac{\sigma^6}{(r-r')^{16}}+\dfrac{\sigma^6}{(r+r')^{16}}\right. \\
\qquad\qquad\qquad\qquad\left.+\dfrac{4}{5(r-r')^{10}}-\dfrac{4}{5(r+r')^{10}}\right], \quad |r-r'|>\sigma \\[2ex]
\dfrac{4\pi\sigma^{12}\varepsilon^2}{rr'}\left[\dfrac{9}{55\sigma^{10}}-\dfrac{4\sigma^{12}}{11(r+r')^{22}}+\dfrac{\sigma^6}{(r+r')^{16}}-\dfrac{4}{5(r+r')^{10}}\right], \quad |r-r'|<\sigma
\end{cases}
$$

(The function is zero when $r+r'<\sigma$ and equal to 4π times the square of the LJ potential (see equation (3.44)) when $r=0$ and $r'>\sigma$.) We take for model 2 the function $\zeta_{\mathrm{MMF}}=\zeta_{\mathrm{LJ}}^{(1)}-\beta\zeta_{\mathrm{LJ}}^{(2)}/2$ with bulk value $\mu_{\mathrm{lr}}^{\mathrm{MMF}}=\mu_{\mathrm{lr}}^{\mathrm{LJ1}}-\beta\mu_{\mathrm{lr}}^{\mathrm{LJ2}}/2$, where $\mu_{\mathrm{lr}}^{\mathrm{LJ2}}=512\pi\sigma^3\rho_b\varepsilon^2/315$.

The external potential is the LJ potential,

$$
V_{\mathrm{ext}}(r)=\phi_{\mathrm{LJ}}(r)=4\varepsilon\left(\frac{\sigma^{12}}{r^{12}}-\frac{\sigma^6}{r^6}\right). \tag{3.44}
$$

Next we will discuss the numerical ways which can be used to solve the equation.

Chapter 4

Numerical Analysis

4.1 Integral Equations

The equation that is evaluated in this thesis is of the form

$$
\ln(y(x)) + \int\limits_0^\infty \left(G_i(\{\widetilde{y}_j(x)\})w^{(i)}(x,t) + K(x,t)y(t) \right)\mathrm{d}t = f(x),
$$

$$
\text{with} \quad \widetilde{y}_i(x) = \int y(t)w^{(i)}(x,t)\mathrm{d}t.
$$

(4.1)

Here the three weights $w^{(i)}$ are separable (i.e., $w^{(i)}(x,t) = \sum g_j^{(i)}(x)p_j^{(i)}(t)$) but not symmetric (i.e., $w^{(i)}(x,t) \neq w^{(i)}(t,x)$). The integral itself has constant limits of integration. The function K in this integral is symmetric but not separable, nor can it be approximated as such.

An equation in which the unknown function appears under an integral sign is called an integral equation. Such equations have been studied extensively in mathematics and different classes of equations can be distinguished. The complicating factor in equation (4.1) is the term $G(\{\widetilde{y}_i(x)\})$ and it makes this equation not fit in any general classification. We may, however, find ways to solve it in the literature by examining other classes. The most studied type is the class of linear integral equations. These can generally be written as

$$
\alpha y(x) = f(x) + \lambda \int\limits_a^{L(x)} K(x,t)y(t)\mathrm{d}t,
$$

(4.2)

where y is the unknown function, f is a known function and K is another known function of two variables often called the *kernel*. The names corresponding to different cases of the general linear integral are given in table

Table 4.1: Classification of linear integral equations.

Case 1		Case 2	
$\alpha=0$	first kind	$\alpha\neq0$	second kind
$f(x)=0\forall x\in(a,L)$	homogeneous	$\exists x\in(a,L):f(x)\neq0$	inhomogeneous
$L(x)=b$	Fredholm	$L=x$	Volterra

4.1. Integral equations can be solved or approximated in several ways and this may depend on the form of the kernel. For example, inhomogeneous Volterra integral equations of the first or second kind with a difference kernel (i.e., $K(x,t)=K(x-t)$) has a convolution form, i.e.,

$$\alpha y(x) - \int_0^x K(x-t)y(t)\mathrm{d}t = f(x). \qquad (4.3)$$

This can be solved using a Laplace transform and inverse transform given by,

$$\breve{f}(s) = \int_0^\infty f(x)\mathrm{e}^{-sx}\mathrm{d}x \quad\text{and}\quad f(x) = \frac{1}{2\pi i}\int_{c-i\infty}^{c+i\infty} \widetilde{f}(s)\mathrm{e}^{sx}\mathrm{d}s \qquad (4.4)$$

respectively (which exist for piecewise continuous f with $|f(x)|<M\mathrm{e}^{\sigma_0 x}$ for some $M>0$ and $\sigma_0\geq0$), since the transforms of equation (4.3) has the simple form $\alpha\breve{y}(s)-\breve{K}(s)\breve{y}(s)=\breve{f}(s)$. A similar expression can be found for inhomogeneous Fredholm integral equations of the first or second kind with a difference kernel on the entire axis using a Fourier transform and its inverse transform, respectively given by

$$\widetilde{f}(u) = \int_{-\infty}^\infty f(x)\mathrm{e}^{-iux}\mathrm{d}x \quad\text{and}\quad f(x) = \frac{1}{2\pi}\int_{-\infty}^\infty \widetilde{f}(u)\mathrm{e}^{-iux}\mathrm{d}u. \qquad (4.5)$$

In order for the transform of a function to exist, the function must be integrable.

4.1.1 Intermezzo: convolution theorem

After some manipulation we can write our integrals over the unknown function in a convolution form,

$$n_\alpha(r) = \frac{1}{r}\int \rho(r')r'\omega_C^{(\alpha)}(r-r')\mathrm{d}r' \qquad (4.6)$$

Showing here

$$n_2(r) = \frac{1}{r} \int\limits_{|r-R|}^{r+R} \rho(r')r'[2\pi R]\mathrm{d}r' \qquad \text{so} \quad \omega_C^{(2)}(r) = 2\pi R\Theta(R-r),$$

$$n_3(r) = \frac{1}{r} \int\limits_{|r-R|}^{r+R} \rho(r')r'[\pi(R^2-(r-r')^2)]\mathrm{d}r' \quad \text{so} \quad \omega_C^{(3)}(r) = \pi(R^2-r^2)\Theta(R-r),$$

$$(4.7)$$

$$n_{V2}(r) = \frac{\partial n_3}{\partial r} = \frac{1}{r^2} \int\limits_{|r-R|}^{r+R} \rho(r')r'[\pi(R^2-(r-r')^2)]\mathrm{d}r'$$

$$+ \frac{1}{r} \int\limits_{|r-R|}^{r+R} \rho(r')r'[-\pi(2(r-r'))]\mathrm{d}r' \quad \text{so} \quad \omega_C^{(V2)}(r) = -2\pi r\Theta(R-r).$$

We can write n_{V2} as a sum of two convolution integrals where the first integral has a kernel $\omega_C^{(3)}$ and a prefactor of r^{-2} (compared to r^{-1} of equation (4.6)), whereas the second integral has the kernel $\omega_C^{(V2)}$. Note that we did not include the part $r<R$ for n_3; it is in principle not necessary to do so, because the density should vanish because of the external potential. Also note that these weights $\omega_C^{(\alpha)}$ are defined differently than $\omega^{(\alpha)}$ in the overview, section 3.3. The transform of

$$rn_\alpha(r) = \int \rho(r')r'\omega_C^{(\alpha)}(r-r')\mathrm{d}r' \quad \text{is} \quad \widetilde{rn_\alpha(r)}(k) = \widetilde{r\rho(r)}(k)\,\widetilde{\omega}_C^{(\alpha)}(k). \quad (4.8)$$

The r in front of n_α becomes r^2 for $\alpha=V2$.

For the long ranged part, the term involving ζ in equation (3.43), we can for the case that $|r-r'|>\sigma$ distinguish two terms which are a function of $r-r'$ and $r+r'$, that is

$$\frac{1}{r}\int \rho(r')\frac{16\pi\sigma^6\varepsilon}{5}\left[\frac{\sigma^6}{4(r-r')^{10}} - \frac{5}{8(r-r')^{10}}\right]\mathrm{d}r' = \frac{+1}{r}\int c\rho(r')v(r-r')\mathrm{d}r',$$

$$\frac{1}{r}\int \rho(r')\frac{16\pi\sigma^6\varepsilon}{5}\left[\frac{-\sigma^6}{4(r+r')^{10}} + \frac{5}{8(r+r')^{10}}\right]\mathrm{d}r' = \frac{-1}{r}\int c\rho(r')v(r+r')\mathrm{d}r',$$

$$(4.9)$$

where $c=16\pi\sigma^6\varepsilon/5$ and v is the function between first large brackets. The Fourier transform of r-times the right-hand sides become respectively

$$\widetilde{c\rho(r)}(k)\,\widetilde{v}(k) \quad \text{and} \quad -\,\widetilde{c\rho(r)}(-k)\,\widetilde{v}(k). \quad (4.10)$$

The last result can be shown after a change of variables $r' \to -r'$. For the case that $|r-r'| < \sigma$ and also for the other models, similar expressions can be obtained.

We cannot exploit the separability of the kernels $w^{(i)}$ because of the structure of G_i. It has fractions and logarithms in the unknown function and it would not improve the expressions. Because of this same reason a series expansion of the solution in terms of base functions won't work either: we cannot solve for the coefficients.

We *can* write equation (4.1) in the form

$$y(x) - \int_a^b K(x, t, y(t)) \mathrm{d}t = f(x), \qquad (4.11)$$

where we allow the possibility of integrating over y. This is called the Urysohn equation of the second kind. A solution for these kind of equations is usually found by the successive approximation method,

$$y_{n+1}(x) = f(x) + \int_a^b K(x, t, y_n(t)) \mathrm{d}t. \qquad (4.12)$$

Discretized we arrive at a system of nonlinear equations,

$$y_i - \sum_{i=1}^n A_j K_{ij}(y_j) = f_i, \quad i = 1, \ldots, n, \qquad (4.13)$$

with the approximate values y_i of the solutions $y(x)$ at nodes $x_1, \ldots, x_n$, where $f_i = f(x_i)$ and $K_{ij}(y_j) = K(x_i, t_j, y_j)$ and A_j are the coefficients of the integration method (Riemann, Trapezoidal, Gauss Quadrature,...).

4.1.2 Intermezzo: Picard iteration

Such an iterative procedure is called a Picard iteration. Our equation can be written also be written in this form, since it is an integral equation of the second kind,

$$\rho_{n+1}(r) = \Lambda^{-3} \exp \left[\beta(\mu - V_{\mathrm{ext}}) \right.$$

$$\left. - \int_0^\infty \left(\frac{\partial \Phi(r')}{\partial n_\alpha} \bigg|_{\rho_n} \omega^{(\alpha)}(r, r') + \rho_n(r')\beta\zeta(r, r') \right) r'^2 \mathrm{d}r' \right]. \qquad (4.14)$$

In this iteration process, we must be careful that $n_3 < 1$ strictly for every iteration, since we have a term $\ln(1-n_3)$. Therefore it is necessary to use a relaxation parameter $\alpha \in (0,1)$ and use the following as next approximation,

$$\rho_{n+1}(r) = \alpha \rho'_{n+1}(r) + (1-\alpha)\rho_n(r). \tag{4.15}$$

Here ρ'_{n+1} is obtained by putting ρ_n in equation (4.14). Since n_3 scales linearly with ρ, higher bulk densities require smaller values for α. The trick is to choose α small enough such that the process does not break down, but big enough for fast enough convergence. It can be chosen such that ρ_{n+1} gives the lowest value for the grand potential, since this is what we want to minimize:

$$\Omega[\rho] = \int_0^\infty \left(f_{\text{id}}(r) + f_{\text{hs}}(r) + f_{\text{lr}}(r) + (V_{\text{ext}}(r) - \mu)\rho(r) \right) 4\pi r^2 \mathrm{d}r$$

$$\text{where} \quad f_{\text{id}}(r) = \beta \rho(r)(\ln\Lambda^3 \rho(r) - 1),$$
$$f_{\text{hs}}(r) = \Phi(\rho(r)), \tag{4.16}$$
$$f_{\text{lr}}(r) = \frac{1}{2}\rho(r) \int_0^\infty \rho(r')\zeta(r,r')r'^2 \mathrm{d}r',$$
$$\text{and} \quad V_{\text{ext}}(r) = \phi_{\text{LJ}}(r).$$

There has been done a lot of research of integral equations. Some approximations only work for relatively simple non-linear integral equations, not for the equation we evaluate in this work with weighted forms of the unknown. We will continue with the implementation of the problem.

Chapter 5

Implementation

Let $L=m\sigma$ be the total length of the system, that is $m\in\mathbb{N}$ particle diameters. We take m large enough such that the system shows bulk behavior (the density profile is flat). Furthermore, we take N grid-points per particle diameter, taken to be odd. The total number of grid-points is $M=m(N-1)+1$. The recursive relation (4.14) becomes, with iteration number n,

$$\boldsymbol{\rho}'_{n+1}[r_k] = \Lambda^{-3}\exp\left(\beta(\mu-\boldsymbol{\phi}_{\mathrm{LJ}}[r_k]) - \beta\boldsymbol{\mu}^n_{\mathrm{hs}}[r_k] - \beta\boldsymbol{\mu}^n_{\mathrm{lr}}[r_k]\right). \tag{5.1}$$

In the bulk of the system, that is for $k\in[(N-1)/2, M-(N-1)/2]$, we have for the hard-sphere (local) chemical potential $\boldsymbol{\mu}^n_{\mathrm{hs}}$ (i.e., the derivatives of the hard-sphere free energy expressions (2.91) or (2.92), see also section 3.3) and the weighted density (cf. equation (2.84))

$$\boldsymbol{\mu}^n_{\mathrm{hs}}[r_k] = \frac{1}{\beta}\sum_\alpha\sum_{l=k-(N-1)/2}^{k+(N-1)/2} \frac{\partial\Phi[r_l]}{\partial\mathbf{n}^n_\alpha}\omega^{(\alpha)}[r_k,r_l]r_l^2\frac{1}{N-1} \tag{5.2}$$

$$\text{with } \mathbf{n}^n_\alpha[r_k] = \sum_{l=k-(N-1)/2}^{k+(N-1)/2} \boldsymbol{\rho}_n[r_l]\omega^{(\alpha)}[r_k,r_l]r_l^2\frac{1}{N-1}$$

Here $1/(N-1)$ is the grid-spacing. When $k\in[0,(N-1)/2)$ the bounds of the summation index over l change to $[(N-1)/2-k,(N-1)/2+k)$ for $\alpha\neq3$, and to $[0...(N-1)/2+k)$ for $\alpha=3$. This is due to the definition of the functions ω^α; the third function is also defined for $r\in[0,R-r]$ whereas the others are not. For $k\in((N-1)/2, M-1]$ we use a reflexive boundary condition. This means that for l that are outside of the grid (i.e., $l\in[M, M+(N-1)/2]$) we take

$$\boldsymbol{\rho}_n[r_l] = \boldsymbol{\rho}_n[r_{2(M-1)-l}]. \tag{5.3}$$

We can use reflexive boundary conditions since the range of the convolution is small (half a particle diameter) and the density profile should be flat at the end of the domain.

For the long ranged part (cf. equation(4.16)) we take

$$\boldsymbol{\mu}_{\mathrm{lr}}^{\mathrm{n}}[r_k] = \sum_{l=0}^{M-1} \boldsymbol{\rho}_{\mathrm{n}}[r_l]\zeta[r_k, r_l]r_l^2 \frac{1}{N-1} + \boldsymbol{\rho}_{\mathrm{n}}[r_{M-1}]\mathbf{b}[r_k] \tag{5.4}$$

$$\text{with } \mathbf{b}[r_k] = \int_L^\infty \zeta(r_k, r')r'^2 \mathrm{d}r'.$$

So the part of the convolution that is outside the grid is added as a source, where the density is taken to be constant. This is not taken to be the bulk density ρ_{b}, but the last point of the grid $\boldsymbol{\rho}_{\mathrm{n}}[r_{M-1}]$. In the former case a discontinuity in the density, that is a difference of the bulk density and the endpoint of the solution $(\rho_{\mathrm{b}} - \boldsymbol{\rho}_{\mathrm{n}}[r_{M-1}])$, would lead to another external force. Here the discretized external potential (cf. equation (2.132)) is

$$\boldsymbol{\phi}_{\mathrm{LJ}}[r_k] = 4\varepsilon\left(\frac{\sigma^{12}}{r_k^{12}} - \frac{\sigma^6}{r_k^6}\right) - 4\varepsilon\left(\frac{\sigma^{12}}{L^{12}} - \frac{\sigma^6}{L^6}\right). \tag{5.5}$$

The last term is necessary in order to make sure that the potential has a range of exactly L, so $\phi_{\mathrm{LJ}}(r) = 0$ for all $r \geq L$. This is again necessary since the bulk chemical potential is taken to be a value of constant density when there is no external potential. A nonzero value of the external potential at the end of the grid would greatly influence the solution, even though it is small ($\sim 10^{-6}$). It is not necessary to have a zero potential for some range of grid-points at the end of the system, but it is necessary that there is no 'jump' discontinuity, which would result in an external force.

For a flat density profile where the density is equal to the bulk density ρ_b, it is important that all the discrete summations yield the exact value of the integral because the local chemical potentials ($\boldsymbol{\mu}_{\mathrm{hs}}$ and $\boldsymbol{\mu}_{\mathrm{lr}}$) must add up to the bulk chemical potential μ. That is, all the row sums of the matrices in the calculation of the weighted densities n_α and of $\boldsymbol{\mu}_{\mathrm{lr}}$ must be as close to a constant as possible. Specifically, we must have for all $k \in [0, M-1]$ that

$$\sum_{l=0}^{M-1} \omega^{(2)}[r_k, r_l]r_l^2 \to \pi\sigma^2,$$

$$\sum_{l=0}^{M-1} \omega^{(V2)}[r_k, r_l]r_l^2 \to 0, \tag{5.6}$$

$$\sum_{l=0}^{M-1} \omega^{(3)}[r_k, r_l] r_l^2 \rightarrow \frac{\pi\sigma^3}{6} \qquad (5.7)$$

and

$$\sum_{l=0}^{M-1} \zeta_{\text{LJ}}^{(1)}[r_k, r_l] r_l^2 + \mathbf{b}_{\text{LJ}}^{(1)}[r_k] \rightarrow -\frac{32\pi\sigma^3\varepsilon}{9},$$

$$\sum_{l=0}^{M-1} \zeta_{\text{WCA}}[r_k, r_l] r_l^2 + \mathbf{b}_{\text{WCA}}[r_k] \rightarrow -\frac{4\pi r_{\text{req}}^3 \varepsilon}{3}\left(1+\frac{4\sigma^6}{r_{\text{eq}}^6}-\frac{4\sigma^{12}}{3r_{\text{eq}}^{12}}\right), \qquad (5.8)$$

$$\sum_{l=0}^{M-1} \zeta_{\text{LJ}}^{(2)}[r_k, r_l] r_l^2 + \mathbf{b}_{\text{LJ}}^{(2)}[r_k] \rightarrow \frac{512\pi\sigma^3\varepsilon^2}{315}.$$

In figures 5.1 and 5.2 we see the error for the discrete sums of $\omega^{(V2)}$ and $\omega^{(3)}$ for a system length L of 10σ. The error for a trapezoidal integration method is $\mathcal{O}(N^{-2})$ and for a Riemann integration method $\mathcal{O}(N^{-1})$. The function $\omega^{(V2)}$ scales as r^{-2} and $\omega^{(3)}$ scales as r^{-1}, hence the difference in shape of the curves. The function $\omega^{(2)}$ is linear in r' and hence exact for Riemann and trapezoidal integration. Similar scaling behavior holds for the different ζ.

The grand potential as in equation (4.16) is calculated as follows.

$$\Omega[\boldsymbol{\rho}_{\text{n}}] = \sum_{k=0}^{M-1} \left(\mathbf{f}_{\text{id}}^{\text{n}}[r_k] + \mathbf{f}_{\text{hs}}^{\text{n}}[r_k] + \mathbf{f}_{\text{lr}}^{\text{n}}[r_k] + (\boldsymbol{\phi}_{\text{LJ}}[r_k]-\mu)\boldsymbol{\rho}_{\text{n}}[r_k] \right) 4\pi r_k^2 \frac{1}{N-1}$$

$$\text{where} \quad \mathbf{f}_{\text{id}}^{\text{n}}[r_k] = \beta\boldsymbol{\rho}_{\text{n}}[r_k](\ln\Lambda^3\boldsymbol{\rho}_{\text{n}}[r_k]-1),$$

$$\mathbf{f}_{\text{hs}}^{\text{n}}[r_k] = \Phi(\boldsymbol{\rho}_{\text{n}}[r_k]), \qquad (5.9)$$

$$\mathbf{f}_{\text{lr}}^{\text{n}}[r_k] = \frac{1}{2}\boldsymbol{\rho}_{\text{n}}[r_k]\left(\sum_{l=0}^{M-1} \boldsymbol{\rho}_{\text{n}}[r_l]\zeta[r_k, r_l] r_l^2 \frac{1}{N-1}+\boldsymbol{\rho}_{\text{n}}[r_{M-1}]\mathbf{b}[r_k] \right),$$

and the external potential $\boldsymbol{\phi}_{\text{LJ}}$ is as in equation (5.5). Note that we cut off the sum over k at M. We can do this because we assume that the length of the system L is chosen such that the density is flat at the end of the system and the local chemical potentials ($\boldsymbol{\mu}_{\text{id}}$, $\boldsymbol{\mu}_{\text{hs}}$ and $\boldsymbol{\mu}_{\text{lr}}$) add up to the constant μ. This means that we leave out a constant term in Ω and it has no influence on the *minimum* of the functional, even though Ω is an extensive property (it scales with the size of the system). That is, we do not include $\mathbf{f}_{\text{id}}^{\text{n}}[r_k]$, $\mathbf{f}_{\text{hs}}^{\text{n}}[r_k]$ and $\mathbf{f}_{\text{lr}}^{\text{n}}[r_k]$ for $k \geq M$ because they are all constant by assumption ($\boldsymbol{\rho}_{\text{n}}[r_k]=\rho_b$ for $k \geq M$).
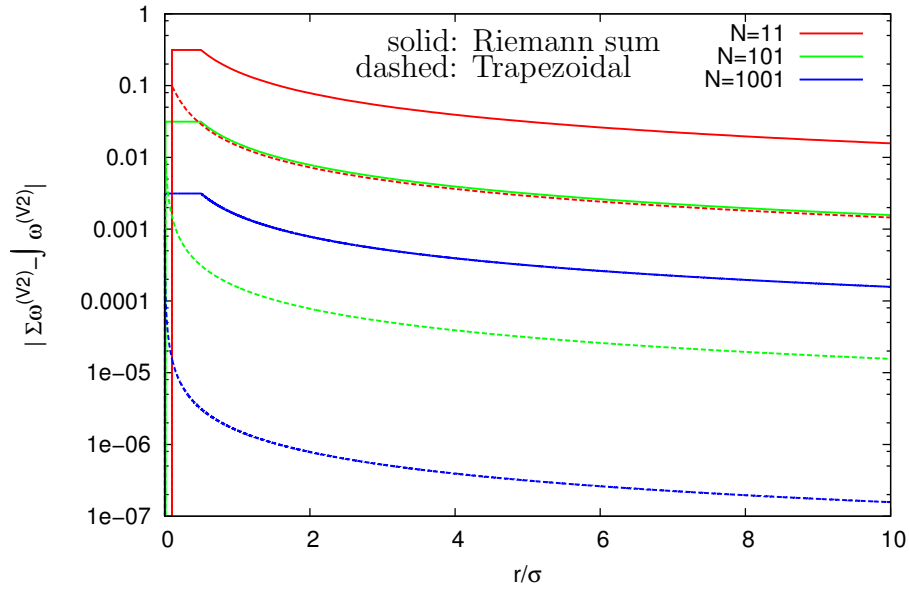
Figure 5.1: The error of the discrete sums of the rows of the matrix $\omega^{(V2)}$, for a different number of points in the bandwidth N. Here $L=10\sigma$.
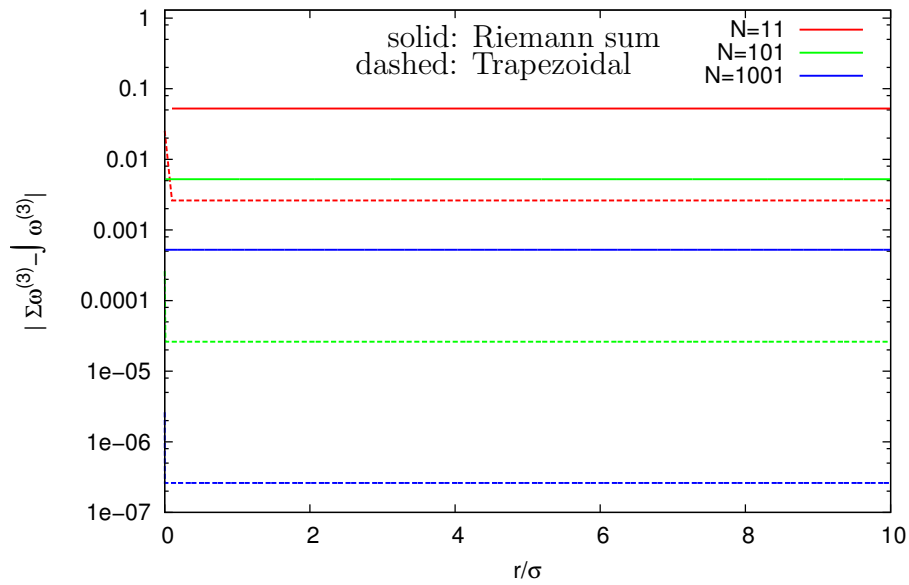

Figure 5.2: The error of the discrete sums of the rows of the matrix $\omega^{(3)}$, for a different number of points in the bandwidth N. Here $L=10\sigma$.

It is necessary to use a relaxation if the initial condition (IC) is not close to the solution,

$$\boldsymbol{\rho}_{n+1} = (1-\alpha)\boldsymbol{\rho}_n + \alpha\boldsymbol{\rho}'_{n+1}. \tag{5.10}$$

We cannot use $\alpha=1$ because the vector $\mathbf{n}_3^n$ can become larger than 1 when $\boldsymbol{\rho}'_{n+1}$ from equation 5.1 is used. From the equations in the overview we see that $\mathbf{n}_3^n \geq 1$ gives values which are not a number. Physically, for bulk systems, the quantity n_3 reduces to the packing fraction $\xi=\pi\rho\sigma^3/6$, which is the fraction of space which is occupied. Naturally this cannot be larger than 1. For inhomogeneous systems ρ *can* (locally) be larger than $6/\pi\sigma^3$, as long as the *weighted* density n_3 remains smaller than 1. This means that curves with large narrow peaks can be solutions.

We can search for an optimal value for α. It must be large enough to give fast convergence and small enough to prevent divergence. In figure 5.3 we plot optimal constant α for a density range for a system of hard spheres (so no perturbation) with ϕ_{LJ} (the Lennard-Jones potential) as external potential. Here we mean by optimal, that we minimize $\|\boldsymbol{\rho}_{100}-\boldsymbol{\rho}_{99}\|_2$ with respect to α. We do this optimizing with the Newton-Raphson method,

$$\alpha_{i+1} = \alpha_i - \frac{f(\alpha_i)}{f'(\alpha_i)}, \tag{5.11}$$

where f is $\|\boldsymbol{\rho}_{100}-\boldsymbol{\rho}_{99}\|_2$ for a given α and f' is the (numerically calculated) derivative of f with respect to α. The tolerance is chosen as 10^{-5}. In figure 5.3 we see that for higher bulk densities, a lower coupling parameter is needed. This makes sense since for high densities there is more tendency to large oscillations and more care is needed. Also a larger effective diameter increases the (hard sphere part of the) free energy and also lower values for α are needed as we see from the figure. In some sense this is still not the optimal choice for α since there is a different optimum for a minimal Ω in every iteration. We can calculate the minimum for Ω as a function of α for every iteration. In figure 5.4 we see that not for every iteration there is a minimal α. In figure 5.5 we see that after a large value for α, the maximum value for n_3 increases in the following iteration. Thereafter a low value for α is needed and the result is an oscillating behavior for the optimal coupling parameter α_n per iteration n. We also observe that the functional does not decrease monotonously and requires less iteration than the optimal constant α. The error of the norm also shows oscillating behavior, but at some point the differences in the grand potential for different α are so small that the optimization algorithm picks the initial guess for α_n, see figure 5.7. The optimized version is stopped after 200 iterations, that's why the errors are not the same, when the iteration process stops. The plots 5.4-5.7 are made without perturbation term, with
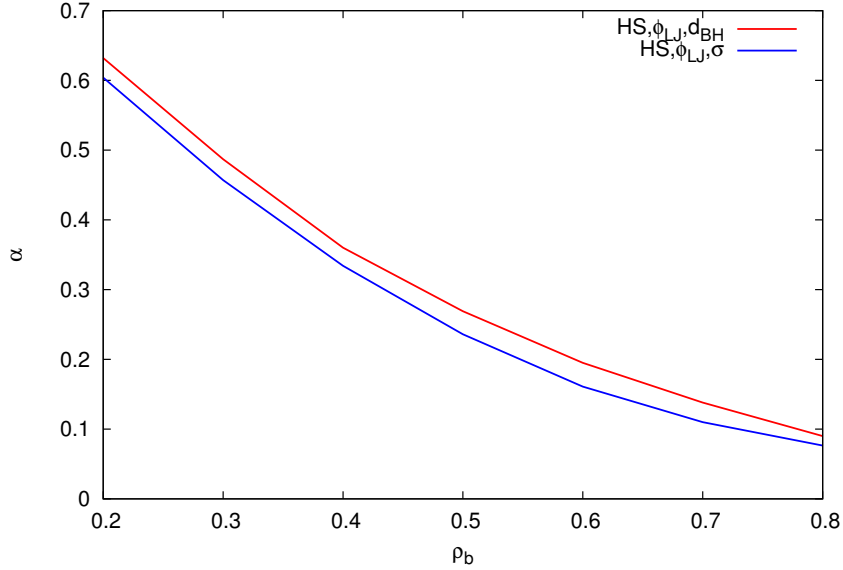
Figure 5.3: The optimal coupling parameter for the model without the perturbation as a function of bulk density, for an effective diameter of $d_{\mathrm{BH}}=0.973\sigma$ and σ respectively.

effective diameter σ, $kT=1.0$ and $\rho_b=0.9$ and the curves are with constant coupling parameter has $\alpha_{\mathrm{opt}}=0.0619$ (from figure 5.3). We conclude that the cost for finding an optimal, iteration varying coupling parameter does not decrease the total computational cost. Nor can we find a basic structure in the variation of α_n.

The stopping criterion in out models is the 2-norm of the difference of the solution in the last two iterations,

$$\| \boldsymbol{\rho}_{\mathrm{n}+1}-\boldsymbol{\rho}_{\mathrm{n}} \|_2 < \epsilon, \tag{5.12}$$

where for safety we take $\epsilon=10^{-8}$, but 10^{-7} or 10^{-6} also suffice. The initial condition is taken to be ρ_b on the whole domain. In the absence of the external potential the systems then converges in a single iteration.

In figure 5.9 we see a typical convergence plot for model 1A. It shows the ratio of the error made in the kth iteration with respect to the $k-1$st iteration for the hs part, the lr part and for the density (resp. eqs. (5.2), (5.4) and (5.1)). We see that this does not become constant; at best eventually linear. When the error becomes very small (smaller than 10^{18}) the ratio starts fluctuating for the hs and lr part. These are rounding errors, as the error is very small.
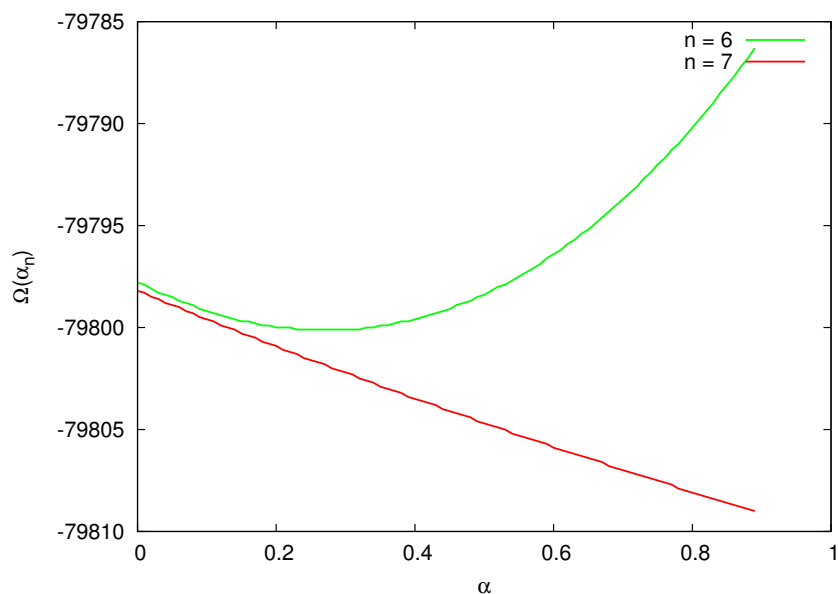
Figure 5.4: Here we see Ω after iteration 6 and 7 respectively, as a function of the coupling parameter.
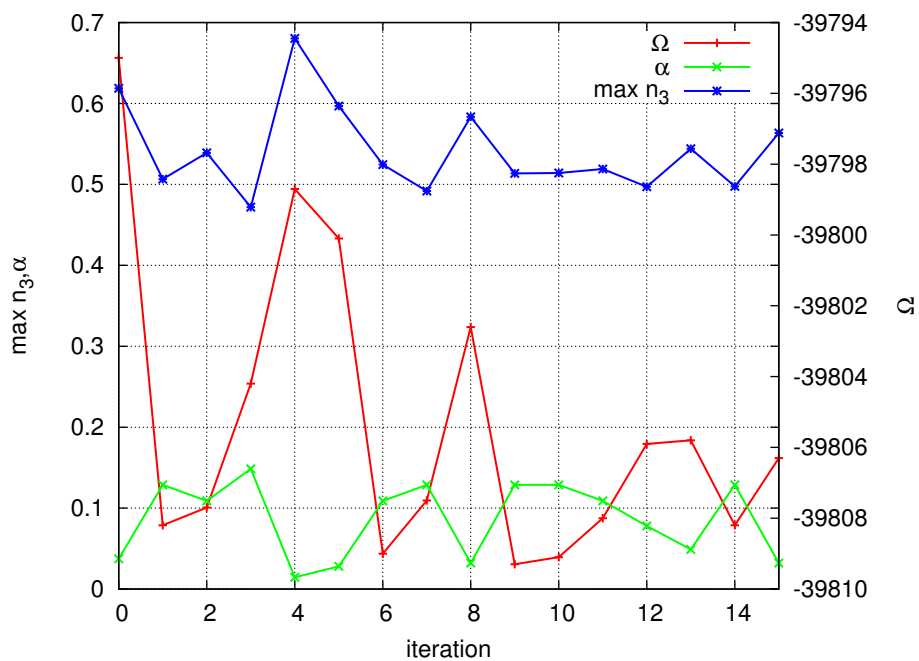
Figure 5.5: The grand potential Ω on the right, and the maximal value of n_3 and the optimal value for α_n on the left for the first few iterations.
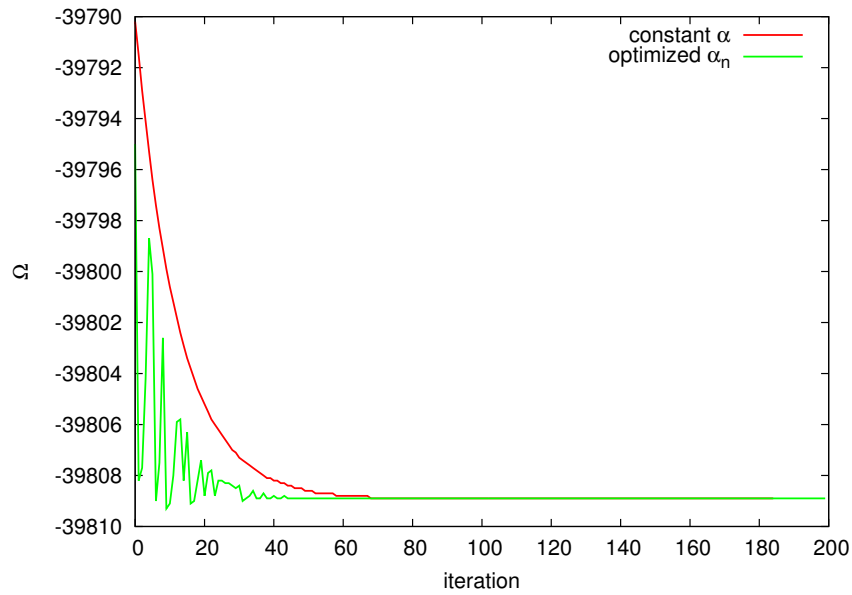
Figure 5.6: The functional Ω per iteration for a constant α and an optimized α_n. There is no perturbation term included, effective diameter σ, kT=1.0 and ρ_b=0.9 and the curves are with constant α_{opt}=0.0619

Figure 5.7: The error between two consecutive iterations per iteration for a constant α and an optimized α_n. There is no perturbation term included, effective diameter σ, kT=1.0 and ρ_b=0.9 and the curves are with constant α_{opt}=0.0619

Figure 5.8: The error per iteration compared to the solution in iteration 100 ($\| \boldsymbol{\rho}_{100} - \boldsymbol{\rho}_{\mathrm{n}} \|_2$). There is no perturbation term included, effective diameter σ, $kT = 1.0$ and $\rho_b = 0.9$ and the curves are with constant $\alpha_{\mathrm{opt}} = 0.0619$

In figure 5.10 we can see the ratio of the error made in the kth iteration with respect to the $k-1$st iteration for the density (eq. (5.1)) for different relaxation parameters. We see that with a larger relaxation parameter α, the problem converges faster. But when it is chosen too large, the convergence in the first iterations is not guaranteed.

The grid spacing $1/(N-1)$ is taken to be 0.01. In figure 5.11 we see that a larger grid spacing would lead to inaccurate solutions, because of the oscillating behavior of the curves.
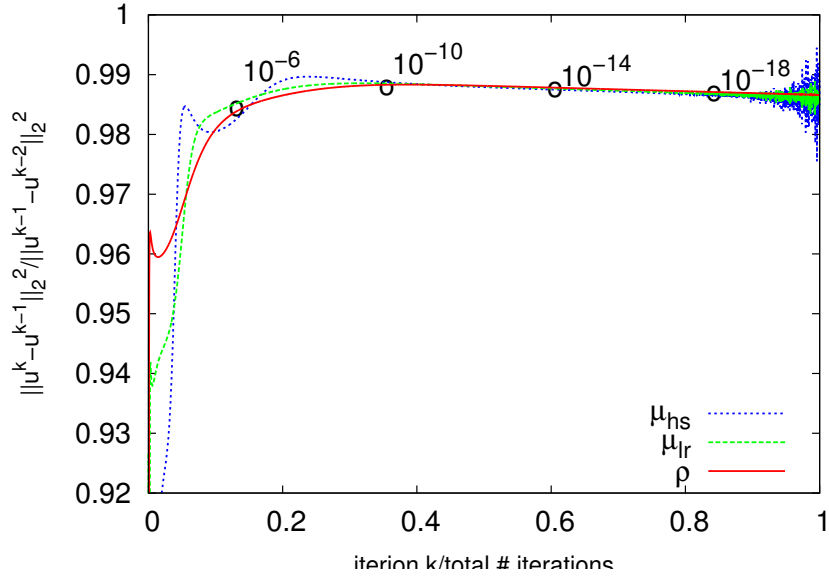
Figure 5.9: The ratio of two consecutive updates for the components ($\boldsymbol{\mu}_{\text{hs}}$ and $\boldsymbol{\mu}_{\text{lr}}$ in resp. eqs. (5.2) and (5.4)) and the density ($\boldsymbol{\rho}$ eq. (5.1)) of the equation we are solving (see section 3.3). The relaxation parameter α is 0.025 (see eq. (5.10)) and the allowed error ϵ^2 is 10^{-21} The labeled points in the graph indicate how small the error is. The initial condition is $\rho_{\text{bulk}}=0.9$ on the whole domain.
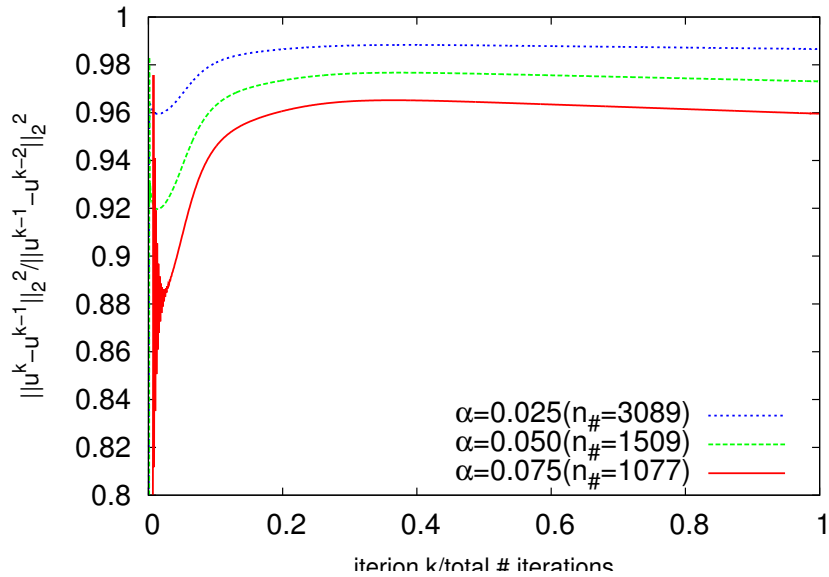
Figure 5.10: The ratio of two consecutive updates for $\boldsymbol{\rho}$ (see eq. (5.1)) for different relaxation parameters α (see eq. (5.10)) and the allowed error ϵ^2 is 10^{-21} The initial condition is $\rho_{\text{bulk}}=0.9$ on the whole domain.

82
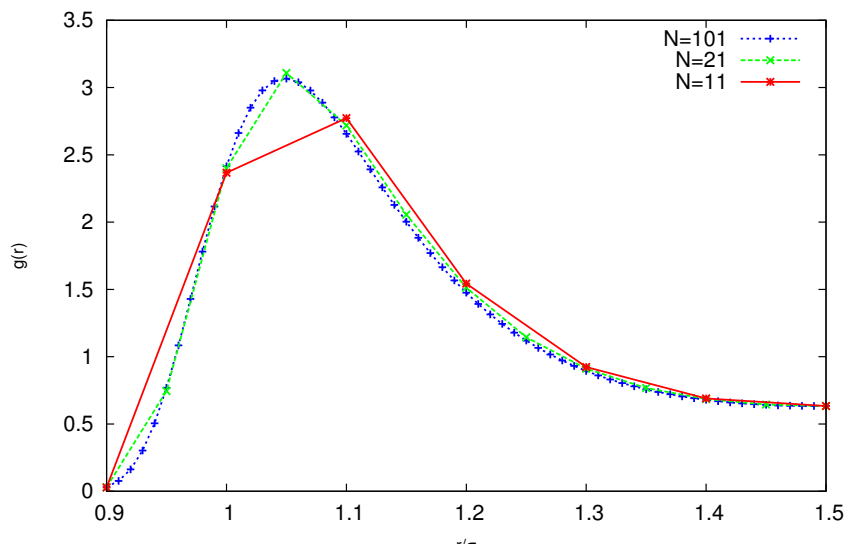
Figure 5.11: Radial distribution function for results with grid spacing $1/(N-1)$ of 0.01, 0.05 and 0.1 respectively.

Chapter 6

Results

In this chapter we will apply the models described before. In table 6.1 an overview of the models and their names is given. The results are presented in reduced coordinates. This means that the quantities are unitless, the reduced temperature is given by $T^*=kT/\varepsilon$ and the reduced density by $\rho^*=\rho\sigma^3$. Essentially we rescale the units of energy and distance. Numerically, we put $\sigma=1$ and $\varepsilon=1$. Note that it is not important how we scale the mass m in the thermal wavelength Λ, since the constant also appears in the bulk chemical potential μ and they cancel, see equation (3.43).

Table 6.1: An overview of the models and how they are referred to.

Abbreviation	Description	section
HS	Reference system, (no perturbation)	
BH	Mean Field (BH-split), high density approx.	3.2.1
WCA	Mean Field (WCA-split), high density approx.	3.2.2
MMF	Modified Mean Field, low density approx.	3.2.3

First we discuss the limiting cases of the reduced density. In section 6.1 we discuss the low density limit and in section 6.2 we discuss high densities. The work in these sections is all done with the WB hard-sphere function. In section 6.3 we compare the RF and WB versions. Next, in section 6.4, we evaluate fluid properties which follow from the radial distribution function.

6.1 Low Densities

In figure 6.1 radial distribution functions are shown for temperatures T^*=1.1, T^*=1.2 and T^*=1.3 for a density of ρ_b^*=0.1. The molecular dynamic results show a first solvation shell and a small second shell. The MMF model closely follows the second shell, whereas the HS model fails to predict any structure beyond the first shell. The magnitude of the first shell decreases with increasing temperature and is systematically overestimated the MMF model and underestimated by the HS model, see table 6.2. For T^*=1.3 the peaks get close. (The effective diameter is taken to be σ, but in the low density limit it does not play a large role)

Table 6.2: Maximal point for the radial distribution functions of figure 6.1.

T^*	MD	MMF	HS
1.1	2.600	2.656	2.377
1.2	2.335	2.392	2.185
1.3	2.166	2.157	2.122

In figure 6.2 we see rdf's at a temperature of T^*=1.3 and bulk densities ρ_b^*=0.1, ρ_b^*=0.2, ρ_b^*=0.3 and ρ_b^*=0.4. We observe that the perturbation decreases the first peak for a density of ρ_b^*=0.4, while it increases the peak for densities of ρ_b^*=0.1 and 0.2. The MMF model starts to overestimate the oscillations also for the second solvation shell. The HS model reveals also a second peak, that is, it predicts stronger correlations. The interpolation (or extrapolation) between the HS and MMF curves are not linear in ε, but quadratic; see figure 6.3 and section 3.2.3. The contribution to the second shell is apparent. In figure 6.4 results are shown for model 2 with an effective diameter of 0.968σ (which follows from equation (2.131)), that means that the free energy density of the reference system is lower compared to an effective diameter of σ and the result is that the particle density becomes larger. An effective diameter larger than σ leads for low densities to lower particle densities which can also be seen in figure 6.4. The plots with an arbitrary effective diameter of 1.03σ show that such an effective diameter does not lead to better results for higher densities.

In figure 6.5 a typical plot for all models in the low density regime is given. The LJ model does not differ much from the HS model (i.e., the perturbation is so small that it barely makes a difference) and the WCA model is too attractive, resulting in high particle densities.
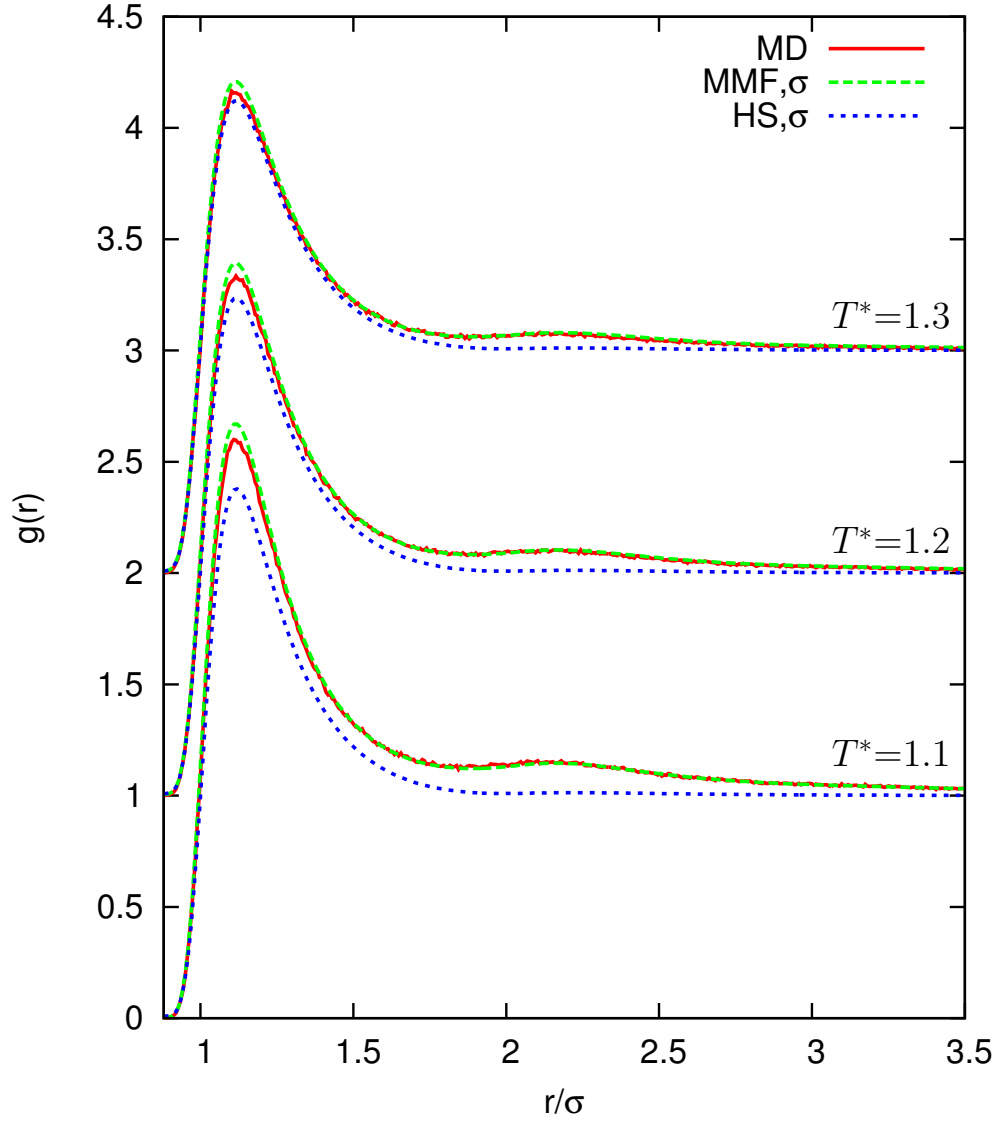
Figure 6.1: Radial distribution functions for soft particles for a density of ρ_b^*=0.1, obtained from correlation around a soft particle in the origin as an external potential. The MD results are from [1]. The lines for temperatures $T^* = 1.2$ and $T^* = 1.3$ are for clarity shifted up by 1 and 2 units respectively. The effective diameter for the reference system is taken to be σ.
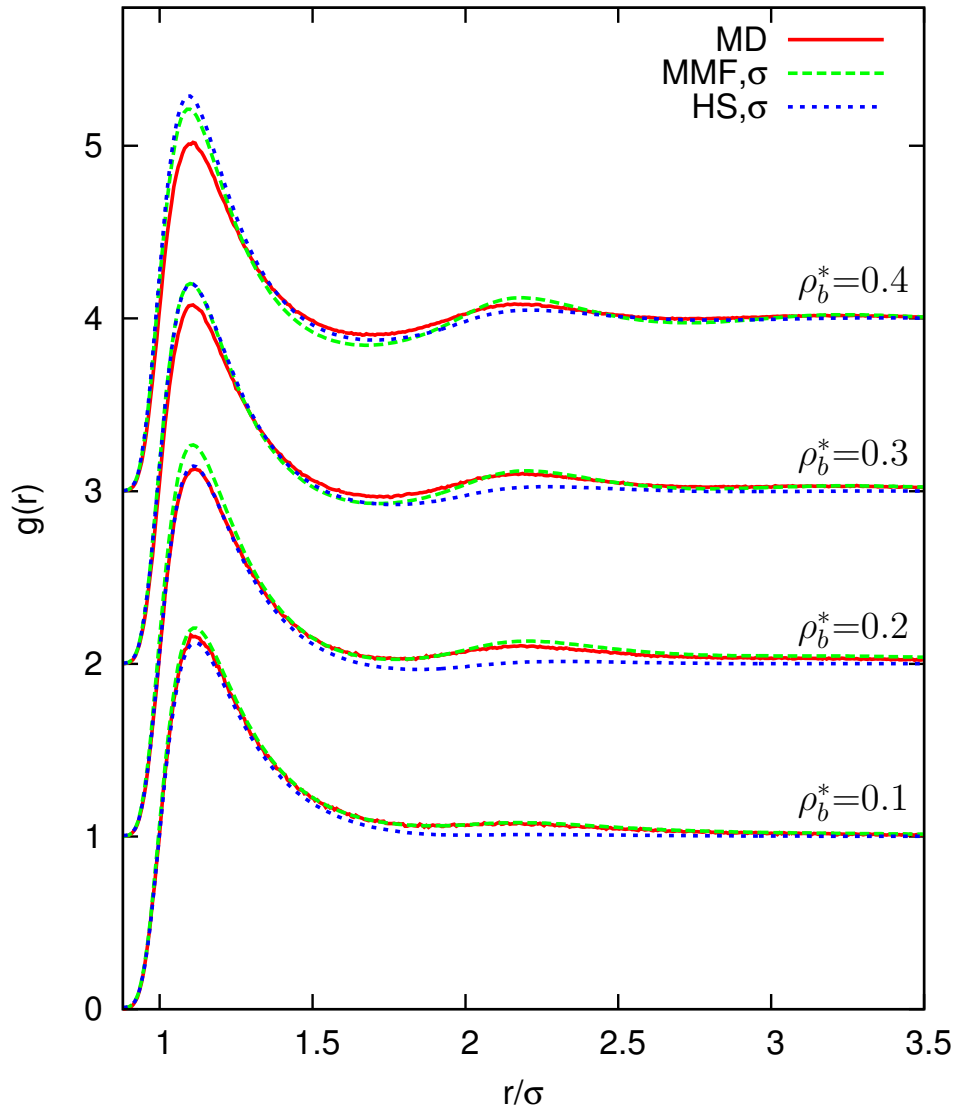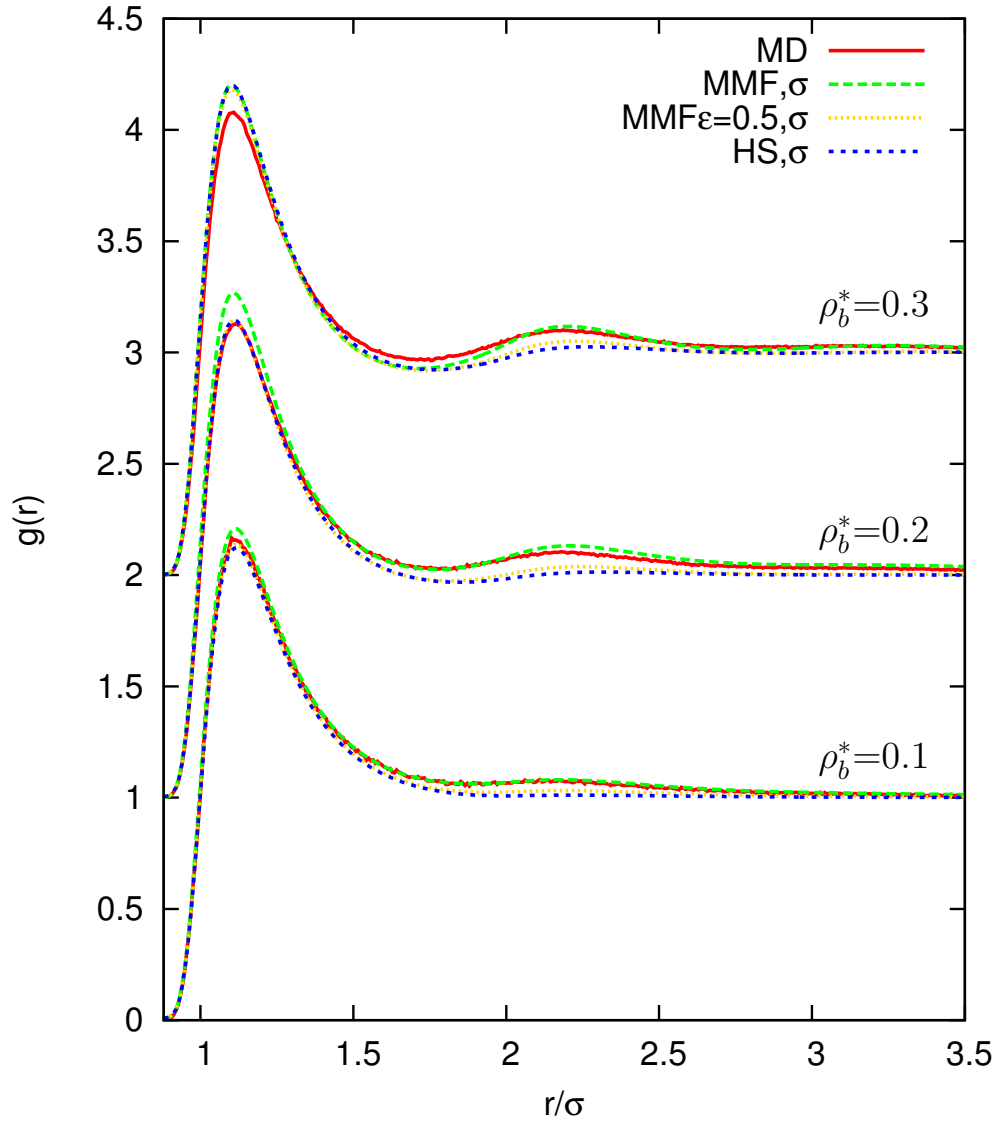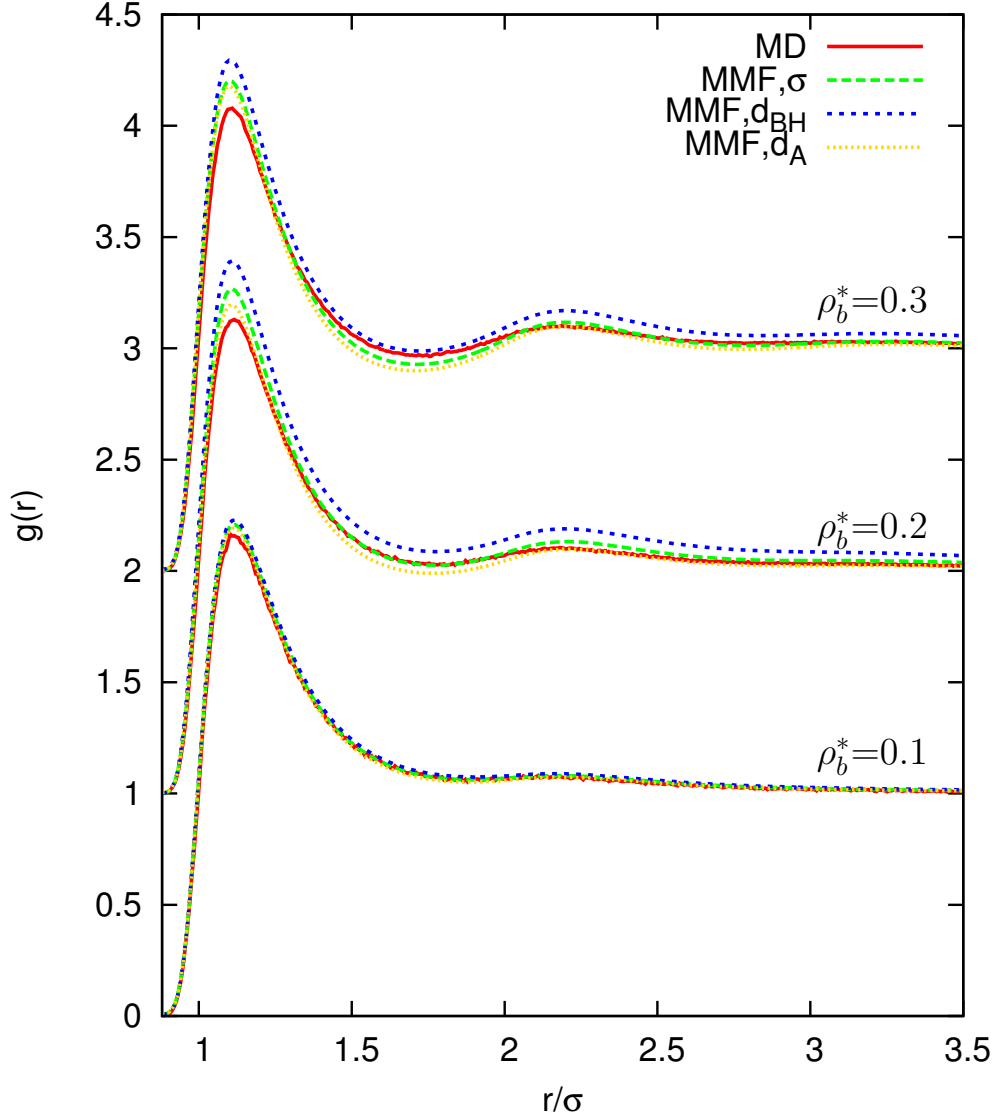
Figure 6.2: Radial distribution functions for soft particles at a temperature of $T^*=1.3$, obtained from correlation around a soft particle in the origin as an external potential. The MD results are from [1]. The lines for temperatures $\rho^*=0.2$, $\rho^*=0.3$ and $\rho^* = 0.4$ are for clarity shifted up by 1, 2 and 3 units respectively. The effective diameter for the reference system is taken to be σ.

Figure 6.3: Radial distribution functions for soft particles at a temperature of T^*=1.3, obtained from correlation around a soft particle in the origin as an external potential. The MD results are from [1]. The lines for temperatures ρ^*=0.2 and ρ^*=0.3 are for clarity shifted up by 1 and 2 units respectively. The effective diameter for the reference system is taken to be σ.

Figure 6.4: Radial distribution functions for soft particles at a temperature of $T^*=1.3$, obtained from correlation around a soft particle in the origin as an external potential. The MMFσ lines are the low density approximation with effective diameter σ, the MMF$d_{\mathrm{BH}}=0.968\sigma$ are lines with smaller repulsions and MMF$d_{\mathrm{A}}=1.03\sigma$ are lines with larger repulsions. The MD results are from [1]. The lines for temperatures $\rho^*=0.2$ and $\rho^*=0.3$ are for clarity shifted up by 1 and 2 units respectively.
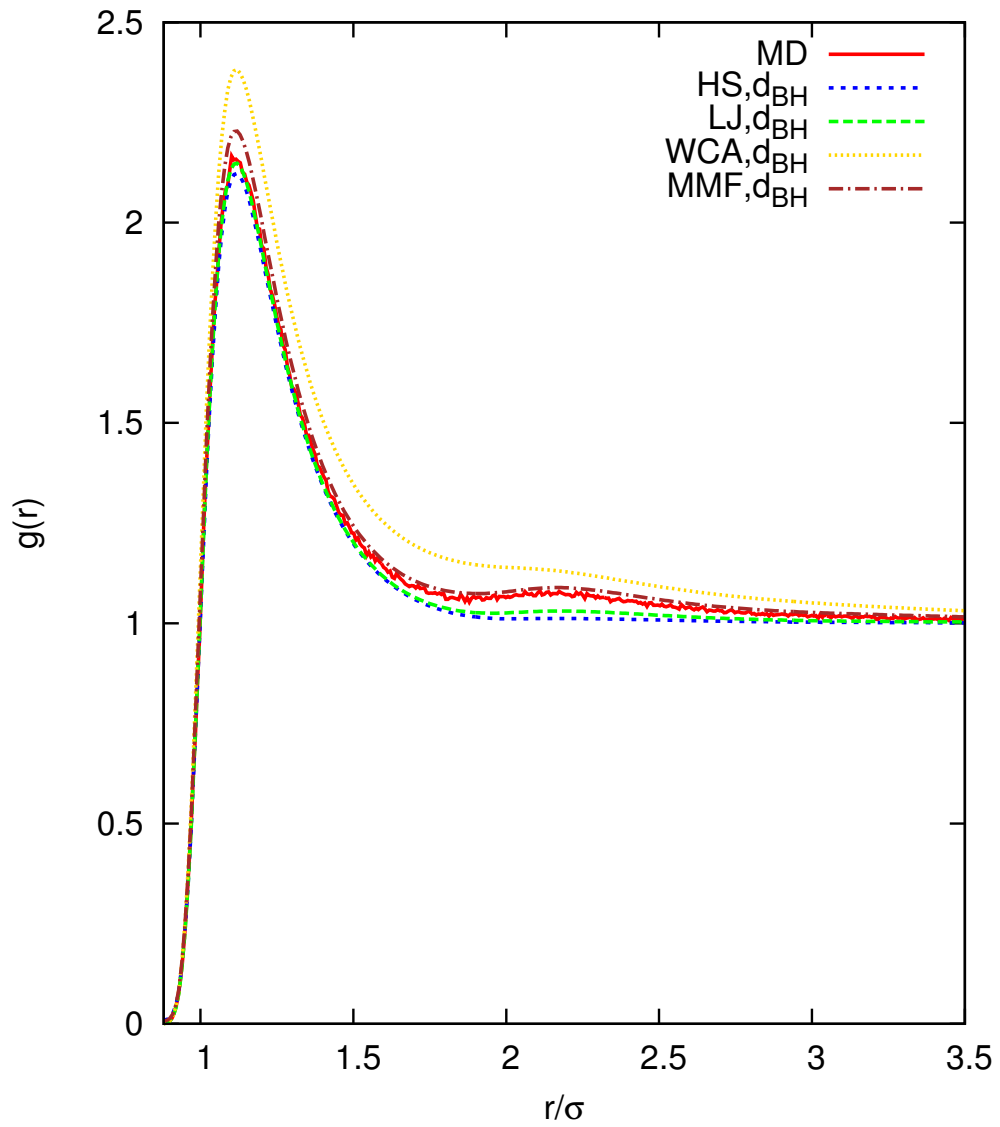
Figure 6.5: Radial distribution functions for soft particles at a temperature of T^*=1.3 and a density of ρ^*=0.1, obtained from correlation around a soft particle in the origin as an external potential. The MD results are from [1] and the effective diameter d_{BH} is 0.967σ.

6.2 High Densities

It is known that for high densities the repulsive forces are dominant, since the particles are on average so close together that they are mainly repulsive. The attractive forces can be treated as a uniform background force. For the test-particle method and inhomogeneous density profiles this also holds, except perhaps near the particle itself. In figure 6.6 we see a plot of the HS and WCA model for a high density range (ρ^*=0.6, 0.7, 0.8 and 0.9) for a temperature of T^*=1.0 compared with simulations. Indeed we see that the repulsions dominate: the perturbation has little or no effect for r>2σ and the curves agree with the molecular dynamics. (The deviation from MD for the second shell for the highest densities (ρ^*=0.9) are typical for the FMT approach, see e.g. [18] for a density profile of hard spheres near a hard wall with similar behavior.)

The reference system (HS) however overestimates the first shell and the perturbation (WCA) to some extent corrects for this. When the perturbation becomes stronger (i.e., for increased ε in ζ) we obtain a measure for the strength of the short-ranged attractions. In table 6.3 we give the values as a function of density and temperature obtained by trial and error to let the first solvation shell agree with the simulations. For the effective diameter we use the BH effective diameter, see table 6.3. Note that for a homogeneous system the WCA effective diameter is larger than σ. We find that for inhomogeneous (liquid) densities this is too high, as also observed by Tang who calculated profiles in slit-like pores.[32] In figures 6.7, 6.8 and 6.9 we show the profiles with the adjusted perturbation corresponding to table 6.3. We see perfect agreement for ρ^*=0.7, but for higher densities the oscillations are a bit out of phase, which is due to the reference system. A higher effective diameter will shift the peaks to the left but also increases the magnitude. The perturbation cannot correct for, this since it decreases the magnitude of the first peak but only increases the others further, see figure 6.10 for an example with a large value for α. This means that we are not able to obtain better results by using other effective diameters.

Note that adapting the values of ε in the perturbation does not mean that we change the interaction potential, but merely that we correct for the non-homogeneity of the correlation between the particles since we assume that g is uniform in this mean field approximation. Since the perturbation has no effect for long ranges we may assume that the radial distribution function for the inhomogeneous system has the value of ε from table 6.3 and then continuously approaches 1.

In figure 6.11 we see again that the LJ model is similar to the HS model, although it does overestimate the oscillations beyond the first peak. Contrary

to the low density limit, now the WCA model gives better solutions and the MMF model overestimates the correlations. This is vice versa to figure 6.5. We conclude that the actual shape of the approximation of the long ranged interactions makes a difference, not merely the magnitude.

Table 6.3: The interaction strength $\varepsilon := \varepsilon(T^*, \rho^*)$ as a function of density and temperature, and the BH effective diameter $d_{\mathrm{BH}} := d_{\mathrm{BH}}(T^*)$ according to equation (2.131).

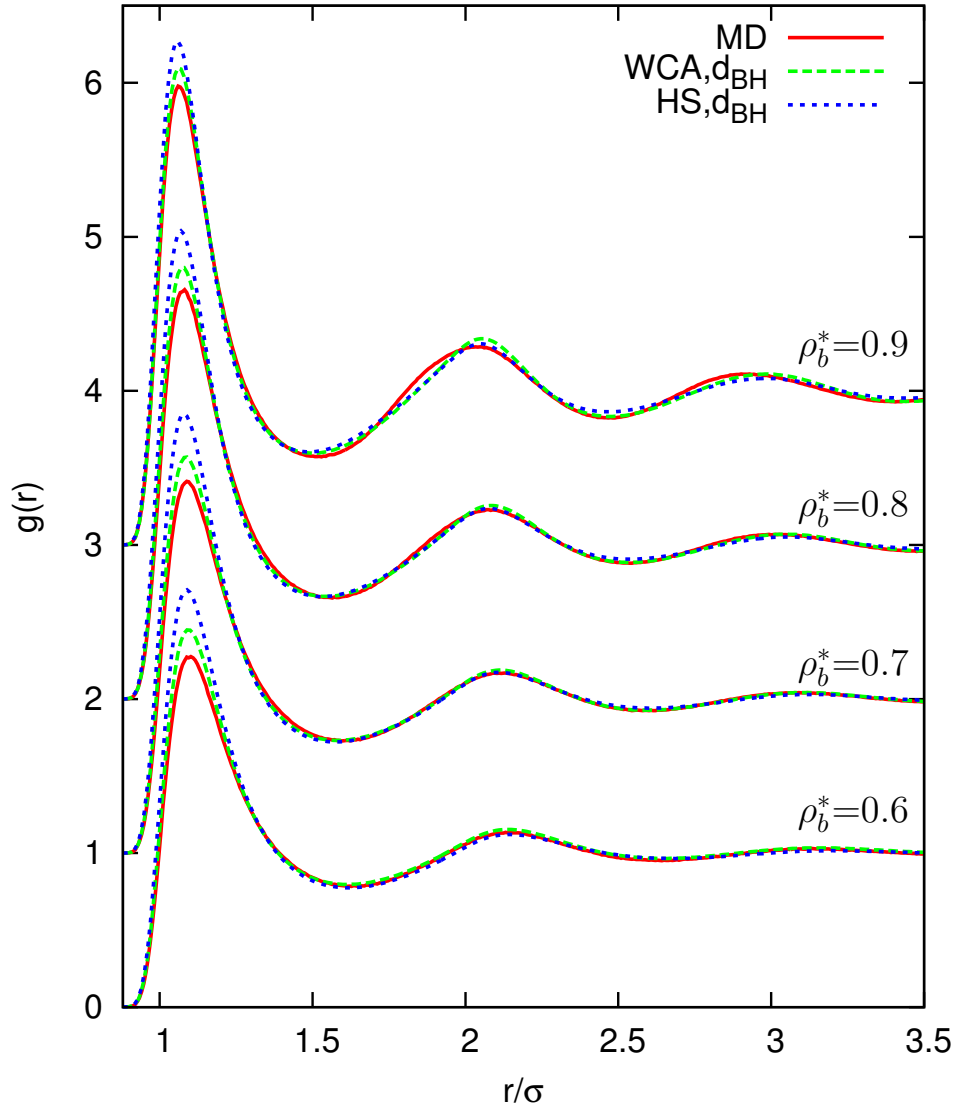| $T^* \backslash \rho^*$	0.7	0.8	0.9	d_{BH}/σ
0.9	1.17	1.30	1.40	0.977
1.0	1.22	1.35	1.45	0.975
1.1	1.26	1.38	1.50	0.973
1.2	1.30	1.42	1.55	0.969
1.3	1.33	1.47	1.65	0.967

Figure 6.6: Radial distribution functions for soft particles at a temperature of $T^*=1.0$, obtained from correlation around a soft particle in the origin as an external potential. The MD results are from [1]. The lines for densities $\rho^*=0.7$, $\rho^*=0.8$ and $\rho^*=0.9$ are for clarity shifted up by 1, 2 and 3 units respectively. The effective diameter for the reference system is taken to be $d_{\mathrm{BH}}=0.973\sigma$.
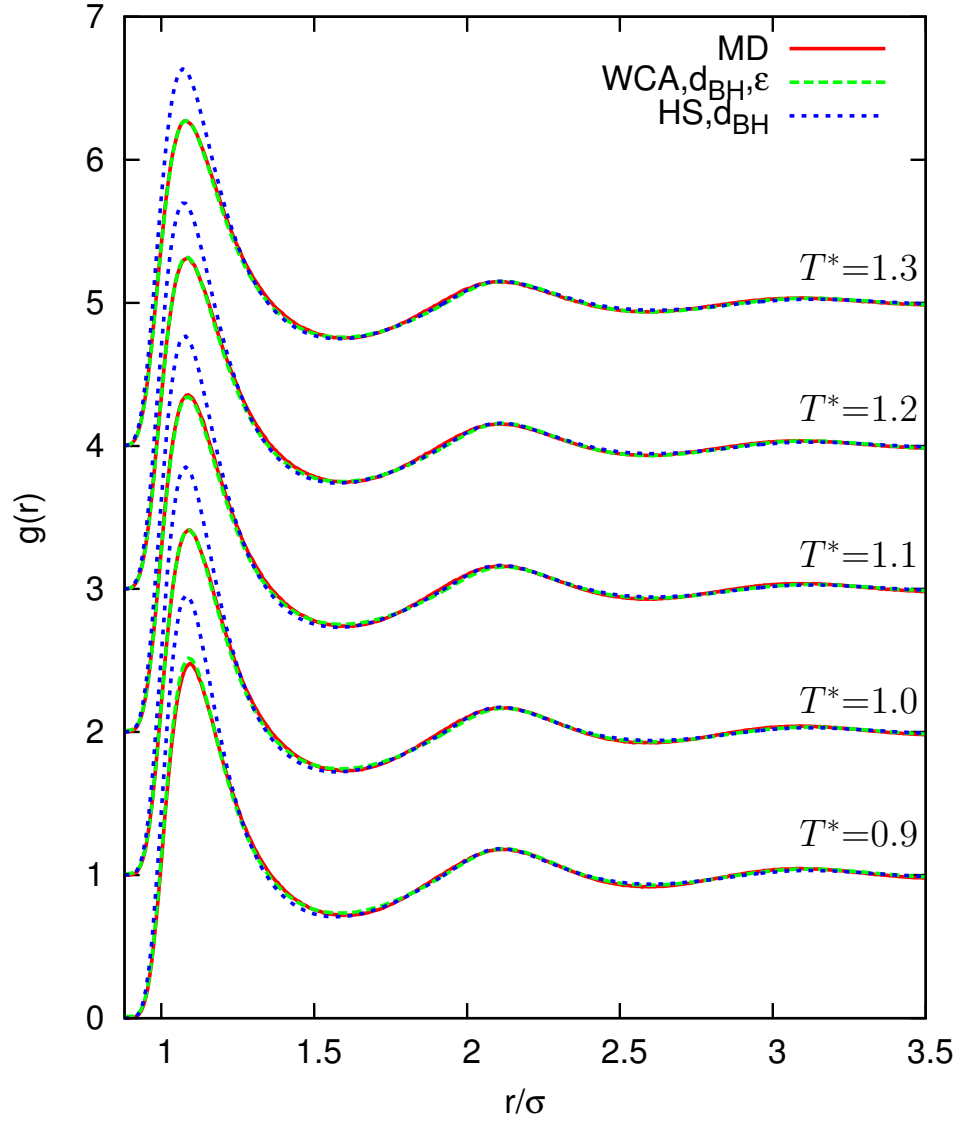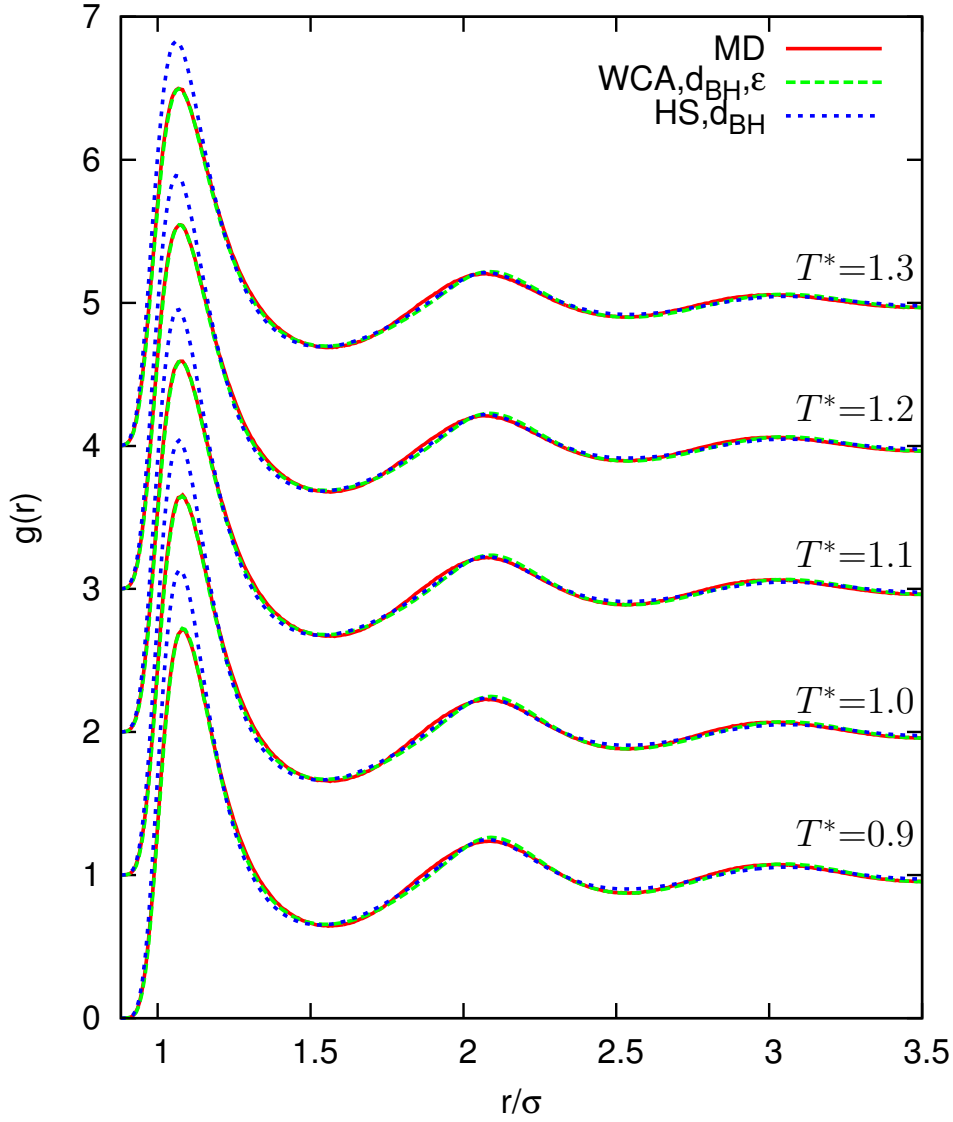
Figure 6.7: Radial distribution functions for soft particles at a density of ρ^*=0.7, obtained from correlation around a soft particle in the origin as an external potential. The MD results are from [1]. The lines for T^*=1.0, 1.1, 1.2 and 1.3 are for clarity shifted up by 1, 2, 3 and 4 units respectively. The effective diameter for the reference system is taken to be d_{BH} as also given in table 6.3.

Figure 6.8: Radial distribution functions for soft particles at a density of $\rho^*{=}0.8$, obtained from correlation around a soft particle in the origin as an external potential. The MD results are from [1]. The lines for $T^*{=}1.0, 1.1, 1.2$ and 1.3 are for clarity shifted up by 1, 2, 3 and 4 units respectively. The effective diameter for the reference system is taken to be d_{BH} as also given in table 6.3.
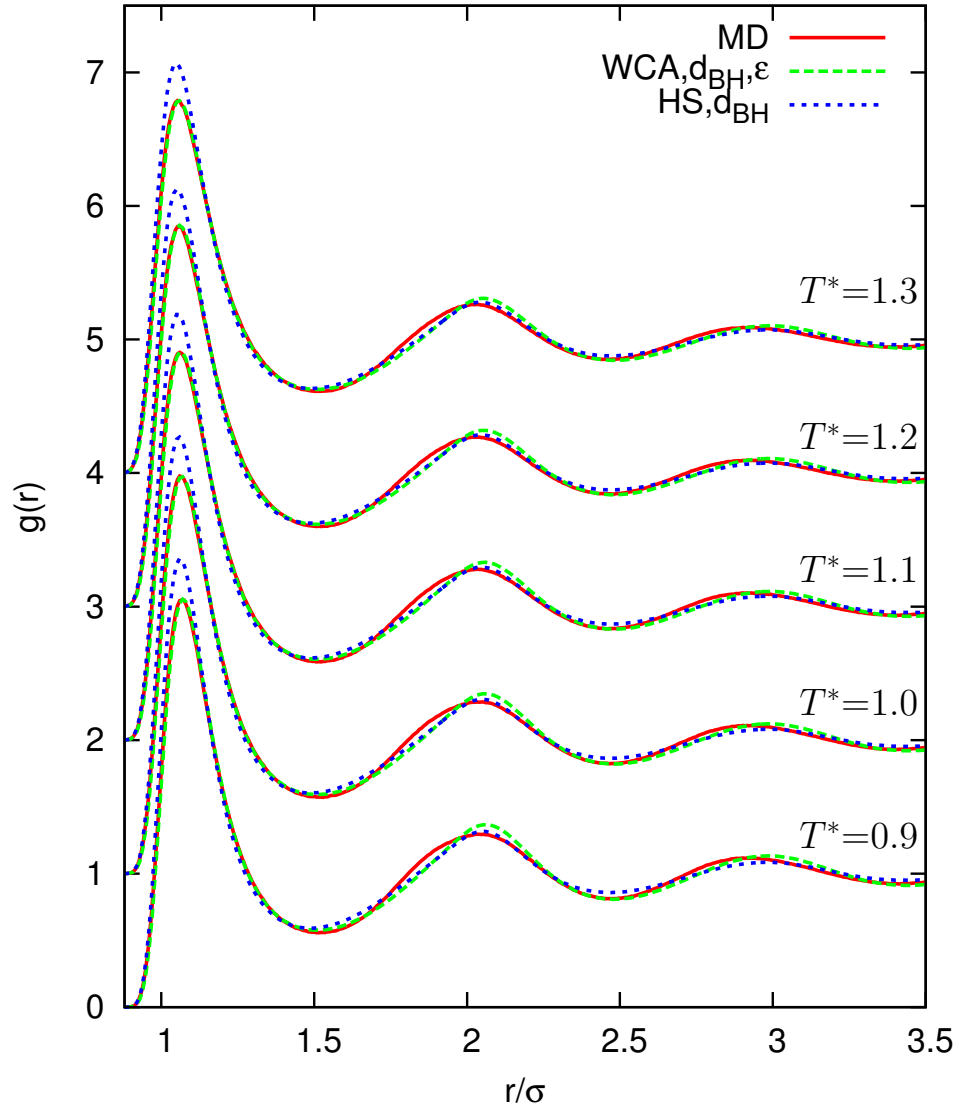
Figure 6.9: Radial distribution functions for soft particles at a density of ρ^*=0.9, obtained from correlation around a soft particle in the origin as an external potential. The MD results are from [1]. The lines for T^*=1.0, 1.1, 1.2 and 1.3 are for clarity shifted up by 1, 2, 3 and 4 units respectively. The effective diameter for the reference system is taken to be d_{BH} as also given in table 6.3.
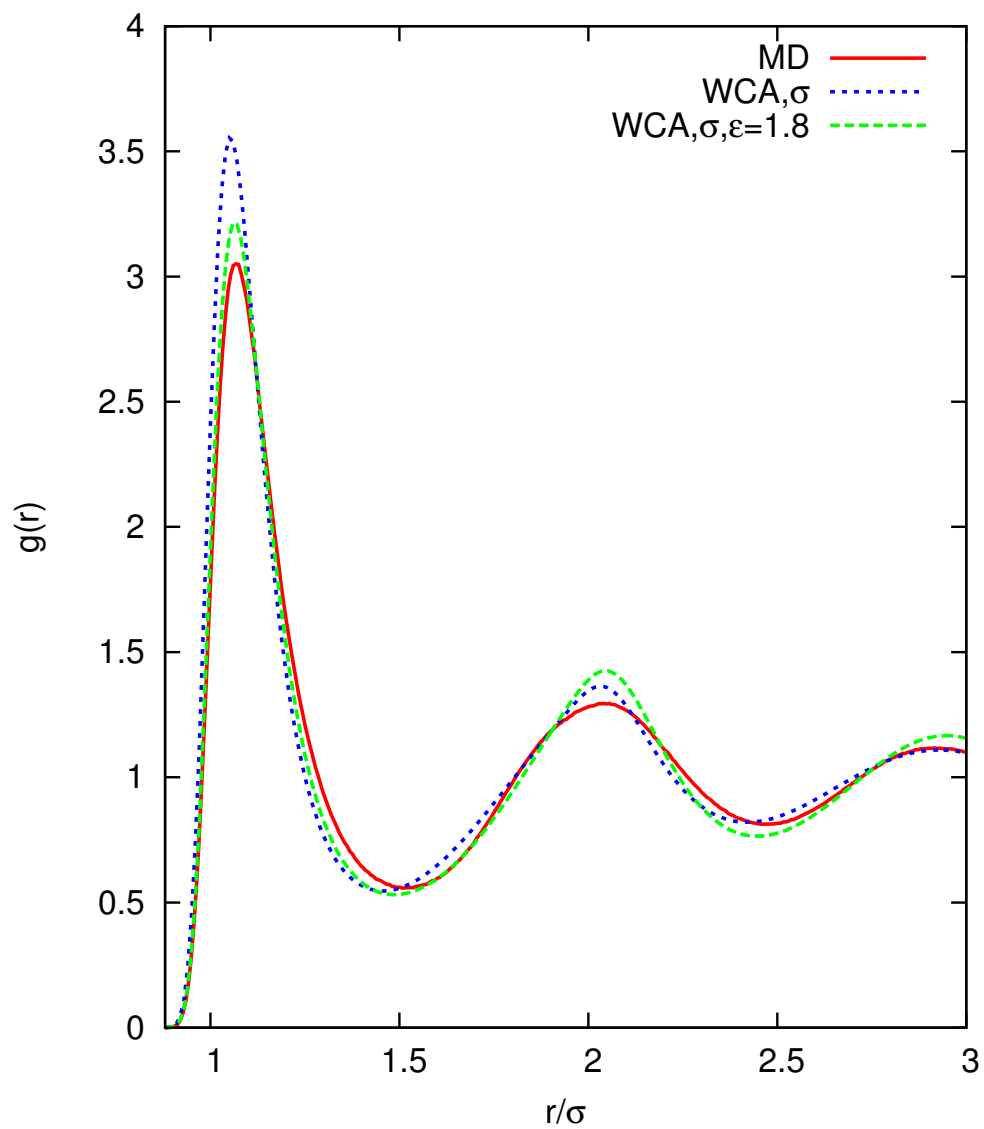
Figure 6.10: Radial distribution functions for soft particles at a density of ρ^*=0.9 and temperature T^*=0.9, obtained from correlation around a soft particle in the origin as an external potential. The WCA line is the mean field approximation with the WCA split where the perturbation strength ε=1.8 and the HS lines are lines without the perturbation. The MD results are from [1]. The effective diameter d_{BH} is 0.975σ.
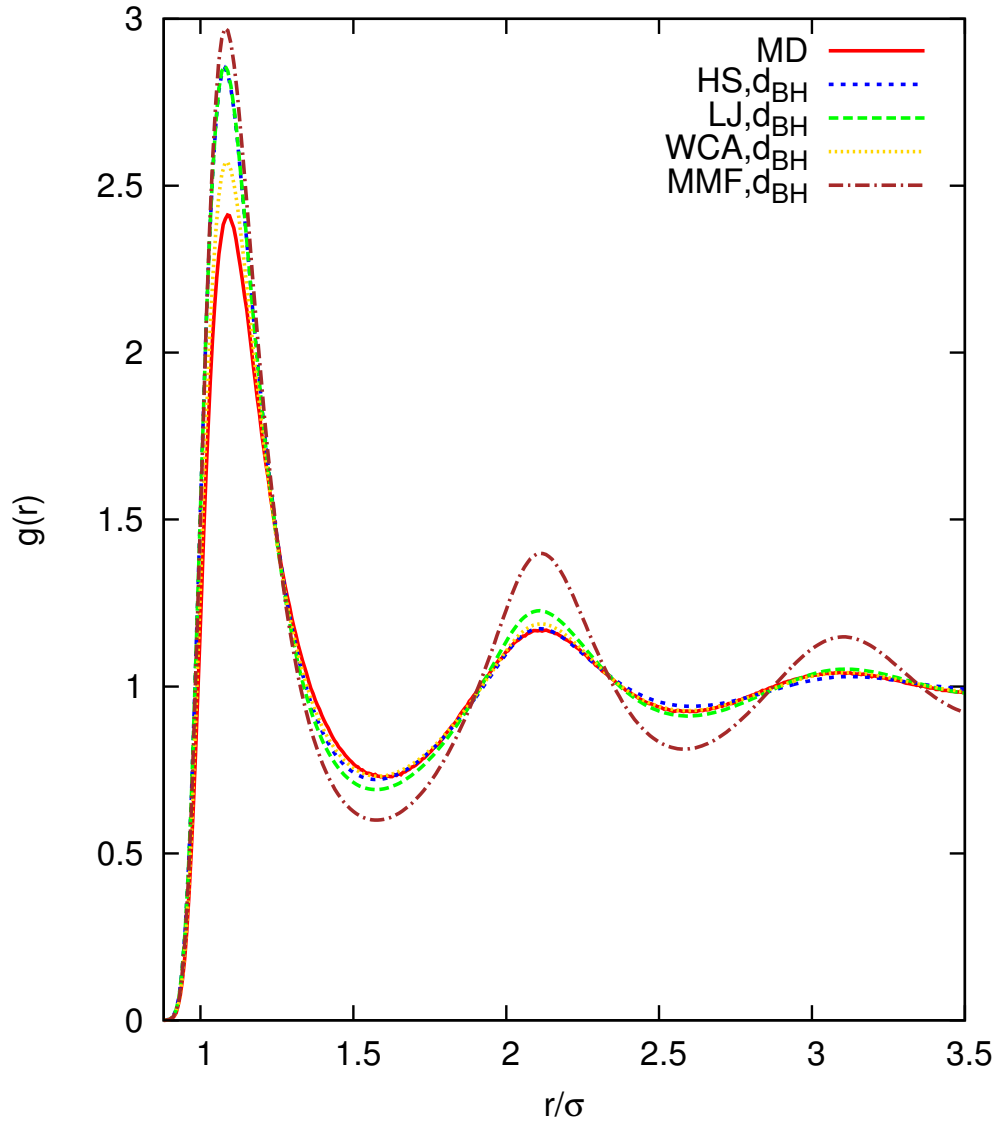
Figure 6.11: Radial distribution functions for soft particles at a temperature of T^*=1.0 and a density of ρ^*=0.7, obtained from correlation around a soft particle in the origin as an external potential. The effective diameter d_{BH} is 0.973σ.

6.3 Reference Systems Compared

All the previous plots in this chapter where done with the WB version of
FMT. Here we will look at the effect of the RF function on the solutions.
The homogeneous limit of the WB and RF expression are the CS and PY
expression respectively, see equation (2.141) and (2.140). The free energy
expressions and their derivatives with respect to density (hard-sphere chem-
ical potential) are shown in figure 6.12. The PY curves overestimate the
(almost exact) CS curves, but they do have the same (correct) low density
limit. We observe that also the low density limits of the density profiles are
the same. For the high density limit we may note that the oscillations for
the RF version are a bit larger (which is wrong compared to simulations)
but the differences are very small, see figure 6.13. The effect of the effective
diameter is similar to the results we have seen in the previous sections of this
chapter. We conclude that for these curves the RF or WB reference system
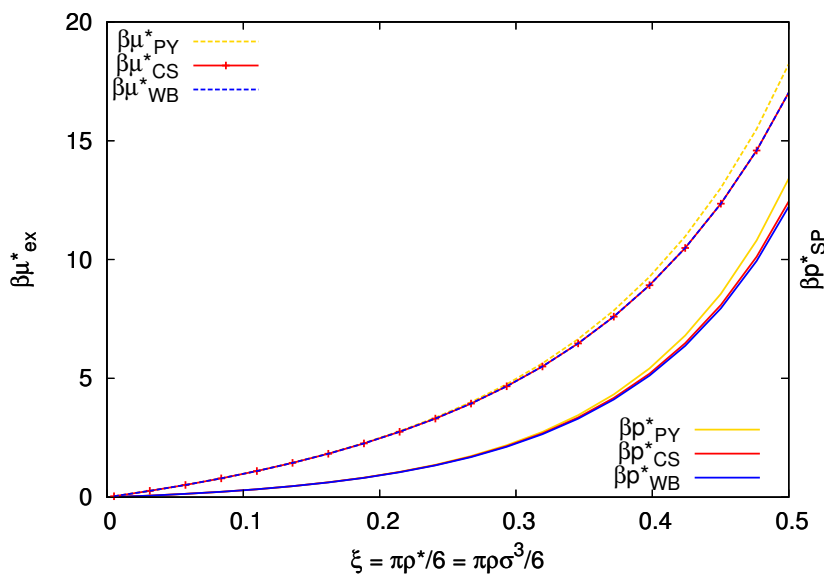do not vary much.

Figure 6.12: Scaled particle pressure (eq. (2.89), lower three lines) and hard-
sphere chemical potential (upper three lines) for the Percus-Yevick (eq.(2.140) in
yellow), Carnahan Starling (2.141) in red) and White Bear (eq. (2.92) in blue)
free energy density versus packing fraction. The PY pressure overestimates the
empirical CS results by 7% in the high density limit, whereas the WB version
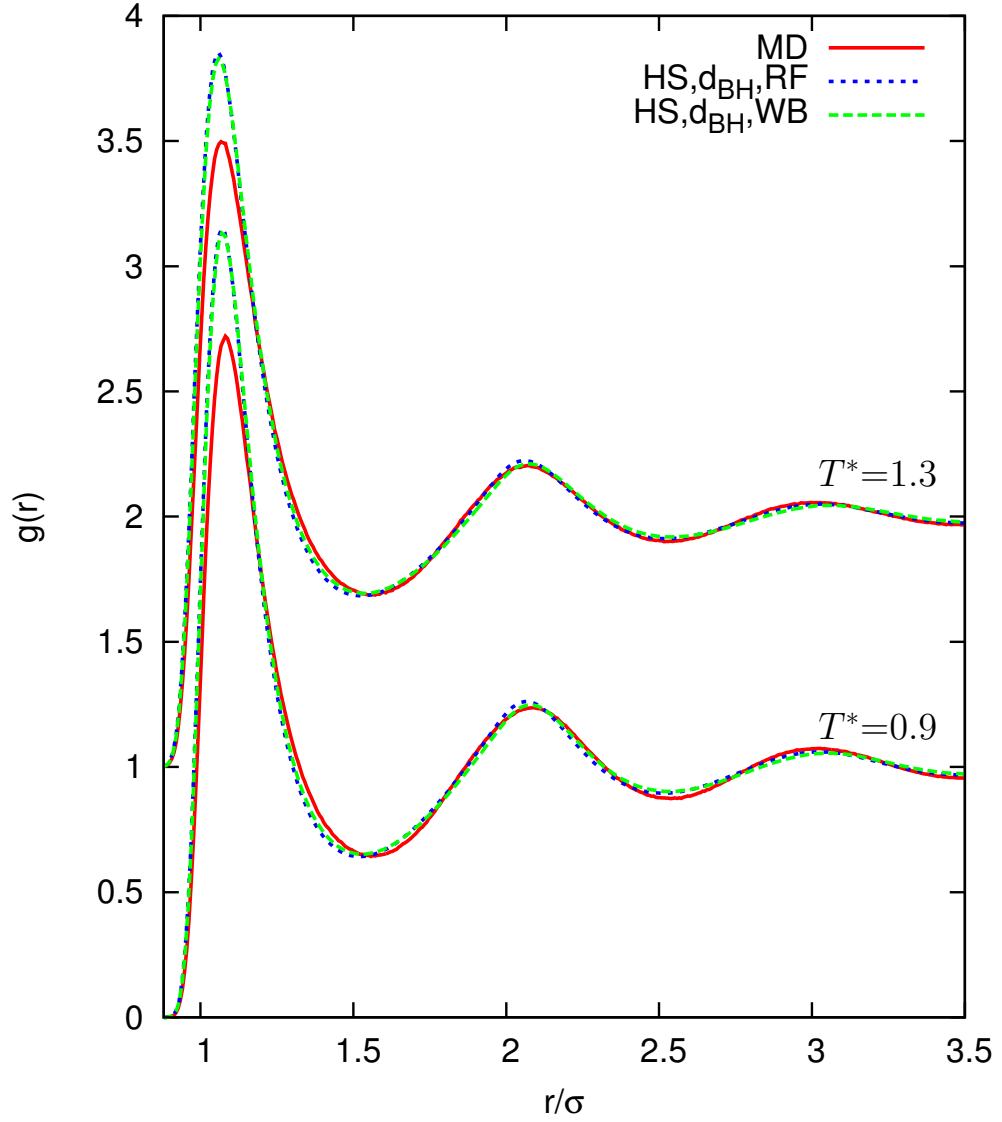deviates by 2% at most.

Figure 6.13: Radial distribution functions for soft particles at a temperature of $\rho^*=0.8$, obtained from correlation around a soft particle in the origin as an external potential for the HS model. The MD results are from [1]. The lines for temperatures $T^*=1.3$ are for clarity shifted up by 1 units. The effective diameter for the reference system is taken to be $d_{BH}(T^*)$.

100

6.4 Thermodynamic Properties

We will evaluate system properties that we can derive from the radial distribution functions. The data in table 6.2 can be fitted by

$$\varepsilon(\rho^*, T^*) = -0.1497 + 1.27\rho^* + 1.047T^*. \qquad (6.1)$$

(Fit obtained from Matlab.)

From equation (2.119) and (2.120) we can calculate respectively the (excess) internal energy and the pressure (or the compressibility factor $Z = \beta p/\rho$) from the radial distribution function and compare these also to simulation data. In figure 6.14 we see that the properties are sensitive to small deviations in g. For example, the HS and LJ model did not give much different results for g, but they can be seen to differ in the corresponding thermodynamic properties. When the maxima of the rdf's are larger than simulations, the corresponding compressibility factor will be larger as can be seen from equation (2.120) (remember that the interaction potential is negative). For high densities the WCA model behaves the best as we have seen before, but from figure 6.14 we see that the results for Z are still significantly off. The curves with the by trial and error fitted ε from equation (6.1) are off, but this is the result of the underestimation of the first local minimum. This shows the sensitivity of the properties with respect to g. Note that Z is always positive since the temperature, pressure and density are. In figure 6.14 we however see a negative pressure for low temperatures. What this means is that they do not represent physical (stable) state, but that does not stop me from calculating Z under these circumstances, nor Mr. Verlet from simulating it.

In figure 6.15 we see a plot of the internal energy calculated from equation (2.119). We see reversed over- and underestimation du to the flip in the sign of the weight function of g in equation (2.119) (the derivative of the interaction potential has (mostly) an opposite sign of the interaction potential itself). We see similar curves results for all the data published in [49]. This means that the temperature and density scaling is correct.

We can also try to fit the WCA model to this data, now with the effective diameter of the reference system and the perturbation strength as the fitting parameters. That is, we want to find the solutions of

$$U_{\text{WCA}}(d, \varepsilon) = U_{\text{MD}} \quad \text{and} \quad Z_{\text{WCA}}(d, \varepsilon) = Z_{\text{MD}}, \qquad (6.2)$$

where we calculate U_{WCA} and Z_{WCA} from equation (2.119) and (2.120) respectively. We use a Newton-Raphson method, where the derivatives are calculated using central differences. Typically 4 iterations were needed.
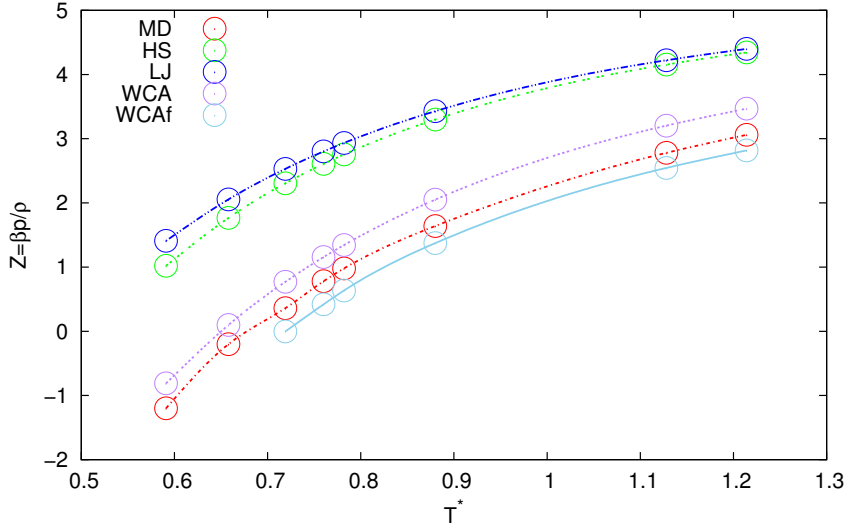
Figure 6.14: The compressibility factor $Z=\beta p/\rho$ for different models at a density of $\rho^*=0.85$ for various temperatures. The effective diameter for the reference system is taken to be $d_{\mathrm{BH}}(T^*)$. The WCAf line has values for ε from equation 6.1 (in the range of the fit). The MD results are from [49].
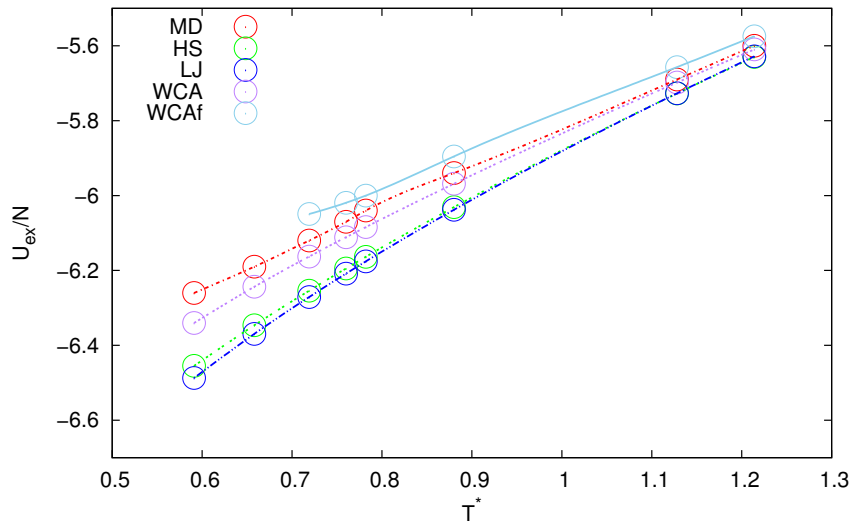

Figure 6.15: The compressibility factor excess energy $U/\langle N \rangle$ for different models at a density of $\rho^*=0.85$ for various temperatures. The effective diameter for the reference system is taken to be $d_{\mathrm{BH}}(T^*)$. The WCAf line has values for ε from equation 6.1 (in the range of the fit). The MD results are from [49].

The results are shown in table 6.4. We see that a higher temperature leads to a smaller effective diameter and a larger ε.

Table 6.4: The effective diameter d_{BH} and the interaction strength ε, such that the WCA model corresponds to the data in [49].

ρ^*	T^*	d_{BH}	ε
0.85	2.889	0.947661	2.04415
0.85	2.202	0.951399	1.61112
0.85	1.214	0.967579	1.28332
0.85	1.128	0.968345	1.23475
0.85	0.880	0.974918	1.20793
0.85	0.786	0.976948	1.16875
0.85	0.782	0.979169	1.21915
0.85	0.760	0.979037	1.19921
0.85	0.719	0.979543	1.18791
0.85	0.658	0.983388	1.19241
0.85	0.591	0.986408	1.22914
0.75	2.849	0.942655	1.49443
0.75	1.304	0.955824	1.07518
0.75	1.071	0.964429	1.12553
0.75	1.069	0.962209	1.06517
0.75	0.827	0.965580	1.08400

We could also show a phase diagram is discussed in section 2.8, but it would be redundant. The plots we have shown here already show that the models overestimate the (liquid) pressure. This results in an underestimation of the liquid saturation curve.

Chapter 7

Conclusions and Outlook

In this work we have presented accurate models for radial distribution functions of soft spheres in the high and low density limit, using the test-particle method. We used fundamental measure theory (FMT) to describe the hard sphere repulsions and approximated the inter-particle correlations in the inhomogeneous system by known limiting cases.

In figure 7.1 we see radial distribution functions without perturbation (so no attractions are taken into account) for a temperature $T^*=1.3$ for a wide density range. We note by comparison with simulations that attractions are important for low densities near the second solvation shell (the second peak) and for high densities near the first solvation shell (the first peak). In this work we constructed models which correct for both, not by expanding around a hard-sphere system but by using known limiting behavior. Physically, in the high density limit, attractive forces can be approximated as a uniform background field, except perhaps near the particle itself. Therefore we were able to obtain a measure for these short ranged correlations due to the long ranged forces by fitting the perturbation to MD simulations, for even better accuracy.

Generally it is not merely the magnitude of the perturbation that plays a role: the shape of the perturbation matters, since each model is only accurate in a certain density or temperature range. We have seen that the low density model does not give accurate results for high densities and vice versa.

The work presented here is just another step forward in the calculation of radial distribution functions using FMT and the test-particle method. In particular, we have learned something about the behavior of correlations in (strongly) inhomogeneous density profiles. A next step could be calculating density profiles of *non-spherical* soft particles like ellipsoids or diatomic molecules with an LJ-like interaction. In appendix C we show a theoretical
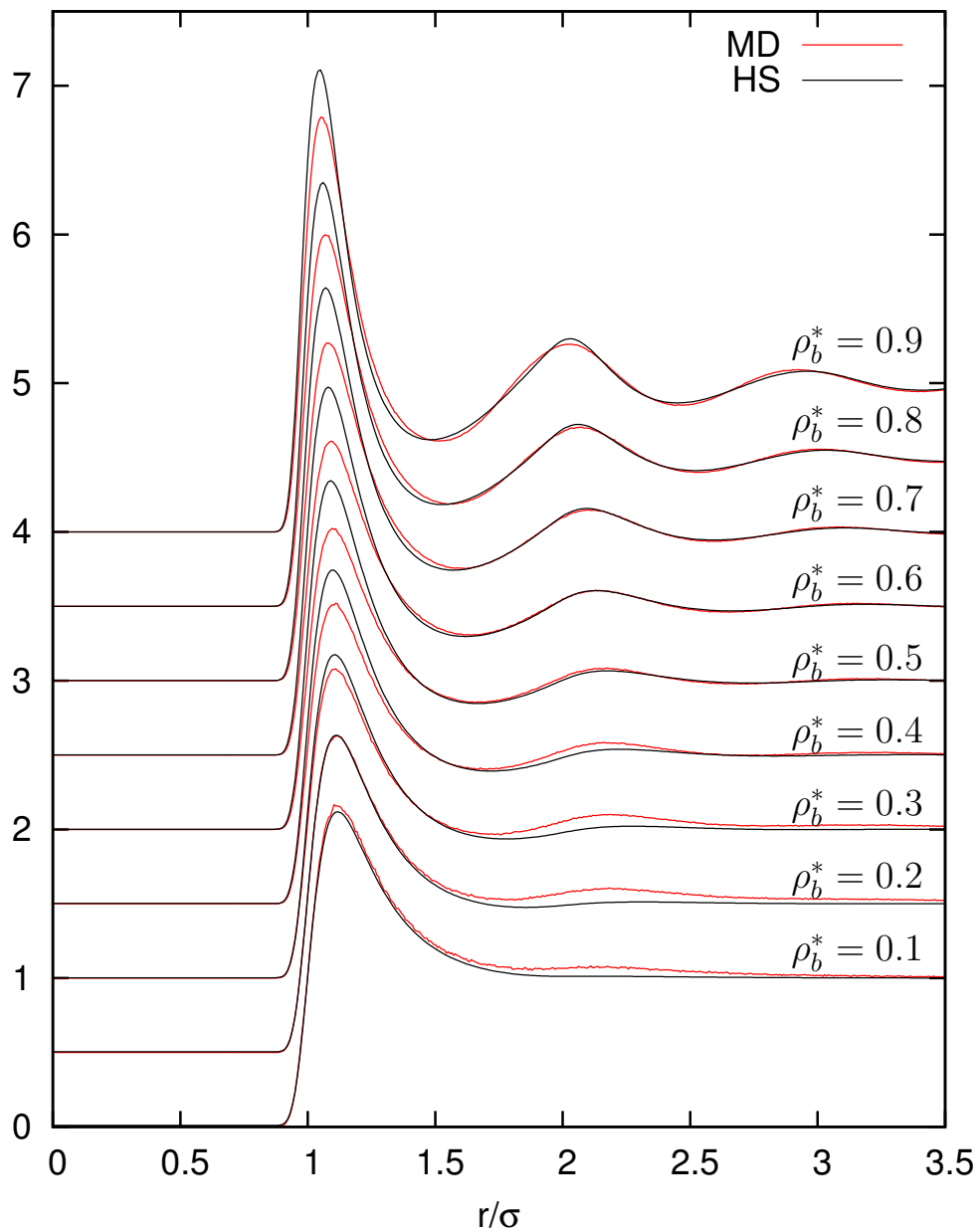
Figure 7.1: Radial distribution functions for hard spheres around an LJ particle for different bulk densities at $T^*=1.3$. The diameter of the hard spheres is given by the BH effective diameter eq. (2.131). For clarity the lines are shifted up (all lines approach one in the limit of r to infinity). The Molecular Dynamic results are from [1].

extension of the model to quadrupoles, since it is not straightforward. When in general more complex particles are used or higher particle distributions need to be calculated, a lot of symmetry is lost. In general, three dimensions need to be calculated numerically and on top of that, the system is in general not invariant under rotation of the test-particle anymore. Higher numerical efficiency might be obtained using the convolution sums as discussed in section 4.1.1. When the fast Fourier transform (FFT) is used, the calculations are done at a cost of $\mathcal{O}(N \log N)$ compared to $\mathcal{O}(N^2)$ when the sums are just evaluated, but the number of grid points must be a power of 2 in this case. When a model involves higher dimensions, a gradient descent method might be used. This requires second variations of the functional with respect to the density profile and is computationalwise costly. [47, 48]

Appendix A

Collection of Derivations

A.1   Saddle Point Integration

Approximating an integral of the form

$$I = \int e^{N\phi(x)} \mathrm{d}x \tag{A.1}$$

by the maximum value of the integrand, obtained at a point x_{max} is called the *saddle point integration* method. Expanding the exponent around x_{max} gives,

$$I = \int e^{N(\phi(x_{\mathrm{max}}) - \frac{1}{2}|\phi''(x_{\mathrm{max}})|(x - x_{\mathrm{max}})^2 + \cdots)} \mathrm{d}x, \tag{A.2}$$

since the first derivative of ϕ is zero at x_{max} is zero and the second derivative is negative. When higher order terms are neglected, this becomes,

$$I \approx e^{N\phi(x_{\mathrm{max}})} \int e^{-\frac{N}{2}|\phi''(x_{\mathrm{max}})|(x - x_{\mathrm{max}})^2} \mathrm{d}x \approx \sqrt{\frac{2\pi}{N|\phi''(x_{\mathrm{max}})|}} e^{N\phi(x_{\mathrm{max}})}, \tag{A.3}$$

where in the last step the integration has been extended to the whole real line since the integrand is negligibly small outside the neighborhood of x_{max}. Corrections to the above result can be done by taking higher order terms into account in the expansion. These terms can be treated perturbatively and leads to a series in powers of $1/N$. Alternatively an expansion around other local maxima can be added. Since all these corrections vanish in the thermodynamic limit, we have

$$\lim_{N \to \infty} \frac{\ln I}{N} = \lim_{N \to \infty} \left[\phi(x_{\mathrm{max}}) - \frac{1}{2N} \ln\left(\frac{N\phi''(x_{\mathrm{max}})}{2\pi} \right) + \mathcal{O}(N^{-2}) \right] = \phi(x_{\mathrm{max}}). \tag{A.4}$$

107

A.2 Fourier Transform Step Function

First we show that the convolution product as defined in equation (2.79) (a function of '$\mathbf{r}_{ij}=\mathbf{r}_i-\mathbf{r}_j$') becomes a simple multiplication in Fourier space,

$$
\begin{aligned}
\mathcal{T}(\omega_i^{(\alpha)}\otimes\omega_j^{(\gamma)}(\mathbf{r}=\mathbf{r}_{ij})) &= \int \mathrm{d}\mathbf{r}_{ij}\int \mathrm{d}\mathbf{r}\ \omega_i^{(\alpha)}(\mathbf{r}-\mathbf{r}_i)\omega_j^{(\gamma)}(\mathbf{r}-\mathbf{r}_j)\mathrm{e}^{i\mathbf{k}\cdot\mathbf{r}_{ij}} \\
&= \int \mathrm{d}\mathbf{r}_{ij}\int \mathrm{d}\mathbf{r}'\ \omega_i^{(\alpha)}(\mathbf{r}'-\mathbf{r}_{ij})\omega_j^{(\gamma)}(\mathbf{r}')\mathrm{e}^{i\mathbf{k}\cdot\mathbf{r}_{ij}} \\
&= \int \mathrm{d}\mathbf{r}'\left(\int \mathrm{d}\mathbf{r}_{ij}\ \omega_i^{(\alpha)}(\mathbf{r}'-\mathbf{r}_{ij})\mathrm{e}^{i(-\mathbf{k})\cdot(\mathbf{r}'-\mathbf{r}_{ij})}\right)\omega_j^{(\gamma)}(\mathbf{r}')\mathrm{e}^{i\mathbf{k}\cdot\mathbf{r}'} \\
&= \widetilde{\omega}_i^{(\alpha)}(-\mathbf{k})\widetilde{\omega}_j^{(\gamma)}(\mathbf{k}).
\end{aligned}
\tag{A.5}
$$

For the second equality we used the substitution of variables $\mathbf{r}:=\mathbf{r}'+\mathbf{r}_j$ and for the third $\mathbf{r}'':=\mathbf{r}'-\mathbf{r}_{ij}$ (and by Fubini's theorem we can interchange the order of integration; the functions $(\omega^{(\alpha)})$ are integrable, see equation (2.83)). The Fourier transform of the Heaviside step function is,

$$
\begin{aligned}
\widetilde{\omega}^{(3)}(\mathbf{k}) &= \int \mathrm{d}\mathbf{r}\ \Theta(R-|\mathbf{r}|)\mathrm{e}^{i\mathbf{k}\cdot\mathbf{r}} = 2\pi\int_0^R r^2\mathrm{d}r\int_0^\pi \sin\theta\mathrm{d}\theta\ \mathrm{e}^{ikr\cos\theta} \\
&= \frac{4\pi}{k}\int_0^R r\sin kr\mathrm{d}r = \frac{4\pi}{k}\left(-\frac{r\cos kr}{k}+\frac{\sin kr}{k^2}\right)\Big|_0^R \\
&= 4\pi\frac{\sin kR-kR\cos kR}{k^3},
\end{aligned}
\tag{A.6}
$$

with $k=|\mathbf{k}|$ and the integral over φ vanishes because we can choose the polar axis along $\mathbf{k}$. The result for $\widetilde{\omega}^{(3)}$ as in equation (2.82) is obtained. The result for the vector weight follows via integration by parts,

$$
\begin{aligned}
\widetilde{\omega}^{(V2)}(\mathbf{k}) &= \int \mathrm{d}\mathbf{r}\nabla\Theta(R-|\mathbf{r}|)\mathrm{e}^{i\mathbf{k}\cdot\mathbf{r}} \\
&= \int \mathrm{d}\mathbf{r}\Theta(R-|\mathbf{r}|)i\mathbf{k}\mathrm{e}^{i\mathbf{k}\cdot\mathbf{r}} = -i\mathbf{k}\widetilde{\omega}^{(3)}(\mathbf{k}).
\end{aligned}
\tag{A.7}
$$

The transform of the delta function $\omega^{(2)}$ is (compare with equation (A.6)),

$$
\int \mathrm{d}\mathbf{r}\delta(R-|\mathbf{r}|)\mathrm{e}^{i\mathbf{k}\cdot\mathbf{r}} = \frac{4\pi}{k}\int \delta(R-r)r\sin kr\mathrm{d}r = 4\pi R^2\frac{\sin kR}{kR},
\tag{A.8}
$$

as in equation (2.82). Now we have derived the Fourier transform of the weights and we continue with proving equation (2.78).

The pair exclusion function in Fourier space in terms of the above functions (see eq. (2.78)) readily becomes

$$
\begin{aligned}
&\widetilde{\omega}_i^{(0)}(-\mathbf{k})\widetilde{\omega}_j^{(3)}(\mathbf{k}) + \widetilde{\omega}_i^{(3)}(-\mathbf{k})\widetilde{\omega}_j^{(0)}(\mathbf{k}) \\
&\quad + \widetilde{\omega}_i^{(1)}(-\mathbf{k})\widetilde{\omega}_j^{(2)}(\mathbf{k}) + \widetilde{\omega}_i^{(2)}(-\mathbf{k})\widetilde{\omega}_j^{(1)}(\mathbf{k}) \\
&\quad\quad - \widetilde{\omega}_i^{(V1)}(-\mathbf{k})\widetilde{\omega}_j^{(V2)}(\mathbf{k}) - \widetilde{\omega}_i^{(V2)}(-\mathbf{k})\widetilde{\omega}_j^{(V1)}(\mathbf{k}) \\
&= \frac{\sin kR_i}{kR_i}\frac{4\pi}{k^3}(\sin kR_j - kR_j\cos kR_j) \\
&\quad + \frac{4\pi}{k^3}(\sin kR_i - kR_i\cos kR_i)\frac{\sin kR_j}{kR_j} \\
&\quad + 4\pi R_i^2\frac{\sin kR_i}{kR_i}R_j\frac{\sin kR_j}{kR_j} + R_i\frac{\sin kR_i}{kR_i}4\pi R_j^2\frac{\sin kR_j}{kR_j} \\
&\quad - (-i\mathbf{k})\frac{4\pi(\sin kR_i - kR_i\cos kR_i)}{k^3}(-i\mathbf{k})\frac{(\sin kR_j - kR_j\cos kR_j)}{k^3 R_j} \\
&\quad - (-i\mathbf{k})\frac{(\sin kR_i - kR_i\cos kR_i)}{k^3 R_i}(-i\mathbf{k})\frac{4\pi(\sin kR_j - kR_j\cos kR_j)}{k^3} \\
&= \frac{4\pi}{k^2}(R_i + R_j)\sin kR_i\sin kR_j - (R_i + R_j)\cos kR_i\cos kR_j \\
&\quad + \frac{4\pi}{k^3}(\sin kR_i\cos kR_j + \cos kR_i\sin kR_j) \\
&= \frac{4\pi}{k^3}(\sin k(R_i + R_j) - k(R_i + R_j)\cos k(R_i + R_j)) = \widetilde{\Theta}(R_i + R_j - |\mathbf{r}|).
\end{aligned}
$$

First we worked out the brackets, where some terms drop out (remember that $\mathbf{k}\cdot\mathbf{k}=k^2$ where $|\mathbf{k}|=k$; the terms arising from weights 0 and 3 cancel with part of the vector weights), and then we used goniometric sum rules. This means that the Fourier transform for the '*pair* exclusion function' $\Theta(R_i + R_j - |\mathbf{r}|)$, can be written in terms of functions of single particle characteristics R_i and R_j. These functions are the Heaviside step function ($\omega^{(3)}$, volume), the gradient of the step function w.r.t. $\mathbf{r}$ ($\omega^{(V2)}$, slope) and the derivative of the step function w.r.t. $r=|\mathbf{r}|$ ($\omega^{(2)}$, surface). The other weights ($\omega^{(0)}$, $\omega^{(1)}$ and $\omega^{(V1)}$) are necessary to make pairs having the correct dimension as in equation (2.87).

It turns out that this is not a unique expression of $\Theta(R_i + R_j - |\mathbf{r}|)$ in terms of functions of R_i and R_j. Kierlik and Rosinberg [43] found an equivalent [44] expression in terms of the step function and its first, second and third derivative, hence lacking the vector weights. Here we work in a 1D geometry, where we only are left with a single component of the vector weights. Otherwise the version of [43] would require less computation power, since they have four weights compared to five (1+1+3) for the original version.

A.3 Properties of the Radial Distribution

The average excess potential energy in the grand canonical ensemble follows from

$$
\langle \mathcal{U}_N(\mathbf{r}^N) \rangle = \mathrm{Tr}_{\mathrm{cl}}\, \mathcal{U}_N(\mathbf{r}^N) f_0(\mathbf{r}^N, \mathbf{p}^N; N)
$$

$$
= \sum_{N=2}^{\infty} \frac{1}{N! h^{3N}} \iint \frac{1}{2} \sum_{i \neq j} \phi(r_{ij}) \Xi^{-1} \mathrm{e}^{-\beta(\mathcal{H}_N - \mu N)} \mathrm{d}\mathbf{r}^N \mathrm{d}\mathbf{p}^N
$$

$$
= \frac{1}{2} \sum_{N=2}^{\infty} \left(\frac{\mathcal{Z}_N \mathrm{e}^{\beta \mu N}}{\Xi} \right) \iint \phi(r_{12}) \left(\frac{N(N-1)}{N! \Lambda^3 \mathcal{Z}_N} \int \mathrm{e}^{-\beta \mathcal{U}_N(\mathbf{r}^{(N-2)})} \mathrm{d}\mathbf{r}^{(N-2)} \right) \mathrm{d}\mathbf{r}_1 \mathrm{d}\mathbf{r}_2
$$

$$
= \frac{1}{2} \iint \left(\sum_{N=2}^{\infty} P(N) \rho_N^{(2)}(\mathbf{r}_1, \mathbf{r}_2) \right) \phi(r_{12}) \mathrm{d}\mathbf{r}_1 \mathrm{d}\mathbf{r}_2
$$

$$
= \frac{1}{2} \iint \rho^{(2)}(\mathbf{r}_1, \mathbf{r}_2) \phi(r_{12}) \mathrm{d}\mathbf{r}_1 \mathrm{d}\mathbf{r}_2 = 2\pi \rho \langle N \rangle \int_0^{\infty} \phi(r) g(r) r^2 \mathrm{d}r. \tag{A.9}
$$

We used the definitions of taking averages in the first step (eqs. (2.31), (2.32) and (2.33)). In the second step we wrote the interaction energy as the sum of all pairwise interactions as in equation (2.52). For the third equality we integrated out the momenta (resulting in factors of Λ) and used the fact that all integrals over r give the same $N(N-1)$ integrals. The terms in large brackets are $P(N)$, $\rho_N^{(2)}$ and $\rho^{(2)}$ from equations (2.101), (2.96) and (2.100) respectively. The result for homogeneous densities after the last step (using equations (2.104) and (2.107)) is called the *energy equation*.

In order to derive the *pressure equation*, we start with the *virial equation*

$$
\frac{\beta P}{\rho} = 1 - \frac{\beta}{3\langle N \rangle} \left\langle \sum_{i=1}^{N} \mathbf{r}_i \cdot \nabla \mathcal{U}_N(\mathbf{r}^N) \right\rangle
$$

$$
= 1 - \frac{\beta}{3\langle N \rangle} \sum_{N=2}^{\infty} \frac{1}{N! h^{3N}} \int \sum_{i=1}^{N} \mathbf{r}_i \cdot \nabla_i \left(\sum_{i \neq j} \phi(r_{ij}) \right)
$$

$$
\times \Xi^{-1} \mathrm{e}^{-\beta(\mathcal{H}_N - \mu N)} \mathrm{d}\mathbf{r}^N \mathrm{d}\mathbf{p}^N
$$

$$
= 1 - \frac{\beta}{3\langle N \rangle} \sum_{N=2}^{\infty} \frac{\mathrm{e}^{\beta \mu N}}{N! \Lambda^{3N} \Xi} \frac{1}{2} \sum_{i \neq j} \int \mathbf{r}_{ij} \cdot \nabla_{ij} \phi(r_{ij}) \mathrm{e}^{-\beta \mathcal{H}_N} \mathrm{d}\mathbf{r}^N
$$

$$
= 1 - \frac{\beta}{3\langle N \rangle} \sum_{N=2}^{\infty} \frac{N(N-1)}{2} \frac{\mathrm{e}^{\beta \mu N}}{N! \Lambda^{3N} \Xi} \int \mathbf{r}_{12} \cdot \nabla_{12} \phi(r_{12}) \mathrm{e}^{-\beta \mathcal{U}_N(\mathbf{r}^N)} \mathrm{d}\mathbf{r}^N
$$

$$= 1 - \frac{\beta}{6\langle N \rangle} \iint \left(\frac{1}{\Xi} \sum_{N=2}^{\infty} \frac{\mathrm{e}^{\beta\mu N}}{(N-2)!\Lambda^{3N}} \int \mathrm{e}^{-\beta\mathcal{U}_N(\mathbf{r}^N)} \mathrm{d}\mathbf{r}^{(N-2)} \right)$$
$$\times \, \mathbf{r}_{12} \cdot \nabla_{12}\phi(r_{12}) \mathrm{d}\mathbf{r}_1 \mathrm{d}\mathbf{r}_2$$
$$= 1 - \frac{\beta}{6\langle N \rangle} \iint \rho^{(2)}(\mathbf{r}_1, \mathbf{r}_2) r_{12} \frac{\mathrm{d}\phi(r_{12})}{\mathrm{d}r} \bigg|_{r=r_{12}} \mathrm{d}\mathbf{r}_1 \mathrm{d}\mathbf{r}_2$$
$$= 1 - \frac{\beta V}{6\langle N \rangle} \int \rho^2 g(r) r \frac{\mathrm{d}\phi(r)}{\mathrm{d}r} \mathrm{d}\mathbf{r}$$
$$= 1 - \frac{2\pi\beta\rho}{3} \int \frac{\mathrm{d}\phi(r)}{\mathrm{d}r} g(r) r^3 \mathrm{d}r. \tag{A.10}$$

We used the definitions of taking averages in the first step (eqs. (2.31), (2.32) and (2.33)). In the second step we wrote the interaction energy as the sum of all pairwise interactions as in equation (2.52). For the third equality we integrated out the momenta (resulting in factors of Λ) and for the next that all integrals over space gives $N(N-1)$ times the same value. The terms in large brackets on the next line is $\rho^{(2)}$ from equation (2.100). The result for homogeneous densities after the last step (using equations (2.104) and (2.107)) is called the *pressure equation.*

From equation (2.25) it follows that at equilibrium (i.e., $\mathrm{d}G=\mathrm{d}F=\mathrm{d}\Omega=0$) and for constant temperatures (i.e., $\mathrm{d}T=0$) that

$$N \frac{\partial\mu}{\partial N} = V \frac{\partial p}{\partial N} = \frac{\partial p}{\partial\rho} = \rho \left(\frac{-1}{V} \frac{\partial p}{\partial V} \right) \equiv \rho \chi_T. \tag{A.11}$$

In the last step we defined the isothermal compressibility χ_T. In order to prove the relation of this quantity with the particle fluctuations, we first show the following,

$$\frac{\partial \ln \Xi}{\partial \ln z} = z \frac{\partial \ln \Xi}{\partial z} = \frac{z}{\Xi} \frac{\partial \Xi}{\partial z}. \tag{A.12}$$

Here z is the fugacity (cf. equation (2.105)) and the grand partition function Ξ can from equations (2.31) and (2.33) be written as

$$\Xi = \sum_{N=0}^{\infty} \frac{1}{N!h^{3N}} \iint \mathrm{e}^{-\beta(\mathcal{H}_N - \mu N)} \mathrm{d}\mathbf{r}^N \mathrm{d}\mathbf{p}^N$$
$$= \sum_{N=0}^{\infty} \frac{z^N}{N!} \int \mathrm{e}^{-\beta\mathcal{U}_N(\mathbf{r}^N)} \mathrm{d}\mathbf{r}^N. \tag{A.13}$$

Whence

$$\frac{\partial \Xi}{\partial z} = z \sum_{N=1}^{\infty} N \frac{z^N}{N!} \int e^{-\beta \mathcal{U}_N(\mathbf{r}^N)} d\mathbf{r}^N$$

$$= \frac{\Xi}{z} \sum_{N=0}^{\infty} \frac{N}{N! h^{3N}} \iint \Xi^{-1} e^{-\beta(\mathcal{H}_N - \mu N)} d\mathbf{r}^N d\mathbf{p}^N \qquad (A.14)$$

$$= \frac{\Xi}{z} \mathrm{Tr}_{\mathrm{cl}} N f_0 = \frac{\Xi}{z} \langle N \rangle,$$

and

$$\frac{\partial^2 \Xi}{\partial z^2} = \frac{1}{z^2} \sum_{N=2}^{\infty} N(N-1) \frac{z^N}{N!} \int e^{-\beta \mathcal{U}_N(\mathbf{r}^N)} d\mathbf{r}^N$$

$$= \frac{\Xi}{z^2} \sum_{N=0}^{\infty} \frac{N^2 - N}{N! h^{3N}} \iint \Xi^{-1} e^{-\beta(\mathcal{H}_N - \mu N)} d\mathbf{r}^N d\mathbf{p}^N \qquad (A.15)$$

$$= \frac{\Xi}{z^2} \mathrm{Tr}_{\mathrm{cl}}(N^2 - N) f_0 = \frac{\Xi}{z^2} \langle N^2 - N \rangle = \frac{\Xi}{z^2} (\langle N^2 \rangle - \langle N \rangle).$$

Finally

$$\frac{\partial^2 \ln \Xi}{\partial \ln z^2} = z \frac{\partial}{\partial z} \frac{\partial \ln \Xi}{\partial \ln z} = z \frac{\partial}{\partial z} \left(\frac{z}{\Xi} \frac{\partial \Xi}{\partial z} \right)$$

$$= z \left(\frac{1}{\Xi} \frac{\partial \Xi}{\partial z} - \frac{z}{\Xi^2} \left(\frac{\partial \Xi}{\partial z} \right)^2 + \frac{z}{\Xi} \frac{\partial \Xi}{\partial z} \right) \qquad (A.16)$$

$$= \langle N \rangle - \langle N \rangle^2 + (\langle N^2 \rangle - \langle N \rangle)$$

$$= \langle N^2 \rangle - \langle N \rangle^2.$$

Now we arrive at

$$\frac{\langle N^2 \rangle - \langle N \rangle^2}{\langle N \rangle} = \frac{1}{\langle N \rangle} \frac{\partial^2 \ln \Xi}{\partial \ln z^2} = \frac{1}{\langle N \rangle} \frac{\partial}{\partial \ln z} \frac{\partial \ln \Xi}{\partial \ln z} = \frac{1}{\langle N \rangle} \frac{\partial \langle N \rangle}{\partial \ln z}$$

$$= \frac{1}{\langle N \rangle} \frac{\partial \langle N \rangle}{\partial \beta \mu}. \qquad (A.17)$$

In the last step we used the chain rule

$$\frac{\partial}{\partial \ln z} = \frac{\partial z}{\partial \ln z} \frac{\partial}{\partial z} = z \frac{\partial \beta \mu}{\partial z} \frac{\partial}{\partial \beta \mu} = z \frac{\partial \beta \mu}{\partial z} \frac{\partial}{\partial \beta \mu} = z \frac{1}{z} \frac{\partial}{\partial \beta \mu} \qquad (A.18)$$

and the definition of the fugacity

$$\frac{\partial z}{\partial \beta \mu} = \Lambda^{-3} e^{\beta \mu} = z. \qquad (A.19)$$

We used equations (A.11) and (A.17) in the first step of equation (2.121). (Since we work in the grand canonical ensemble we switch to the average number of particles in equation (A.11)).

A.4 Second Order Free Energy Term in λ

The derivative of the second particle density function with respect to the coupling parameter λ can in the grand canonical ensemble from equation (2.102) be written as

$$
\begin{aligned}
\frac{\partial \rho_\lambda^{(2)}}{\partial \lambda} = & \frac{-1}{\Xi^2} \frac{\partial \Xi}{\partial \lambda} \sum_{N=2}^{\infty} \frac{z^N}{(N-2)!} \int e^{-\beta \mathcal{U}_N} d\mathbf{r}^{(N-2)} \\
& + \frac{1}{\Xi} \sum_{N=2}^{\infty} \frac{z^N}{(N-2)!} \int e^{-\beta \mathcal{U}_N}(-\beta \mathcal{U}_N') d\mathbf{r}^{(N-2)},
\end{aligned}
\tag{A.20}
$$

where z is the fugacity (cf. (2.105)). The derivative of the grand partition function becomes,

$$
\begin{aligned}
\frac{\partial \Xi}{\partial \lambda} &= \sum_{N=2}^{\infty} \frac{z^N}{N!} \int e^{-\beta \mathcal{U}_N}(-\beta \mathcal{U}_N') d\mathbf{r}^N \\
&= -\beta \sum_{N=2}^{\infty} \frac{z^N}{N!} \int e^{-\beta \mathcal{U}_N} \mathcal{W}_N d\mathbf{r}^N \\
&= -\beta \sum_{N=2}^{\infty} \frac{z^N}{N!} \frac{N(N-1)}{2} \int e^{-\beta \mathcal{U}_N} \phi(\mathbf{r}_1, \mathbf{r}_2) d\mathbf{r}^N \\
&= -\frac{\beta \Xi}{2} \iint \left(\frac{1}{\Xi} \sum_{N=2}^{\infty} \frac{z^N}{(N-2)!} \int e^{-\beta \mathcal{U}_N} d\mathbf{r}^{(N-2)} \right) \phi(\mathbf{r}_1, \mathbf{r}_2) d\mathbf{r}_1 d\mathbf{r}_2 \\
&= -\frac{\beta \Xi}{2} \iint \rho_\lambda^{(2)}(\mathbf{r}_1, \mathbf{r}_2) \phi(\mathbf{r}_1, \mathbf{r}_2) d\mathbf{r}_1 d\mathbf{r}_2.
\end{aligned}
\tag{A.21}
$$

On the first line we integrated out already the momenta (see equation (2.33)), resulting in terms including z and $\mathcal{U}_N' = \mathcal{W}_N$ is the derivative with respect to the coupling parameter λ, see equation (2.126). Next we recognize that all the terms in $\mathcal{W}_N$ are equal, resulting in $N(N-1)/2$ terms. After that we can integrate out $N-2$ spatial variables resulting in $\rho_\lambda^{(2)}$.

The second term in equation (A.20) becomes

$$
\begin{aligned}
-\frac{\beta}{\Xi} & \sum_{N=2}^{\infty} \frac{z^N}{(N-2)!} \int e^{-\beta \mathcal{U}_N} \mathcal{W}_N d\mathbf{r}^{(N-2)} \\
&= -\frac{\beta}{\Xi} \sum_{N=2}^{\infty} \frac{z^N}{(N-2)!} \int e^{-\beta \mathcal{U}_N} \mathcal{W}_N d\mathbf{r}^{(N-2)} \\
&= -\frac{\beta}{\Xi} \sum_{N=2}^{\infty} \frac{z^N}{(N-2)!} \sum_{i=1}^{N} \sum_{j=1}^{i} \int e^{-\beta \mathcal{U}_N} \phi_p(\mathbf{r}_i, \mathbf{r}_j) d\mathbf{r}^{(N-2)}
\end{aligned}
$$

113

$$= -\frac{\beta}{\Xi} \sum_{N=2}^{\infty} \frac{z^N}{(N-2)!} \left(\phi_p(\mathbf{r}_1, \mathbf{r}_2) \int e^{-\beta \mathcal{U}_N} d\mathbf{r}^{(N-2)} \right.$$

$$+ (N-2) \int \phi_p(\mathbf{r}_1, \mathbf{r}_3) e^{-\beta \mathcal{U}_N} d\mathbf{r}^{(N-2)}$$

$$+ (N-2) \int \phi_p(\mathbf{r}_2, \mathbf{r}_3) e^{-\beta \mathcal{U}_N} d\mathbf{r}^{(N-2)}$$

$$\left. + \frac{(N-2)(N-3)}{2} \int \phi_p(\mathbf{r}_3, \mathbf{r}_4) e^{-\beta \mathcal{U}_N} d\mathbf{r}^{(N-2)} \right).$$

In the first two steps we put in the perturbation potential ϕ_p and in the last step we see that there is one term in $\mathcal{W}_N$ that is not integrated over, $2(N-2)$ terms that are partially integrated over (by one parameter) and $(N-2)(N-3)/2$ terms that are fully integrated out. After some manipulation we can write the expression in terms of particle density functions, we only need to exclude the integrals over the perturbed potential. The result is

$$-\beta \left\{ \phi_p(\mathbf{r}_1, \mathbf{r}_2) \frac{1}{\Xi} \sum_{N=2}^{\infty} \frac{z^N}{(N-2)!} \int e^{-\beta \mathcal{U}_N} d\mathbf{r}^{(N-2)} \right.$$

$$+ \int \phi_p(\mathbf{r}_1, \mathbf{r}_3) \left(\frac{1}{\Xi} \sum_{N=3}^{\infty} \frac{z^N}{(N-3)!} \int e^{-\beta \mathcal{U}_N} d\mathbf{r}^{(N-3)} \right) d\mathbf{r}_3$$

$$+ \int \phi_p(\mathbf{r}_2, \mathbf{r}_3) \left(\frac{1}{\Xi} \sum_{N=3}^{\infty} \frac{z^N}{(N-3)!} \int e^{-\beta \mathcal{U}_N} d\mathbf{r}^{(N-3)} \right) d\mathbf{r}_3$$

$$\left. + \frac{1}{2} \int \phi_p(\mathbf{r}_3, \mathbf{r}_4) \left(\frac{1}{\Xi} \sum_{N=3}^{\infty} \frac{z^N}{(N-4)!} \int e^{-\beta \mathcal{U}_N} d\mathbf{r}^{(N-4)} \right) d\mathbf{r}_3 d\mathbf{r}_4 \right\}.$$

The parts within large brackets are 3rd, 3rd and 4th particle distribution functions respectively. The second part of the first term in equation (A.20) gives also rise to a 2-particle density function. We arrive at

$$\frac{\partial \rho_\lambda^{(2)}}{\partial \lambda} = -\beta \left\{ \phi_p(\mathbf{r}_1, \mathbf{r}_2) \rho_\lambda^{(2)}(\mathbf{r}_1, \mathbf{r}_2) \right.$$

$$+ \int \rho_\lambda^{(3)}(\mathbf{r}_1, \mathbf{r}_2, \mathbf{r}_3)(\phi_p(\mathbf{r}_1, \mathbf{r}_3) + \phi_p(\mathbf{r}_2, \mathbf{r}_3)) d\mathbf{r}_3 \qquad \text{(A.22)}$$

$$\left. + \frac{1}{2} \int [\rho_\lambda^{(4)}(\mathbf{r}_1, \mathbf{r}_2, \mathbf{r}_3, \mathbf{r}_4) - \rho_\lambda^{(2)}(\mathbf{r}_1, \mathbf{r}_2) \rho_\lambda^{(2)}(\mathbf{r}_3, \mathbf{r}_4)] \phi_p(\mathbf{r}_3, \mathbf{r}_4) d\mathbf{r}_3 d\mathbf{r}_4 \right\}.$$

The last term in the last integral is due to the first line of equation (A.20). As we can see, higher order density functions are involved.

A.5 1D Radial FMT Stencils

When the density profiles have radial symmetry (i.e., $\rho(\mathbf{r}){=}\rho(r)$) then the weighted densities from equation (2.84) can be simplified to an integration over a single parameter,

$$n_\alpha(\mathbf{r}) = \int r'^2 \mathrm{d}r' \rho(r') \int \mathrm{d}\varphi' \int \sin\theta' \mathrm{d}\theta' \omega^{(\alpha)}(|\mathbf{r}{-}\mathbf{r}'|). \qquad (\text{A.23})$$

To explain the integration limits we refer to figure 3.2 and eq. (3.18). From the weights $\omega^{(\alpha)}$ in eq. (2.83) we see that the integration bounds should be limited to the *inner* part of the shell in fig. 3.2 with *radius* $R{=}\sigma/2$. This means that there are only contributions when $r'{\in}(r{-}R, r{+}R)$ for a given $r{>}R$ and the *maximal* azimuth angle γ follows from $R^2{=}r^2{+}r'^2{-}2rr'\cos\gamma$.

For the volumetric integral $(\omega^{(3)}(\mathbf{r}){=}\Theta(R{-}|\mathbf{r}|))$ we obtain for $r{>}R$,

$$\begin{aligned}
n_3(r) &= \int r'^2 \mathrm{d}r' \rho(r') \int \mathrm{d}\varphi' \int \sin\theta' \mathrm{d}\theta' \Theta(R{-}\sqrt{r^2{+}r'^2{-}2rr'\cos\theta'}) \\
&= \int_{r-R}^{r+R} 2\pi r'^2 \mathrm{d}r' \rho(r') \int_0^\gamma \sin\theta' \mathrm{d}\theta' = \int_{r-R}^{r+R} \mathrm{d}r' \rho(r') \pi \frac{r'}{r}(R^2{-}(r{-}r')^2).
\end{aligned} \qquad (\text{A.24})$$

When $r{<}R$ a simple sketch convinces us that the azimuth runs from '0' to 'π' when $r'{<}R{-}r$ and from '0' to 'γ' when $r'{>}R{-}r$, see figure A.1. The result in equation (3.16) follows immediately.
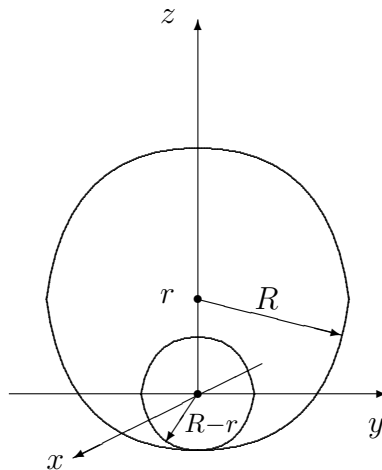

Figure A.1: A sketch of the geometry when $r{<}R$. The spherical shell with radius R crosses the $xy-$plane. The case that $r'{<}R{-}r$ is treated separately.

115

In order to find the second weighted density (with $\omega^{(2)}(\mathbf{r}) = \delta(R - |\mathbf{r}|)$) we first define $\tau(r, r', \theta') = R - \sqrt{r^2 + r'^2 - 2rr'\cos\theta'}$ for a shorthand notation. Then,

$$n_2(r) = \int r'^2 \mathrm{d}r' \rho(r') \int \mathrm{d}\varphi' \int \delta(\tau(r, r', \theta')) \sin\theta' \mathrm{d}\theta' \tag{A.25}$$

$$= \int_{r-R}^{r+R} 2\pi r'^2 \mathrm{d}r' \rho(r') \int_0^\pi \sin\theta' \left(\frac{\partial\tau(r, r', \theta')}{\partial\theta'} \right)^{-1} \mathrm{d}\Theta(\tau(r, r', \theta')),$$

where we assumed that $r > R$ and used the relation $\mathrm{d}\Theta(x)/\mathrm{d}x = \delta(x)$ and the chain rule $(\delta(ax) = (\mathrm{d}ax/\mathrm{d}x)^{-1} \mathrm{d}\Theta(ax)/\mathrm{d}x)$. With

$$\frac{\partial\tau(r, r', \theta')}{\partial\theta'} = \frac{-rr'\sin\theta'}{\sqrt{r^2 + r'^2 - 2rr'\cos\theta'}} = \frac{-rr'\sin\theta'}{\sqrt{\kappa(r, r', \theta')}}, \tag{A.26}$$

where we defined $\kappa(r, r', \theta') = r^2 + r'^2 - 2rr'\cos\theta'$, the integration over the azimuth angle (θ') becomes,

$$\int_0^\pi \sin\theta' \frac{-\sqrt{\kappa(r, r', \theta')}}{rr'\sin\theta'} \mathrm{d}\Theta(\tau(r, r', \theta')) \tag{A.27}$$

$$= \left(\frac{-\sqrt{\kappa(r, r', \theta')}}{rr'} \Theta(\tau(r, r', \theta')) \Big|_0^\pi - \int_0^\pi \Theta(\tau(r, r', \theta')) \frac{-\sin\theta'}{\sqrt{\kappa(r, r', \theta')}} \mathrm{d}\theta' \right)$$

$$= -\frac{|r+r'|}{rr'} \Theta(R - |r+r'|) + \frac{|r-r'|}{rr'} \Theta(R - |r-r'|) + \int_0^\pi \frac{\sin\theta'\Theta(\tau(r, r', \theta'))}{\sqrt{\kappa(r, r', \theta')}} \mathrm{d}\theta',$$

after integration by parts. When $r > R$ the upper bound in the last integral is 'γ' and it becomes,

$$\int_0^\gamma \frac{\sin\theta'}{\sqrt{r^2 + r'^2 - 2rr'\cos\theta'}} \mathrm{d}\theta' = \frac{\sqrt{r^2 + r'^2 - 2rr'\cos\theta'}}{rr'} \Big|_0^\gamma = \frac{R - |r-r'|}{rr'}. \tag{A.28}$$

The overall result of equation (A.27) becomes $-0 + |r-r'| + (R - |r-r'|)/rr' = R/rr'$ and the result in equation (3.16) follows by putting this in equation (A.25). When $r < R$ and $r' \in (R - r, R + r)$, which is the part within the circles in figure A.1, the same holds. When $r < R$ and $r' \in (0, R - r)$, which is the inner circle in figure A.1, the upper bound becomes 'π' and the overall result is $-|r+r'| + |r-r'| + (|r+r'| - |r-r'|)/rr' = 0$. This explains absolute signs in the lower bounds of the integral over r' in eq. (3.16), that is, the exclusion of the inner circle in figure A.1.

Similarly for the vector weighted density $\mathbf{n}_{V2}(r)=n_{V2}(r)\hat{\mathbf{r}}$ (with $\omega^{(V2)}(\mathbf{r})=\nabla\Theta(R-|\mathbf{r}|)=\delta(R-|\mathbf{r}|)\mathbf{r}/r$) we obtain, with the same shorthand notation for τ and κ as we used before ($R-\sqrt{r^2-r'^2-2rr'\cos\theta'}$ resp. $r^2-r'^2-2rr'\cos\theta'$),

$$n_{V2}(r) = \int r'^2 \mathrm{d}r'\rho(r') \int \mathrm{d}\varphi' \int \sin\theta'\mathrm{d}\theta'\delta(\tau(r,r',\theta'))\frac{\mathbf{r}-\mathbf{r'}}{|\mathbf{r}-\mathbf{r'}|} \tag{A.29}$$

$$= \int\limits_{r-R}^{r+R} 2\pi r'^2 \mathrm{d}r'\rho(r') \int\limits_0^\pi \frac{(r-r'\cos\theta')\hat{\mathbf{z}}}{\sqrt{\kappa(r,r',\theta')}}\sin\theta'\left(\frac{\partial\tau(r,r',\theta')}{\partial\theta'}\right)^{-1}\mathrm{d}\Theta(\tau(r,r',\theta'))$$

$$= \int\limits_{r-R}^{r+R} 2\pi r'^2 \mathrm{d}r'\rho(r') \int\limits_0^\pi \frac{(r-r'\cos\theta')\hat{\mathbf{z}}}{\sqrt{\kappa(r,r',\theta')}}\sin\theta'\frac{-\sqrt{\kappa(r,r',\theta')}}{rr'\sin\theta'}\mathrm{d}\Theta(\tau(r,r',\theta'))$$

$$= \int_{r-R}^{r+R} \frac{2\pi r'^2}{rr'}\mathrm{d}r'\rho(r') \int_0^\pi (r'\cos\theta'-r)\hat{\mathbf{z}}\mathrm{d}\Theta(\tau(r,r',\theta'))\hat{\mathbf{z}},$$

where on the second line the x and y components become zero because of the integration over the polar angle φ', since we put $\mathbf{r}-\mathbf{r'}=-r'\sin\theta'\cos\varphi'\hat{\mathbf{x}}-r'\sin\theta'\sin\varphi'\hat{\mathbf{y}}+(r-r'\cos\theta')\hat{\mathbf{z}}$ and we used integration by parts, see equation (A.26). The integral over the azimuth becomes

$$\int_0^\pi \frac{2\pi r'}{r}(r'\cos\theta'-r)\mathrm{d}\Theta(\tau(r,r',\theta')) \tag{A.30}$$

$$= \left(\frac{2\pi r'}{r}(r'\cos\theta'-r)\Theta(\tau(r,r',\theta'))\Big|_0^\pi - \int\limits_0^\pi \Theta(\tau(r,r',\theta'))\frac{2\pi r'^2}{r}(-\sin\theta')\mathrm{d}\theta'\right)$$

$$= \frac{2\pi r'}{r}(-r'-r)\Theta(R-|r+r'|) - \frac{2\pi r'}{r}(r'-r)\Theta(R-|r-r'|) + \int\limits_0^\gamma \frac{2\pi r'^2}{r}\sin\theta'\mathrm{d}\theta'$$

after again integration by parts. The last integral has upper bound 'γ' as a result of the Heaviside function in the integrand (assuming that $r>R$) and the result is $0-2\pi r'(r'-r)/rr'-2\pi r'^2(\cos\gamma-1)/rr'=\pi r'(r^2-r'^2+R^2)/r^2$. When $r<R$ and $r'\in(R-r,R+r)$, which is part within the circles in figure A.1, the same holds. When $r<R$ and $r'\in(0,R-r)$, i.e., the inner circle in figure A.1, the upper bound becomes 'π' and $-|r+r'|+|r-r'|+(|r+r'|-|r-r'|)/rr'=0$ is the overall result. Note that we put r along the $z-$axis, so $\hat{\mathbf{r}}=\hat{\mathbf{z}}$.

The result for the vector weight can also be obtained via the relation $n_{V2}(r)\hat{\mathbf{r}} = -\hat{\mathbf{r}}\mathrm{d}n_3(r)/\mathrm{d}r$ and realizing that when $r<R$ and $r'\in(0,R-r)$ the weight has to vanish due to symmetry. This relation follows from the definition of the weight as a gradient of a Dirac delta function.

Basically, the one dimensional effective weights $\omega^{(\alpha)}$ can be written as,

$$\omega^{(2)}(r,r') = 2\pi R \mathbb{1}/(rr'), \quad \omega^{(V2)}(r,r') = \pi(r^2 - r'^2 + R^2)\mathbb{1}/(r^2 r')$$
$$\text{and} \ \ \omega^{(3)}(r,r') = 4\pi\Theta(R-r) + \pi(R^2 - (r-r')^2)\mathbb{1}/(rr'), \tag{A.31}$$

where $\mathbb{1} := \mathbb{1}_{r' \in (|r-R|, r+R)}$ restricts r' to the specified interval. Note that the second stencil is symmetric, $\omega^{(2)}(r,r') = \omega^{(2)}(r',r)$ and so is the third (when $r > R$), but the vector weight is not. When the weights are integrated, the Jacobian over the radial integral (r'^2) should still be put in. This makes that the *total* weights are not symmetric anymore. In the limit of $r \to \infty$, the stencils obtain a limit, independent of r, see figures 3.1 and A.2.
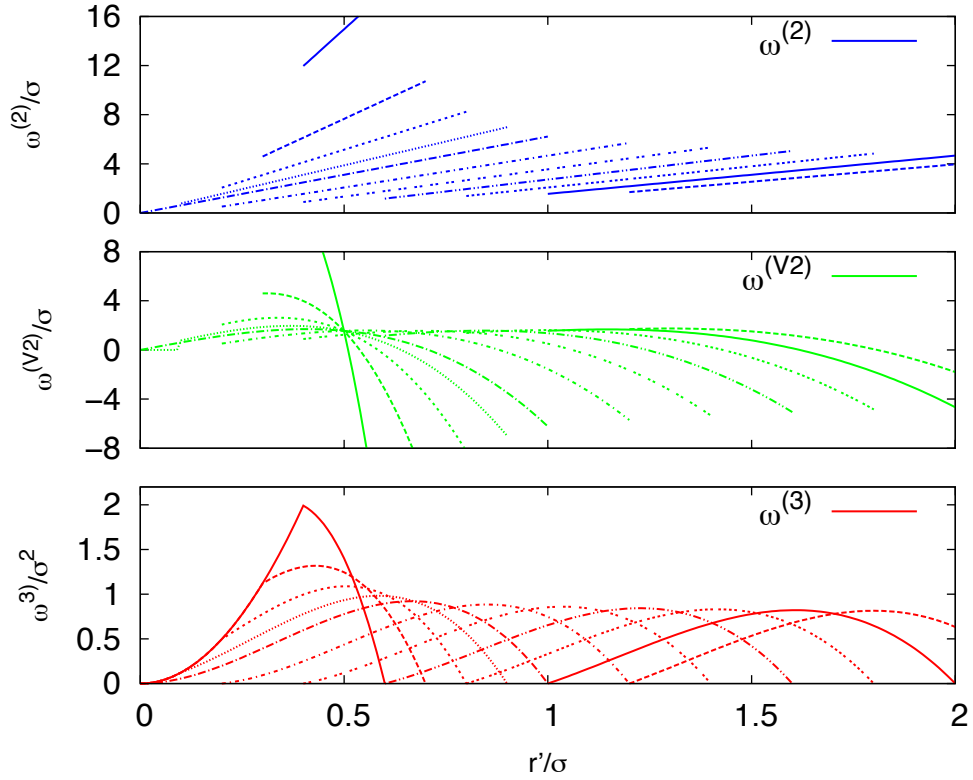

Figure A.2: The weight functions $\omega^{(\alpha)}(r,r')r'^2$ as a function of r' for different r. Each line is centered around r (with the exception of the cases where $r < R = \sigma/2$; then r is half the stencil length for $\omega^{(2)}$ and $\omega^{(V2)}$ whereas for $\omega^{(3)}$, r corresponds to the same r as for the other stencils in this case). It can be seen that the stencils approach a limit as r gets large.

Appendix B

Functional Derivatives

A functional maps a function to a scalar. This means that it depends on all the values of the function on the relevant domain. An example of a linear functional F is

$$F[u] = \int a(x)u(x)\mathrm{d}x, \quad \partial F = \int a(x)\partial u(x)\mathrm{d}x. \tag{B.1}$$

The functional derivative of this becomes then

$$\frac{\delta F}{\delta u(x)} = a(x). \tag{B.2}$$

In general, the functional derivative determines the change in F resulting from a change in u at a particular value of x. In order to calculate the change in F due to a variation in $u(x)$ throughout the range of x it is necessary to integrate over x, as

$$\delta F = F[u+\delta u] - F[u] = \int \frac{\delta F}{\delta u(x)}\delta u(x)\mathrm{d}x. \tag{B.3}$$

For example $F[u] = \int u(x)\ln u(x)\mathrm{d}x$, leads to

$$\begin{aligned} \delta F &= \int [\delta u(x)\ln u(x) + u(x)\delta \ln u(x)]\mathrm{d}x \\ &= \int [\ln u(x) + 1]\delta u(x)\mathrm{d}x, \end{aligned} \tag{B.4}$$

whence

$$\frac{\delta F}{\delta u(x)} = \ln u(x) + 1. \tag{B.5}$$

For the special case that

$$F[u] = u(x') = \int \delta(x-x')u(x)\mathrm{d}x \qquad (\text{B.6})$$

we have

$$\delta F = \int \delta(x-x')\delta u(x)\mathrm{d}x = \delta u(x') \qquad (\text{B.7})$$

and therefore

$$\frac{\delta u(x')}{\delta u(x)} = \delta(x-x'). \qquad (\text{B.8})$$

This means that we can derive equation (3.13) as follows. The derivative of the functional,

$$\mathcal{F}[\rho] = \frac{1}{2} \iint \rho(r_1)\rho(r_2) \frac{\rho(|\mathbf{r}_1-\mathbf{r}_2|)}{\rho_{\text{bulk}}} \phi_{\text{LJ}}(|\mathbf{r}_1-\mathbf{r}_2|)\mathrm{d}\mathbf{r}_1\mathrm{d}\mathbf{r}_2,$$

results in

$$\begin{aligned}
\frac{\delta \mathcal{F}[\rho(\mathbf{r}')]}{\delta\rho(\mathbf{r})} &= \frac{1}{2} \iint \delta(\mathbf{r}_1-\mathbf{r})\rho(r_2) \frac{\rho(|\mathbf{r}_1-\mathbf{r}_2|)}{\rho_{\text{bulk}}} \phi_{\text{LJ}}(|\mathbf{r}_1-\mathbf{r}_2|)\mathrm{d}\mathbf{r}_1\mathrm{d}\mathbf{r}_2 \\
&\quad + \frac{1}{2} \iint \rho(r_1)\delta(\mathbf{r}_2-\mathbf{r}) \frac{\rho(|\mathbf{r}_1-\mathbf{r}_2|)}{\rho_{\text{bulk}}} \phi_{\text{LJ}}(|\mathbf{r}_1-\mathbf{r}_2|)\mathrm{d}\mathbf{r}_1\mathrm{d}\mathbf{r}_2 \\
&\quad + \frac{1}{2} \iint \rho(r_1)\rho(r_2) \frac{\delta(r-|\mathbf{r}_1-\mathbf{r}_2|)}{\rho_{\text{bulk}}} \phi_{\text{LJ}}(|\mathbf{r}_1-\mathbf{r}_2|)\mathrm{d}\mathbf{r}_1\mathrm{d}\mathbf{r}_2 \\
&= \int \rho(r') \frac{\rho(|\mathbf{r}-\mathbf{r}'|)}{\rho_{\text{bulk}}} \phi_{\text{LJ}}(|\mathbf{r}-\mathbf{r}'|)\mathrm{d}\mathbf{r}' \qquad (\text{B.9}) \\
&\quad + \iint \frac{\rho(r)\rho(r')}{2} \frac{\delta(r-|\mathbf{r}-\mathbf{r}'|)}{\rho_{\text{bulk}}} \phi_{\text{LJ}}(|\mathbf{r}-\mathbf{r}'|)\mathrm{d}\mathbf{r}\mathrm{d}\mathbf{r}'.
\end{aligned}$$

More about functional derivatives can be found for example in [5]. Note that the functional derivative also changes the dimension of the outcome, since it omits an integral

Appendix C

An Extension to Quadrupoles

For (linear) quadrupoles the density profile is a function of space as well as of the orientation of the particle. First we separate the spatial and the orientational coordinates i.e.,

$$\rho(\mathbf{r},\omega) = \rho(\mathbf{r})\hat{f}(\mathbf{r},\omega), \tag{C.1}$$

where $\rho(\mathbf{r})$ is the density profile integrated over all particle orientations $\omega=(\theta,\phi)$ (for nonlinear particles there is also assymmetry with respect to the rotation axis χ). This means that

$$\int \hat{f}(\mathbf{r},\omega)\mathrm{d}\omega = \int_0^{2\pi}\int_0^{\pi} \hat{f}(\mathbf{r},\theta,\phi)\sin\theta\mathrm{d}\theta\mathrm{d}\phi = 1. \tag{C.2}$$

We would now write the grand potential Ω as

$$\begin{aligned}
\Omega[\rho(\mathbf{r},\omega)] = &\int f_{\mathrm{id}}(\rho(\mathbf{r}))\mathrm{d}\mathbf{r} + \int f_{\mathrm{hs}}(\rho(\mathbf{r}))\mathrm{d}\mathbf{r} \\
&+ \beta^{-1}\int \rho(\mathbf{r})\int \hat{f}(\mathbf{r},\omega)\ln[4\pi\hat{f}(\mathbf{r},\omega)]\mathrm{d}\omega\mathrm{d}\mathbf{r} \\
&+ \int \rho(\mathbf{r})(V_{\mathrm{ext}}(\mathbf{r},\omega)-\mu)\mathrm{d}\mathbf{r} \\
&+ \frac{1}{2}\iint \mathrm{d}\mathbf{r}_1\mathrm{d}\mathbf{r}_2\rho(\mathbf{r}_1)\rho(\mathbf{r}_2)\iint \mathrm{d}\omega_1\mathrm{d}\omega_2\hat{f}(\mathbf{r}_1,\omega_1)\hat{f}(\mathbf{r}_2,\omega_2) \\
&\qquad g(r_{12},\omega_1,\omega_2)\phi(r_{12},\omega_1,\omega_2).
\end{aligned} \tag{C.3}$$

The third term on the right-hand side represents the loss of entropy due to orientational order. It scales with the logarithm of the probability density function $\hat{f}$ and the average over the all orientations ω is done as in equation

2.32. We let the external potential $V_{\text{ext}}(\mathbf{r}, \omega)$ also depend on the orientation, since we want to fix a quadrupole in the origin and treat it as an external potential. The last term on the right-hand side represent again the long ranged interactions and they will be treated again as a small perturbation because $g(r_{12}, \omega_1, \omega_2)$ is not known exactly. A consequence of the assumption that the perturbation is small is that the amount of ordering is is also small. This means that we can write

$$\hat{f}(\mathbf{r}, \omega) = \frac{1}{4\pi} + \Delta\hat{f}(\mathbf{r}, \omega). \tag{C.4}$$

Here the first term on the right-hand side represents the value for $\hat{f}$ when there is no ordering, that is every possible orientation is equally probable. The second term on the right-hand side is consequently treated as small. Then we can write

$$
\begin{aligned}
\int \hat{f}(\mathbf{r}, \omega) & \ln[4\pi\hat{f}(\mathbf{r}, \omega)]\mathrm{d}\omega \\
&= \int \left(\frac{1}{4\pi} + \Delta\hat{f}(\mathbf{r}, \omega)\right)\ln\left[4\pi\left(\frac{1}{4\pi} + \Delta\hat{f}(\mathbf{r}, \omega)\right)\right] \\
&\approx \int \Delta\hat{f}(\mathbf{r}, \omega) + 2\pi\Delta\hat{f}(\mathbf{r}, \omega)^2 \mathrm{d}\omega \\
&= 2\pi \int \Delta\hat{f}(\mathbf{r}, \omega)^2 \mathrm{d}\omega,
\end{aligned}
\tag{C.5}
$$

where we used a Taylor expansion of $\Delta\hat{f}$ around 0 on the third line and the fact that $\hat{f}$ is normalized on the fourth line. Subsequently we write $\Delta\hat{f}$ in terms of base functions. We take the spherical harmonics $Y_{lm}(\omega)$ for the base functions because they are orthogonal for $\omega = (\theta, \varphi) \in \{(0, \pi), (0, 2\pi)\}$. So

$$\Delta\hat{f}(\mathbf{r}, \theta, \varphi) = \sum_{l=1}^{\infty}\sum_{m=-l}^{l} f_{lm}(\mathbf{r})Y_{lm}(\theta, \varphi). \tag{C.6}$$

Note that there should be no constant in this expression because the integral of $\Delta\hat{f}$ over ω should be zero, as we saw in equation C.5. We obtain an expression in terms of $\Delta\hat{f}$ for the coefficients using the orthogonality relations. We multiply equation C.6 by $Y_{kn}(\theta, \varphi)$ and integrate over the hypersphere ω,

$$
\begin{aligned}
\int_0^{2\pi}\int_0^{\pi} &\Delta\hat{f}(\mathbf{r}, \theta, \varphi)Y_{kn}(\theta, \varphi)\sin\theta\mathrm{d}\theta\mathrm{d}\varphi = \\
&\int_0^{2\pi}\int_0^{\pi}\sum_{l=1}^{\infty}\sum_{m=-l}^{l} f_{lm}(\mathbf{r})Y_{lm}(\theta, \varphi)Y_{kn}(\theta, \varphi)^*\sin\theta\mathrm{d}\theta\mathrm{d}\varphi = f_{kn}(\mathbf{r}),
\end{aligned}
\tag{C.7}
$$

where '*' denotes the complex conjugate. Here we used the relationship

$$\int\limits_{0}^{2\pi}\int\limits_{0}^{\pi} Y_{lm}(\theta,\varphi)Y_{kn}(\theta,\varphi)^{*}\sin\theta\mathrm{d}\theta\mathrm{d}\varphi = \delta_{nm}\delta_{kl}, \qquad (\text{C.8})$$

where δ_{kl} is the Kronecker delta function (1 when $k=l$ and 0 otherwise). Now we can write the 'average loss of entropy per point $\mathbf{r}$' term in equation C.19 (i.e., only the integral over ω in the third term on the right-hand side) like

$$2\pi\int\Delta\hat{f}(\mathbf{r},\omega)^{2}\mathrm{d}\omega = 2\pi\int\left(\sum_{l=1}^{\infty}\sum_{m=-l}^{l}f_{lm}(\mathbf{r})Y_{lm}(\theta,\varphi)\right)^{2}\mathrm{d}\omega$$

$$= 2\pi\sum_{l=1}^{\infty}\sum_{m=-l}^{l}f_{lm}(\mathbf{r})Y_{lm}(\theta,\varphi). \qquad (\text{C.9})$$

In the first step we used the expansion as in equation C.6.
Now we will work out the last term in equation C.19. We will need to make an assumption on $g(r_{12},\omega_1,\omega_2)$. This can be the modified mean field, but the derivation is lengthy. We will show the results for the mean field. The expression of the perturbation potential is given by $\phi_p=\phi_{\text{LJ}}+\phi_{qq}$, where we can write in terms of spherical harmonics, [50]:[1]

$$\phi_{\text{qq}}(r,\omega,\omega_1,\omega_2) = \frac{3}{4}\frac{Q^2}{r^5}[1 - 5(\hat{\boldsymbol{Q}}_1\cdot\hat{\mathbf{r}})^2 - 5(\hat{\boldsymbol{Q}}_2\cdot\hat{\mathbf{r}})^2 + 2(\hat{\boldsymbol{Q}}_1\cdot\hat{\boldsymbol{Q}}_2)^2+$$

$$35(\hat{\boldsymbol{Q}}_1\cdot\hat{\mathbf{r}})(\hat{\boldsymbol{Q}}_2\cdot\hat{\mathbf{r}}) - 20(\hat{\boldsymbol{Q}}_1\cdot\hat{\mathbf{r}})(\hat{\boldsymbol{Q}}_2\cdot\hat{\mathbf{r}})(\hat{\boldsymbol{Q}}_1\cdot\hat{\boldsymbol{Q}}_2) \qquad (\text{C.10})$$

$$= \frac{Q^2}{r^5}\frac{8\pi}{15}\sqrt{70\pi}\sum_{m_1m_2}C(224;m_1m_2m)Y_{2m_1}(\omega_1)Y_{2m_2}(\omega_2)Y_{4m}^{*}(\omega),$$

for $r>\sigma$ and 0 otherwise. In this formula $\hat{\mathbf{Q}}_i$ is the orientation of quadrupole i, $\mathbf{r}$ is the separation vector of the particles with $r = |\mathbf{r}|$, ω_i is the orientation of particle $i = 1, 2$, ω is the orientation of the inter-molecular separation, see figure C.1. The potential for quadrupole-quadrupole plus LJ interactions is shown (and compared to dipole-dipole plur LJ interactions) in figure C.2.

---

[1]The spherical dependent part of an interaction potential for linear particles should be proportional to

$$\sum_{m_1m_2m}C(l_1l_2l;m_1m_2m)Y_{l_1m_1}(\omega_1)Y_{l_2m_2}(\omega_2)Y_{lm}(\omega)^{*},$$

where l_i is the order of pole i (i.e. 1 for dipoles, 2 for quadrupoles etc.) and $l_1 + l_2 = l$, see eq. (A.195a) of [50]. The coefficient can be found by equating this to the Cartesian form for the case that all unit vectors are parallel to the polar axis.
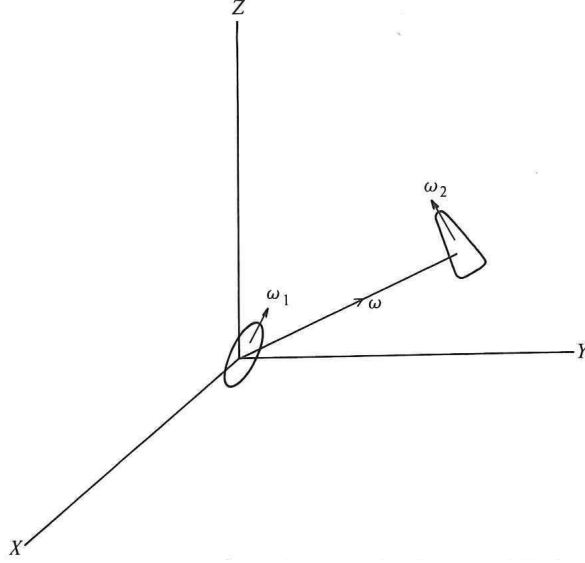
Figure C.1: Geometry of interaction for two linear molecules. Here $\omega_i = \theta_i\varphi_i$ denotes the orientation of the symmetry axis of molecule i, and ω denotes the orientation of the inter-molecular axis. [50]

For convenience the spherical harmonics are given here:

$$Y_{00}(\omega)=\frac{1}{2}\sqrt{\frac{1}{\pi}}, \qquad Y_{40}(\omega)=\sqrt{\frac{1}{\pi}}\frac{3}{16}(35\cos^4\theta-30\cos^2\theta+3),$$

$$Y_{10}(\omega)=\sqrt{\frac{3}{4\pi}}\cos\theta, \qquad Y_{41}(\omega)=\sqrt{\frac{5}{\pi}}\frac{-3}{8}\sin\theta(7\cos^3\theta-3\cos\theta)\mathrm{e}^{i\varphi},$$

$$Y_{11}(\omega)=-\sqrt{\frac{3}{4\pi}}\sqrt{\frac{1}{2}}\sin\theta\mathrm{e}^{i\varphi}, \qquad Y_{42}(\omega)=\sqrt{\frac{5}{2\pi}}\frac{3}{8}\sin^2\theta(7\cos^2\theta-1)\mathrm{e}^{2i\varphi},$$

$$Y_{20}(\omega)=\sqrt{\frac{5}{4\pi}}\frac{1}{2}(3\cos^2\theta-1), \qquad Y_{43}(\omega)=\sqrt{\frac{35}{\pi}}\frac{-3}{8}\sin^3\theta\cos\theta\mathrm{e}^{3i\varphi},$$

$$Y_{21}(\omega)=-\sqrt{\frac{5}{4\pi}}\sqrt{\frac{3}{2}}\sin\theta\cos\theta\mathrm{e}^{i\varphi}, \qquad Y_{44}(\omega)=\sqrt{\frac{35}{2\pi}}\frac{3}{16}\sin^4\theta\mathrm{e}^{4i\varphi},$$

$$Y_{22}(\omega)=\sqrt{\frac{5}{4\pi}}\sqrt{\frac{3}{8}}\sin^2\theta\mathrm{e}^{2i\varphi}, \qquad Y_{lm}(\omega)=(-1)^m Y_{l\underline{m}}^*(\omega),$$

where $\underline{a}\equiv -a$, and the Clebsch-Gordan coefficients $C(l_1,l_2,l;m_1,m_2,m_3)$, in the convention of Rose, can be calculated using Wigner's closed expression
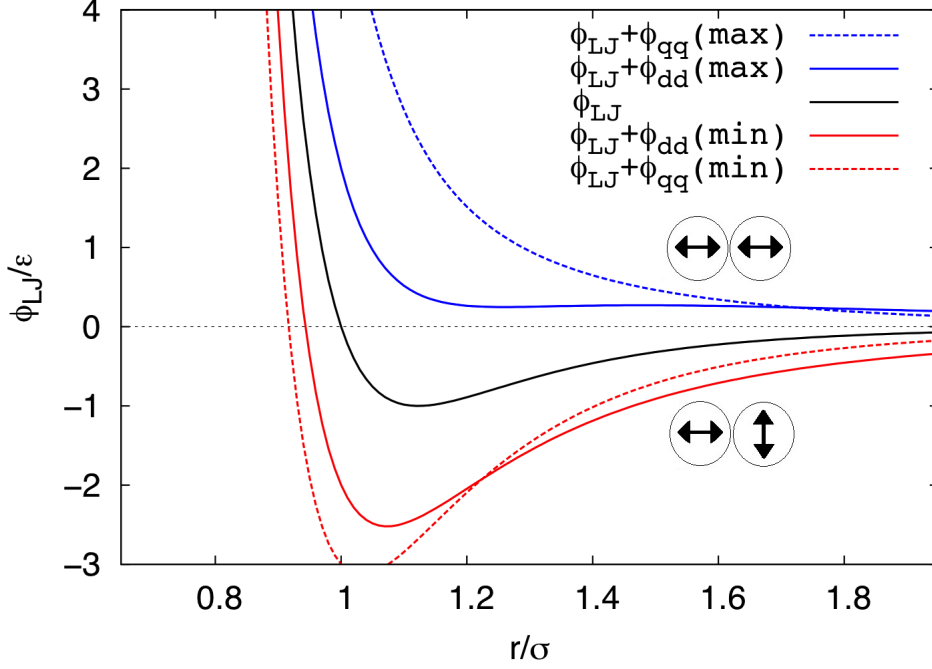
124

Figure C.2: Lennard-Jones potential and the maximal deviation from it for different orientations of dipoles (solid) and quadrupoles (dashed).

[51]:

$$C(j_1, j_2, j_3; m_1, m_2, m_3) = \delta_{m_3, m_1+m_2} \tag{C.11}$$
$$\times \left[(2j_3+1) \frac{(j_3+j_1-j_2)!(j_3-j_1+j_2)!(j_1+j_2-j_3)!(j_3+m_3)!(j_3-m_3)!}{(j_1+j_2+j_3+1)!(j_1-m_1)!(j_1+m_1)!(j_2-m_2)!(j_2+m_2)!} \right]^{1/2}$$
$$\times \sum_\nu \frac{(-1)^{\nu+j_2+m_2}}{\nu!} \frac{(j_2+j_3+m_1-\nu)!(j_1-m_1+\nu)!}{(j_3-j_1+j_2-\nu)!(j_3+m_3-\nu)!(\nu+j_1-j_2-m_3)!},$$

where the sum runs over all ν for which all the factorials are non-negative. The coefficients are only nonzero when $|m_i| \leq j_i$ for $i=1,2,3$, $|j_1-j_2| \leq j_3 \leq j_1+j_2$ and $m_3=m_1+m_2$. Here we need

$$C(112; 000) = \sqrt{2/3}, \quad C(112; \underline{1}10) = \sqrt{1/6}, \quad C(112; 101) = \sqrt{1/2},$$
$$C(112; 112) = 1, \quad C(224; \underline{1}10) = \sqrt{8/35}, \quad C(224; \underline{2}20) = \sqrt{1/70},$$
$$C(224; 000) = \sqrt{18/35}, \quad C(224; \underline{1}10) = \sqrt{8/35} \quad C(224; 101) = \sqrt{3/7},$$
$$C(224; \underline{2}20) = \sqrt{1/70}, \quad C(224; 202) = \sqrt{3/14} \quad C(224; \underline{2}1\underline{1}) = \sqrt{1/14}$$
$$C(224; 112) = \sqrt{4/7}, \quad C(224; 213) = \sqrt{1/2}, \quad C(224; 224) = 1, \quad \text{(C.12)}$$

and others can be found using the following symmetry relations

$$C(j_1 j_2 j_3; m_1 m_2 m_3) = (-1)^{j_1+j_2-j_3} C(j_1 j_2 j_3; \underline{m_1} \underline{m_2} \underline{m_3}) \tag{C.13}$$
$$= (-1)^{j_1+j_2-j_3} C(j_2 j_1 j_3; m_2 m_1 m_3).$$

From now on we assume that we have radial symmetry around the origin. This means that we can integrate out 2 dimensions in the integrals over the unknown $\rho(r)$. We will also have to do this for the potentials. For the quadrupole term we obtain for the spatial part,

$$2\pi \int \frac{Y_{4m}^*(\omega)}{|\mathbf{r}-\mathbf{r'}|^5} \sin\theta \mathrm{d}\theta = 2\pi \int \frac{\sqrt{\pi}^{-1} \frac{3}{16}(35\cos^4\theta' - 30\cos^2\theta' + 3)}{(r'^2 + r^2 - 2rr'\cos\theta')^{5/2}} \sin\theta' \mathrm{d}\theta'$$
$$= 2\sqrt{\pi}\frac{3}{16} \int \frac{35u^4 - 30u^2 + 3}{(r'^2 + r^2 - 2rr'u)^{5/2}} \mathrm{d}u, \tag{C.14}$$

since we still have symmetry over ϕ and therefore all Y_{4m}^* vanish except for $m=0$. In the second step we substituted $u := \cos\theta'$. When $|r-r'| > \sigma$ the bounds of the integrals become 0 and π for θ' (-1 and 1 for u). The result can be obtained by successive integration by parts,

$$\int_{-1}^{1} \frac{35u^4 - 30u^2 + 3}{(r'^2 + r^2 - 2rr'u)^{5/2}} \mathrm{d}u = \frac{8}{3}\frac{1}{rr'} \left(\frac{1}{|r-r'|^3} - \frac{1}{(r+r')^3} \right)$$
$$- \frac{80}{3} \left(\frac{1}{rr'} \right)^2 \left(\frac{1}{|r-r'|} - \frac{1}{(r+r')} \right)$$
$$- 120 \left(\frac{1}{rr'} \right)^3 \left(|r-r'| - (r+r') \right) \tag{C.15}$$
$$- \frac{280}{3} \left(\frac{1}{rr'} \right)^4 \left(|r-r'|^3 - (r+r')^3 \right)$$
$$- \frac{280}{15} \left(\frac{1}{rr'} \right)^5 \left(|r-r'|^5 - (r+r')^5 \right).$$

As $\sqrt{x^2} = |x|$ we can distinguish the cases $r > r'$ and $r < r'$. The result for $r > r'$ and $r < r'$ become respectively

$$\frac{16r'^4(-11r^2 - 7r'^2)}{3r^5(r'-r)^5(r'+r)^5} \quad \text{and} \quad \frac{16r^4(-11r'^2 - 7r^2)}{3r'^5(r-r')^5(r+r')^5}. \tag{C.16}$$

Note that we can simply interchange r and r' in the above expression to distinguish the cases. When $|r-r'| < \sigma$ the bounds of the integrals become γ

126

and π for θ' (-1 and $\cos\gamma$ for u). So

$$
\int\limits_{-1}^{\cos\gamma} \frac{35u^4-30u^2+3}{(r'^2+r^2-2rr'u)^{5/2}}\mathrm{d}u = \frac{1}{3rr'}\left(\frac{1}{\sigma^3}[35s^4-30s^2+3] - \frac{8}{(r+r')^3}\right)
$$

$$
+ \left(\frac{1}{rr'}\right)^2\left(\frac{1}{\sigma}\left[-\frac{140}{3}s^4-\frac{60}{3}s^2\right] - \frac{80}{3}\frac{1}{(r+r')}\right)
$$

$$
+ \left(\frac{1}{rr'}\right)^3\left(\sigma[-140s^4+20s^2] + 120(r+r')\right)
$$

$$
- \frac{280}{3}\left(\frac{1}{rr'}\right)^4\left(\sigma^3 s - (r+r')^3\right)
$$

$$
- \frac{56}{3}\left(\frac{1}{rr'}\right)^5\left(\sigma^5 - (r+r')^5\right),
$$

(C.17)

where s is the dimensionless quantity $(r^2+r'^2-\sigma^2)/2rr'$. Now let ζ_{qq} be $\sqrt{70}\pi^2 Q^2/5$ times equation (C.15) for $|r-r'|>\sigma$ and $\sqrt{70}\pi^2 Q^2/5$ times equation (C.17) for $|r-r'|<\sigma$. The summation over m_1 and m_2 in equation (C.10) can be written in terms of spherical harmonics $Y_{2m_1}(\omega_1)Y_{2\underline{m}_1}(\omega_1)$, where $\underline{m}_1 = -m_1$ (since we must have $m_1+m_2=0$, by the integration over the spatial angles ω in equation (C.14) only $m_1+m_2=m=0$ remains). The integrals over the orientations of the particles (ω_1 and ω_2) become

$$
\iint \Big(C(224;\underline{2}20)Y_{2\underline{2}}(\omega_1)Y_{22}(\omega_2) + C(224;\underline{1}10)Y_{2\underline{1}}(\omega_1)Y_{21}(\omega_2)+
$$

$$
C(224;000)Y_{20}(\omega_1)Y_{20}(\omega_2) + C(224;1\underline{1}0)Y_{21}(\omega_1)Y_{2\underline{1}}(\omega_2)+
$$

$$
C(224;2\underline{2}0)Y_{22}(\omega_1)Y_{2\underline{2}}(\omega_2) \Big)\Delta\hat{f}(r,\omega_1)\Delta\hat{f}(r',\omega_2)\mathrm{d}\omega_1\mathrm{d}\omega_2 =
$$

$$
\sqrt{\frac{1}{70}}\left(f_{2\underline{2}}(r)f_2^2(r') + f_{22}(r)f_{2\underline{2}}(r') \right)+
$$

$$
\sqrt{\frac{1}{6}}\left(f_{2\underline{1}}(r)f_{21}(r') + f_{21}(r)f_{2\underline{1}}(r') \right) + \sqrt{\frac{18}{35}}f_{20}(r)f_{20}(r') =: \psi(r,r').
$$

(C.18)

On the first line we wrote all the sums in equation (C.10) and then integrate over the orientations, as in equation (C.19). For the equality we substituted $\Delta\hat{f}^*$ from equation (C.6) for $\Delta\hat{f}$ and used the orthogonality relation (C.8). Note that we are allowed to use $\Delta\hat{f}^*$ since it must be a real quantity. We obtain an expression in terms of the spatial varying coefficients from equation

(C.7) and we define ψ. Now we can express Ω as

$$\Omega[\rho(r), \{f_{lm}\}] = \int f_{\text{id}}(\rho(r)) r^2 \mathrm{d}r + \int f_{\text{hs}}(\rho(r)) r^2 \mathrm{d}r$$

$$+ \frac{2\pi}{\beta} \int \rho(r) \int \sum_{l=1}^{\infty} \sum_{m=-l}^{l} f_{lm}^2(r) r^2 \mathrm{d}r + \int \rho(r)(V_{\text{ext}}(r) - \mu) r^2 \mathrm{d}r \qquad \text{(C.19)}$$

$$+ \frac{1}{2} \iint r_1^2 r_2^2 \mathrm{d}r_1 \mathrm{d}r_2 \rho(r_1) \rho(r_2) (\zeta_{\text{LJ}}(r_1, r_2) + \zeta_{qq}(r_1, r_2) \psi(r_1, r_2)).$$

Now the equilibrium can be found by minimizing Ω with respect to both ρ and all f_{lm},

$$\frac{\delta \Omega}{\delta \rho(r)} = 0 \quad \text{and} \quad \frac{\delta \Omega}{\delta f_{lm}(r)} = 0, \text{ for } l = 2 \text{ and } m = -2, -1, 0, 1, 2. \text{(C.20)}$$

Note that the f_{lm} also appear in ψ. If and only if the external potential depends on an $f_{l'm'}$, this $f_{l'm'}$ will be nonzero (in this approximation). When the modified mean field is used, also the square of the quadrupole-quadrupole potential is used and the f_{lm} that appear in ψ will all be nonzero. This is a tedious calculation since there appear terms like $Y_{lm}(\omega) Y^*_{\underline{lm}}(\omega)$ which give contributions for all $m=0, 1, 2, 3, 4$ The $f_{l'm'}$ that do not appear in ψ will always be zero, since they only increase the grand potential (which we want to minimize).

This is how the model can be extended to polar particles.

Bibliography

[1] E.S. McGarrity (unpublished data)

[2] Born, M., M.S. Green, A General Kinetc Theory of Liquids, *Cambridge University Press* (Cambridge, 1949)

[3] Levesque D., 1966, *Physica* **32** 1985

[4] Frisch, H., Lebowitz J.L., The Equilibrium Theory of Classical Fluids *Benjamin* (New York, 1964)

[5] Hansen J.P., McDonald R., Theory of Simple Liquids, *Academic Press, INC* (San Diego, 1990)

[6] Percus J.K., 1962, *Phys. Rev. Lett.* **8** 462

[7] Rowlinson J.S. 1965, *Rep. Prog. Phys* **28** 169

[8] Gillan M.J., 1979, *Mol. Phys.* **38** 1781

[9] Percus J.K., Yevick G.J., 1958, *Phys. Rev.* **10** 1

[10] Dale W.D.T., Friedman H.L., 1978, *J. Chem. Phys.* **68** 3391

[11] Baxter L.J., 1966, *Phys. Rev.* **154** 1

[12] Tang Y., Lu C.Y., 1993, *J. Chem. Phys.* **99** 9828

[13] Ebner C., Saam W.F., Stroud D., 1976, *Phys. Rev. A* **14** 2264

[14] Gray G.C., Gubbins K.E., Joslin C.G., Theory of Molecular Fluids Volume II, *The Clarendon Press* (Oxford, 2011)

[15] Rosenfeld Y., 1989, *Phys. Rev. Lett.* **63** 980

[16] Thiele E.J. 1963. *J. Chem. Phys.* **39** 474

[17] Lebowitz J.L., Rowlinson J.S. 1964. *J. Chem. Phys.* **41** 133

[18] Roth R., Evans R., Lang A., Kahl G., 2002, *J. Phys. Condens. Matter*, **14** 12063

[19] Carnahan N.F., Starling K.E., 1969, *J. Chem. Phys.* **51** 635

[20] Mansoori G.A., Carnahan N.F., Starling K.E., Leland T.W., 1971, *J. Chem. Phys.* **54** 1523

[21] Rosenfeld Y., 1994, *Phys. Rev. E* **50** R3318

[22] Rosenfeld Y., 1989, *Mol. Phys.* **86** 637

[23] H. Hansen-Goos, K. Mecke, 2009, *Phys. Rev. Lett.* **102** 018302

[24] H. Hansen-Goos, K. Mecke, 2010, *J. Phys. Condens. Matter* **22** 364107

[25] Esztermann A., Reich H., Schmidt M., 2006, *Phys. Rev E.* **73** 011409

[26] Tarazona P., Rosenfeld Y., 1997, *Phys. Rev. E* **55** R4837

[27] Tarazona P., 2000, *Phys. Rev. Lett.* **84** 694

[28] Oxtoby D.W., 2002, *Ann. Rev. Materials Res.* **32** 39

[29] Löwen H., 2002, *J. Phys. Cond. Matter* **14** 11897

[30] Löwen H., 2003, *J. Phys. Condens. Matter* **15** V1

[31] Yu Y.X., Wu J., 2002, *J. Chem. Phys.* **116** 7094

[32] Tang Y., 2005, *Phys. Rev. A.* **44** 5025

[33] Kierlik E. and Rosinberg M.L. 1991, *J. Chem. Phys.* **123** 204704

[34] Yu Y.X., Wu J., 2002, *J. Chem. Phys.* **117** 10156

[35] Gray C.G., Gubbins K.E., Joslin C.G., Theory of Molecular Fluids, volume 2 *The Clarendon Press*, (Oxford)

[36] Kardar M., Statistical Physics of Particles, *Cambridge University Press* (Cambridge, 2007)

[37] Schroeder D.V., Introduction to Thermal Physics, *Addison Wesley* (Reading, 2000)

[38] http://www.aimath.org/WWN/phasetransition/Defs16.pdf

[39] http://people.virginia.edu/ lz2n/mse305/notes/PD-OneComp.pdf

[40] Groh B., Mulder B., 2000, *Phys. Rev. E* **61** 3811

[41] Teixeira P.I., Telo da Gama M.M., 1991, *J. Phys. Condens. Matter* **3** 111

[42] Henderson D., Barker J.A., Physical Chemistry: An Advanced Treatise vol. VIIIA, *Academic Press*(New York,1971)

[43] Kierlik E., Rosinberg M.L, 1990, *Phys. Rev. A* **42** 3382

[44] Kierlik E., Rosinberg M.L, Bildstein B., Kahl G. 1993, *Phys. Rev. E* **48** 618

[45] Barker J.A., Henderson D., 1967, *J. Chem. Phys.* **47** 4714

[46] Roth R., 2010, *J. Phys. Condens. Matter* **22** 063102

[47] Frink L.J.D., Salinger A.G., 2000, *J. Comp. Phys.* **159** 407

[48] Frink L.J.D., Salinger A.G., 2000, *J. Comp. Phys.* **159** 425

[49] Verlet L., 1967, *Phys. Rev.* **159** 98

[50] Gray C.G., Gubbins K.E., Theory of Molecular Fluids, volume 1 *The Clarendon Press*, (Oxford)

[51] Rose M.E., Elementary theory of angular momentum, *John Wiley & sons Inc.*, (London)